arXiv:1610.01822v1 [cond-mat.mes-hall] 6 Oct 2016

Conductance of closed and open long Aharonov-Bohm-Kondo rings

Zheng Shi[1] and Yashar Komijani[2]

[1] *Department of Physics and Astronomy, University of British Columbia, Vancouver, BC V6T 1Z1, Canada*
[2] *Department of Physics and Astronomy, Rutgers University, Piscataway, New Jersey, 08854, USA*

(Dated: October 7, 2016)

We calculate the finite temperature linear DC conductance of a generic single-impurity Anderson model containing an arbitrary number of Fermi liquid leads, and apply the formalism to closed and open long Aharonov-Bohm-Kondo (ABK) rings. We show that, as with the short ABK ring, there is a contribution to the conductance from the connected 4-point Green's function of the conduction electrons. At sufficiently low temperatures this contribution can be eliminated, and the conductance can be expressed as a linear function of the T-matrix of the screening channel. For closed rings we show that at temperatures high compared to the Kondo temperature, the conductance behaves differently for temperatures above and below v_F/L where v_F is the Fermi velocity and L is the circumference of the ring. For open rings, when the ring arms have both a small transmission and a small reflection, we show from the microscopic model that the ring behaves like a two-path interferometer, and that the Kondo temperature is unaffected by details of the ring. Our findings confirm that ABK rings are potentially useful in the detection of the size of the Kondo screening cloud, the $\pi/2$ scattering phase shift from the Kondo singlet, and the suppression of Aharonov-Bohm oscillations due to inelastic scattering.

I. INTRODUCTION

The Kondo problem, one of the most influential problems in condensed matter physics, emerges from a deceptively unembellished model: a localized impurity spin coupled with a Fermi sea of conduction electrons.[1,2] Perturbation theory in the coupling constant is plagued by infrared divergence, but after much theoretical endeavor[3–5] it has been recognized that the model has a relatively simple low energy behavior. For the single-channel spin-1/2 model, at temperatures well below the Kondo temperature T_K, the impurity spin is "screened" by the conduction electrons, forming a local singlet state. The spatial extent of this singlet state, commonly termed the "Kondo screening cloud", is expected to be $L_K = v_F/T_K$ where v_F is the Fermi velocity. The remaining conduction electrons are well described by a Fermi liquid theory at zero temperature, and acquire a phase shift ($\pi/2$ in the presence of particle-hole symmetry) upon being elastically scattered by the Kondo singlet. Moreover, at finite temperatures, scattering by the Kondo impurity can have both elastic and inelastic contributions[6], and it has been suggested that the inelastic scattering can be the origin of decoherence in mesoscopic structure, as measured for example by weak localization.[6–8]

Advances in semiconductor technology have made it possible to imitate the impurity spin with a quantum dot (QD):[9–13] when the ground state number of electrons in the QD is odd, the QD hosts a nonzero spin at temperatures lower than the charging energy. This possibility has triggered renewed experimental and theoretical interest in mesoscopic manifestations of Kondo physics in QD devices, such as the observation of the length scale L_K, the $\pi/2$ phase shift, and also decoherence effects of inelastic Kondo scattering.

Many mesoscopic configurations have been proposed in order to observe L_K. These include QD-terminated finite quantum wires,[14] and also various geometries with an embedded QD, including finite quantum wires,[15–17] small metallic grains/larger QDs,[18–22] and in particular, closed long Aharonov-Bohm (AB) rings with[23,24] and without[25] external electrodes. (A closed ring conserves the electric current and there is no leakage current.) Another motivation for quantum rings is that they may be used to answer the question of whether or not the inelastic scattering from the Kondo QD can cause decoherence by suppressing the amplitude of AB oscillations. A common feature of all these configurations is that they introduce at least one additional mesoscopic length scale L. When the bare Kondo coupling strength is adjusted so that L_K crosses the scale L, the dependence of observables on other control parameters changes qualitatively. In the closed long AB ring with an embedded QD [also known as the Aharonov-Bohm-Kondo (ABK) ring], for instance, L is the circumference of the ring: it is known that both L_K itself and the conductance through the ring can have drastically different AB phase dependences for $L_K \gg L$ and $L_K \lesssim L$.[23,24] In the "large Kondo cloud" regime $L_K \gg L$, corresponding to a relatively small bare Kondo coupling, the Kondo cloud "leaks" out of the ring and the size of the cloud becomes limited by the ring size. Hence, for a given bare Kondo coupling, L_K can be extremely sensitive to the AB phase at certain values of Fermi energy, varying by many orders of magnitude. This sensitivity is completely lost in the opposite "small Kondo cloud" regime $L_K \lesssim L$, where the bare Kondo coupling is relatively large.

The conductance calculation of ABK rings, however, involves an additional layer of complication[26] that went neglected in a number of early works. In mesoscopic Kondo problems with Fermi liquid electrodes, it is usually convenient to work with the scattering states and rotate to the basis of the so-called screening and non-screening

channels: the screening channel ψ is coupled to the QD and therefore has a nonzero T-matrix, while the non-screening channel ϕ is described by a decoupled non-interacting theory.[24,27–30] A careful evaluation by Kubo formula at finite temperatures reveals that, unlike a QD directly coupled to external leads, the interaction effects on the linear DC conductance of short ABK rings are generally *not* fully encoded by the screening channel T-matrix, or equivalently the two-point function. Instead, there exists a contribution from connected four-point diagrams, corresponding to two-particle scattering processes.[26] This is not in contradiction with the famous Meir-Wingreen formula[31] due to the violation of the proportionate coupling condition.[32] For the short ABK ring, the four-point contribution becomes comparable to the two-point contribution well above the Kondo temperature $T \gg T_K$, but can be approximately eliminated at temperatures low compared to the bandwidth $T \ll t$, by applying the bias voltage and probing the current in a particular fashion. One naturally wonders how this result generalizes to the closed long ring at high and low temperatures, and how it possibly modifies early predictions on conductance,[24] which is again expected to display qualitatively different behaviors for $L_K \gg L$ and $L_K \lesssim L$.

On the other hand, efforts to measure the $\pi/2$ phase shift are mainly concentrated on two-path AB interferometer devices.[33–38] In these devices, electrons from the source lead propagate through two possible paths (QD path and reference path) to the drain lead; the two paths enclose a tunable AB phase φ, and a QD tuned into the Kondo regime is embedded in the QD path. Most importantly, the complex transmission amplitudes through the two paths $t_d e^{i\varphi}$ and t_{ref} should be independent of each other, and the total coherent transmission amplitude at zero temperature $t_{sd} = t_{ref} + t_d e^{i\varphi}$ is the sum of the individual amplitudes (the "two-slit condition"), meaning multiple traversals of the ring are negligible. Using a multi-particle scattering formalism, and assuming that only single-particle scattering processes are coherent, Ref. 39 calculates the conductance of such an interferometer with an embedded Kondo QD in terms of the single-particle T-matrix through the QD, and concludes that the AB oscillations are suppressed by inelastic multi-particle scattering processes due to the Kondo QD.

The two-path interferometer can in principle be realized through open AB rings, where in contrast to closed rings, the propagating electrons may leak into side leads attached to the ring. For a non-interacting QD, Ref. 40 presents the criteria for an open long ring to yield the intrinsic transmission phase through the QD: all lossy arms with side leads should have a small transmission and a small reflection. A small transmission suppresses multiple traversals of the ring and guarantees the validity of the two-slit assumption, while a small reflection prevents electrons from "rattling" (tunneling back and forth) across the QD. However, when the QD is in the Kondo regime, as with the previously discussed closed AB rings, the transmission probability through the QD[41] and even the Kondo temperature[23] may be sensitive to the AB phase and other details of the geometry, hampering the detection of the intrinsic phase shift across the QD. In addition, since the screening channels in the open ABK ring and in the simple embedded QD geometry are usually not the same, it is not obvious that the single-particle T-matrices coincide in the two geometries. These issues are not addressed in Ref. 39, which simply assumes that the two-slit condition is obeyed by the coherent processes, and that the T-matrix of the open ABK ring is identical to that of the QD embedded between source and drain leads. To our knowledge, it has been a mystery whether in certain parameter regimes the open long ABK ring realizes the two-path interferometer with a Kondo QD, where the Kondo temperature and the transmission probability through the QD are independent of the details of other parts of the ring, and the T-matrix of the ring truthfully reflects the T-matrix of the QD.

The aforementioned problems in closed and open ABK rings prompt a unified treatment of linear DC conductance in different mesoscopic geometries containing an interacting QD. Much work has been done on generic mesoscopic geometries,[32,42] but in our formalism presented in this paper we aim to take the connected contribution into account expressly, and refrain from making assumptions about the geometry in question (such as parity symmetry).

We study a QD represented by an Anderson impurity, which is embedded in a junction connecting an arbitrary number of Fermi liquid leads. The junction is regarded as a black box characterized only by its scattering S-matrix and its coupling with the QD, and all leads (including source, drain and possibly side leads) are treated on equal footing. In parallel with Ref. 26 we find that the linear DC conductance is given by the sum of a "disconnected" part and a "connected" part. The disconnected part has the appearance of a linear response Landauer formula, where the "transmission amplitude" is linear in the T-matrix of the screening channel, and indeed reduces at zero temperature to a non-interacting transmission amplitude appropriate for the local Fermi liquid theory. The connected part is again a Fermi surface property, can be eliminated by proper application of bias voltages, and is calculated perturbatively at weak coupling $T \gg T_K$, as well as at strong coupling $T \ll T_K$ provided the local Fermi liquid theory applies.

Our formalism is subsequently applied to long ABK rings. In the case of closed rings, we show that for $T \gg T_K$, the high-temperature conductance does exhibit qualitatively different behaviors as a function of the AB phase for $T \gg v_F/L$ and $T \ll v_F/L$. In the case of open rings, when the small transmission condition is met, we find the mesoscopic fluctuations are suppressed, and the two-path interferometer behavior is indeed recovered at low temperatures. If in addition the small reflection condition is satisfied, the Kondo temperature of the QD and the complex transmission amplitude through the QD are both unaffected by the details of the ring. We then find the conductance at $T \gg T_K$ and $T \ll T_K$, and in particular rigorously calculate the normalized visibility[39] of the AB

oscillations in the Fermi liquid regime. We show that while the deviation of normalized visibility from unity is indeed proportional to inelastic scattering as predicted by Ref. 26, the constant of proportionality depends on non-universal particle-hole symmetry breaking potential scattering. Our findings also suggest that the $\pi/2$ phase shift across the QD is measurable in our two-path interferometer when the criteria of small transmission and small reflection are fulfilled. We stress again that, while we focus on long ABK rings in this paper, our general formalism is applicable to a Kondo impurity embedded in an arbitrary non-interacting multi-terminal mesoscopic structure.

The rest of this paper is outlined below. In Sec. II we provide a formulation of our generalized Anderson model with an interacting QD, separate the screening channel from the non-screening ones, and discuss the effective Kondo model in the local moment regime. In Sec. III the linear DC conductance is calculated using Kubo formula. Disconnected and connected contributions are examined separately, along with the approximate elimination of the latter. Perturbation theories in the weak-coupling and Fermi liquid regimes are employed in Sec. IV; weak-coupling results applicable at high temperatures formally resemble the short ring case. Sec. V applies the abstract formalism to the closed long ring, and Sec. VI studies open long rings and their potential utilization as two-path interferometers. Conclusions and open questions are presented in Sec. VII. In Appendix A, we make contact with early results by applying our formalism in a few other mesoscopic systems. Appendix B consists of details related to the calculation of disconnected contributions. Appendix C is a check of our formalism in the case of a non-interacting QD. Finally, in Appendix D, we perform another consistency check on our scheme of eliminating the connected contribution by calculating it explicitly in the Fermi liquid regime.

II. MODEL

Our generalized tight-binding Anderson model describes N Fermi liquid leads meeting at a junction containing a QD with an on-site Coulomb repulsion. In addition to the QD, the junction comprises an arbitrary configuration of non-interacting tight-binding sites. The full Hamiltonian contains a non-interacting part, a QD part, and a coupling term between the two:

$$H = H_0 + H_T + H_d. \tag{2.1a}$$

The non-interacting part is made up of two terms,

$$H_0 = H_{0,\text{leads}} + H_{0,\text{junction}}; \tag{2.1b}$$

the lead term

$$H_{0,\text{leads}} = -t \sum_{j=1}^{N} \sum_{n=0}^{\infty} \left(c_{j,n}^\dagger c_{j,n+1} + \text{h.c.} \right) \tag{2.1c}$$

models the Fermi liquid leads as semi-infinite nearest-neighbor tight-binding chains with hopping t, where j is the lead index and n is the site index. For simplicity all leads are assumed to be identical, and we temporarily suppress the spin index. $H_{0,\text{junction}}$ is the non-interacting part of the junction; it glues all leads together and often includes additional sites (e.g. representing the arms of an ABK ring), but does not include coupling to the interacting QD. In a typical open ABK ring with electron leakage, two of the leads serve as source and drain electrodes, while the remaining $N-2$ leads mimic the base contacts thorough which electrons escape the junction. In experiments usually the current flowing through the source or the drain is monitored, but the leakage current can also be measured.

Assume that there are M sites in the junction to which the QD is directly coupled; hereafter we refer to these sites as the coupling sites. The coupling to the QD can be written as

$$H_T = -\sum_{r=1}^{M} \left(t_r c_{C,r}^\dagger d + \text{h.c.} \right) \tag{2.1d}$$

where d annihilates an electron on the QD, and $c_{C,r}^\dagger$ creates an electron on the rth coupling site. $c_{C,r}$ may coincide with $c_{j,0}$. In the simplest AB ring, there is only one physical AB phase, which may be incorporated in either $H_{0,\text{junction}}$ or H_T. In more complicated models both $H_{0,\text{junction}}$ and H_T can depend on AB phases.

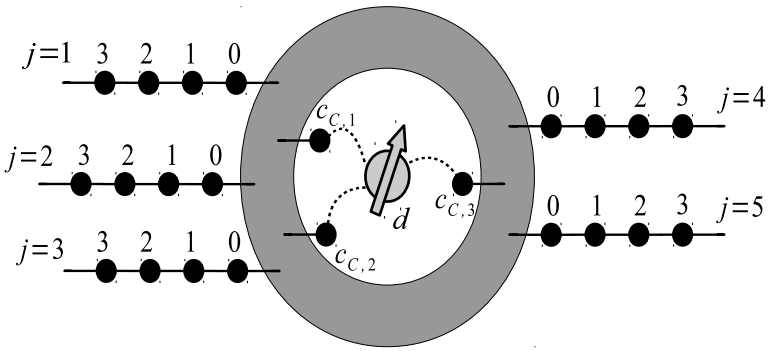

FIG. 1. Sketch of a generic system which allows the application of our formalism. Here $N = 5$ and $M = 3$.

Finally, the Hamiltonian of the interacting QD is given by

$$H_d = \epsilon_d d^\dagger d + U n_{d\uparrow} n_{d\downarrow} \tag{2.1e}$$

where $n_{d\sigma} = d_\sigma^\dagger d_\sigma$. We assume $SU(2)$ spin symmetry throughout the paper.

A generic system with $N = 5$ and $M = 3$ is sketched in Fig. 1, with details of the mesoscopic junction hidden. We will analyze more concrete examples in Secs. V and VI; additional examples, previously studied in Refs. 15, 26, and 30, are provided in Appendix A.

A. Screening and non-screening channels

While it is $H_{0,\text{junction}}$ that ultimately determines the properties of the junction, its details are actually not important in our formalism. Instead, in the following we characterize the model by its background scattering S-matrix and coupling site wave functions. Both quantities are easily obtained from a given $H_{0,\text{junction}}$, and as we show in Sec. III, they play a central role in our quest for the linear DC conductance.

To recast our model into the standard form of an interacting QD coupled to a continuum of states, it is convenient to first diagonalize the non-interacting part of the Hamiltonian H_0 by introducing the scattering basis $q_{j,k}$:

$$H_0 = \int_0^\pi \frac{dk}{2\pi} \sum_{j=1}^{N} \epsilon_k q_{j,k}^\dagger q_{j,k}, \tag{2.2}$$

where $\epsilon_k = -2t\cos k$ is the dispersion relation in the leads, and for simplicity we let the lattice constant $a = 1$. In addition to the scattering states $q_{j,k}$, there may exist a number of bound states with their energies outside of the continuum, but since their wave functions decay exponentially away from the junction region, they do not affect linear DC transport properties.

The scattering basis operator $q_{j,k}$ annihilates a scattering state electron incident from lead j with momentum k, and obeys the anti-commutation relation $\left\{q_{j,k}, q_{j',k'}^\dagger\right\} = 2\pi\delta_{jj'}\delta(k-k')$. The corresponding wave function has the following form on site n in lead j',

$$\chi_{j,k}(j', n) = \delta_{jj'} e^{-ikn} + S_{j'j}(k) e^{ikn}; \tag{2.3a}$$

and on coupling site r,

$$\chi_{j,k}(r) = \Gamma_{rj}(k). \tag{2.3b}$$

In other words, for an electron incident from lead j, $S_{j'j}$ is the background reflection or transmission amplitude in lead j', and Γ_{rj} is the wave function on coupling site r. The scattering S-matrix S is unitary: $S^\dagger S = 1$.

From its wave function, $q_{j,k}$ can be related to $c_{j,n}$ and $c_{C,r}$:

$$c_{j,n} = \int_0^\pi \frac{dk}{2\pi} \sum_{j'=1}^{N} \left[\delta_{jj'} e^{-ikn} + S_{jj'}(k) e^{ikn}\right] q_{j',k}, \tag{2.4a}$$

and

$$c_{C,r} = \int_0^\pi \frac{dk}{2\pi} \sum_{j'=1}^{N} \Gamma_{rj'}(k) q_{j',k}. \tag{2.4b}$$

We now express H_T in the scattering basis. Inserting Eq. (2.4b) into Eq. (2.1d), we find the QD is only coupled to one channel in the continuum, i.e. the screening channel:

$$H_T = -\int_0^\pi \frac{dk}{2\pi} V_k \left(\psi_k^\dagger d + \text{h.c.}\right), \tag{2.5}$$

where the screening channel operator $\psi_k^\dagger$ is defined by

$$\psi_k^\dagger = \frac{1}{V_k} \sum_{j=1}^{N} \sum_{r=1}^{M} t_r \Gamma_{r,j}^*(k) q_{j,k}^\dagger, \tag{2.6}$$

and the normalization factor $V_k > 0$ is defined by

$$V_k^2 = \sum_{j=1}^{N} \sum_{r,r'=1}^{M} t_r t_{r'}^* \Gamma_{rj}^*(k) \Gamma_{r'j}(k) = \text{tr}\left[\Gamma^\dagger(k) \lambda \Gamma(k)\right]. \tag{2.7}$$

This ensures $\left\{\psi_k, \psi_{k'}^\dagger\right\} = 2\pi\delta(k-k')$. Here we also introduce the $M \times M$ Hermitian QD coupling matrix λ,

$$\lambda_{rr'} = t_r t_{r'}^*. \tag{2.8}$$

It will be useful to define a series of non-screening channels $\phi_{l,k}$ orthogonal to ψ, where $l = 1, \cdots, N-1$. The ϕ channels are decoupled from the QD. In a compact notation we can write the transformation from the scattering basis to the screening–non-screening basis as

$$\Psi_k \equiv \begin{pmatrix} \psi_k \\ \phi_{1,k} \\ \cdots \\ \phi_{N-1,k} \end{pmatrix} = \mathbb{U}_k \begin{pmatrix} q_{1,k} \\ q_{2,k} \\ \cdots \\ q_{N,k} \end{pmatrix}, \tag{2.9}$$

where $\mathbb{U}$ is a unitary matrix. The first row of $\mathbb{U}$ is known:

$$\mathbb{U}_{1,j,k} = \frac{1}{V_k} \sum_{r=1}^{M} t_r^* \Gamma_{rj}(k). \tag{2.10}$$

As long as $\mathbb{U}$ stays unitary, its remaining matrix elements can be chosen freely without affecting physical observables. Ψ_k now also diagonalizes H_0,

$$H_0 = \int_0^\pi \frac{dk}{2\pi} \epsilon_k \left(\psi_k^\dagger \psi_k + \sum_{l=1}^{N-1} \phi_{l,k}^\dagger \phi_{l,k}\right); \tag{2.11}$$

we shall also need the inverse transformation,

$$q_{j,k} = \mathbb{U}^*_{1,j,k}\psi_k + \sum_{l=1}^{N-1} \mathbb{U}^*_{l+1,j,k}\phi_{l,k}. \tag{2.12}$$

B. Kondo model

In the local moment regime of the Anderson model,[1,2] we can perform the Schrieffer-Wolff transformation[43] on ψ to obtain an effective Kondo model with a reduced bandwidth and a momentum-dependent coupling:

$$H = H_0 + \int \frac{dkdk'}{(2\pi)^2} \left(J_{kk'}\psi^\dagger_k \frac{\vec{\sigma}}{2}\psi_{k'} \cdot \vec{S}_d + K_{kk'}\psi^\dagger_k\psi_{k'} \right), \tag{2.13a}$$

where all momenta are between $k_F - \Lambda_0$ and $k_F + \Lambda_0$ with Fermi wave vector k_F, $0 < \Lambda_0 \ll k_F$ is the initial momentum cutoff, and the dispersion is linearized near the Fermi energy as $\epsilon_k = v_F\,(k - k_F)$. For the tight-binding model $v_F = 2t \sin k_F$.

The interaction consists of a spin-flip term J,

$$J_{kk'} = V_k V_{k'}\,(j_k + j_{k'})\,, \tag{2.13b}$$

$$j_k = \frac{1}{\epsilon_k - \epsilon_d} + \frac{1}{U + \epsilon_d - \epsilon_k} \approx j, \tag{2.13c}$$

and a particle-hole symmetry breaking potential scattering term K,

$$K_{kk'} = \frac{1}{4} V_k V_{k'}\,(\kappa_k + \kappa_{k'})\,, \tag{2.13d}$$

$$\kappa_k = \frac{1}{\epsilon_k - \epsilon_d} - \frac{1}{U + \epsilon_d - \epsilon_k} \approx \kappa. \tag{2.13e}$$

The energy cutoff is initially $D_0 \equiv v_F\Lambda_0$. When we reduce the running energy cutoff from D to $D+dD$ ($0 < -dD \ll D$) to integrate out the high-energy degrees of freedom in the narrow strips of energy $(-D, -D - dD)$ and $(D + dD, D)$, K is exactly marginal in the renormalization group (RG) sense, whereas J is marginally relevant and obeys the following RG equation:

$$-\frac{d\,(\nu J_{kk'})}{d\ln D} = \frac{1}{2}\left(\nu J_{k,k_F+\Lambda}\nu J_{k_F+\Lambda,k'} + \nu J_{k,k_F-\Lambda}\nu J_{k_F-\Lambda,k'}\right), \tag{2.14}$$

or equivalently

$$-\frac{dj}{d\ln D} = \nu j^2 \left(V^2_{k_F+\Lambda} + V^2_{k_F-\Lambda}\right), \tag{2.15}$$

where ν is the density of states per channel per spin, $\nu = 1/(2\pi v_F)$. Therefore, renormalization of the Kondo coupling is controlled by the momentum-dependent normalization factor V_k^2, defined in Eq. (2.7). j is the only truly independently renormalized coupling constant despite the appearance of Eq. (2.14); this follows from the fact that the screening channel is the only channel coupled to the QD.[15]

The prototype Kondo model possesses a momentum-independent coupling function, $J_{kk'} \approx 2jV^2_{k_F}$. As a result, spin-charge separation occurs and the Kondo interaction is found to be exclusively in the spin sector.[44] The charge sector is nothing but a non-interacting theory with a particle-hole symmetry breaking phase shift due to the potential

scattering term K, while at very low energy scales the spin sector renormalizes to a local Fermi liquid theory with $\pi/2$ phase shift.

On the other hand, in a mesoscopic geometry V_k^2 often exhibit fluctuations on a mesoscopic energy scale E_V. (More precisely, E_V can be defined as the energy corresponding to the largest Fourier component in the spectrum of V_k^2.) In the presence of a characteristic length scale L, E_V may be of the order of the Thouless energy v_F/L; however this is not necessarily the case, with a counterexample provided by the open long ABK ring in Sec. VI where E_V is of the order of the bandwidth $4t$.Well above E_V, V_k^2 appears featureless and can be approximated by its mean value $\overline{V_k^2}$ with respect to k. The Kondo temperature T_K can be loosely defined as the energy cutoff at which the dimensionless coupling $2\nu j\overline{V_k^2}$ becomes $O(1)$. As briefly sketched in Sec. I, there are two very different parameter regimes of the Kondo temperature:[15,24]

a) The small Kondo cloud regime $T_K \gg E_V$. For $E_V \sim v_F/L$, the size of the Kondo screening cloud $L_K \equiv v_F/T_K \ll L$; hence the name. In this regime, the bare Kondo coupling is sufficiently large, so that $2\nu j\overline{V_k^2}$ renormalizes to $O(1)$ before it "senses" any mesoscopic fluctuation. By approximating $V_k^2 \approx \overline{V_k^2}$, Eq. (2.15) has a solution

$$j(D) \approx \frac{j_0}{1 + 2\nu j_0 \overline{V_k^2} \ln \frac{D}{D_0}}, \tag{2.16}$$

where j_0 is the bare Kondo coupling constant at the initial energy cutoff D_0. Eq. (2.16) gives the "background" Kondo temperature

$$T_K \approx T_K^0 \equiv D_0 \exp\left(-\frac{1}{2\nu j_0 \overline{V_k^2}}\right), \tag{2.17}$$

independent of the mesoscopic details of the geometry. For $T \ll T_K$, the low-energy effective theory is also conjectured to be a Fermi liquid, but the T-matrix (or the phase shift) of the screening channel is not yet known with certainty.[15,22]

b) The very large Kondo cloud regime $T_K \ll E_V$. For $E_V \sim v_F/L$, $L_K \gg L$. In this regime, the bare Kondo coupling is very small, and j does not begin to renormalize significantly until the energy cutoff is well below E_V. The variation of V_k^2 is hence negligible in the resulting low energy theory, $V_k^2 \approx V_{k_F}^2$, but $V_{k_F}^2$ may be significantly different from $\overline{V_k^2}$. The Kondo temperature is thus highly sensitive to the mesoscopic details of $V_{k_F}^2$, and the low-energy effective theory is another local Fermi liquid theory, with parameters also sensitive to the mesoscopic details.

III. LINEAR DC CONDUCTANCE

In this section we calculate the DC conductance tensor of the system in linear response theory, generalizing the results in Ref. 26 to our multi-terminal setup. The result is presented as the sum of a disconnected contribution and a connected one (Fig. 2). By "disconnected" and "connected", we are referring to the topology of the corresponding Feynman diagrams: a disconnected contribution originates from a Feynman diagram without any cross-links, and can always be written as the product of two two-point functions. The disconnected contribution has a simple Landauer form, and is quadratic in the T-matrix of the screening channel ψ. The connected contribution is also shown to depend on properties near the Fermi surface only, but it is usually difficult to evaluate analytically except at high temperatures, or at low temperatures if the Fermi-liquid perturbation theory is applicable. Nevertheless, just as with the short ABK ring, the connected contribution can be approximately eliminated at temperatures low compared to another mesoscopic energy scale $T \ll E_{\text{conn}}$.

A. Kubo formula in terms of screening and non-screening channels

The linear DC conductance tensor $G_{jj'}$ is defined through $\langle I_j \rangle = \sum_{j'} G_{jj'} V_{j'}$, where I_j is the current operator in lead j, and $V_{j'}$ is the applied bias voltage on lead j'. I_j is given by $I_j = -ed N_j/d\bar{t}$, where $\bar{t}$ is the real time variable, and

$$N_j \equiv \sum_{n=0}^{\infty} c_{j,n}^\dagger c_{j,n} \tag{3.1}$$

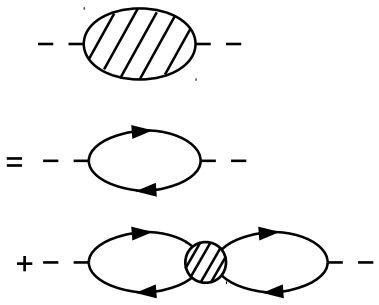

FIG. 2. Disconnected and connected contributions to the density-density correlation function. All Ψ fermion propagators are fully dressed.

is the density operator in lead j. $G_{jj'}$ is then given by the Kubo formula

$$G_{jj'} = \frac{e^2}{h} \lim_{\Omega \to 0} (2\pi i \Omega) \, G'_{jj'} (\Omega) \,, \tag{3.2}$$

where the retarded density-density correlation function is

$$G'_{jj'} (\Omega) \equiv -i \int_0^\infty d\bar{t} e^{i\Omega^+ \bar{t}} \left\langle \left[N_j (\bar{t}) \,, N_{j'} (0) \right] \right\rangle \tag{3.3}$$

and $\Omega^+ \equiv \Omega + i0^+$. The retarded correlation function can be obtained by means of analytic continuation $i\omega_p \to \Omega^+$ from its imaginary time counterpart,

$$\mathcal{G}'_{jj'} (i\omega_p) = - \int_0^\beta d\tau e^{i\omega_p \tau} \left\langle T_\tau N_j (\tau) \, N_{j'} (0) \right\rangle , \tag{3.4}$$

where $\omega_p = 2p\pi/\beta$ is a Matsubara frequency, $\beta = 1/T$ is the inverse temperature, and T_τ is the imaginary time-ordering operator.

To calculate the correlation function we need the density operator N_j written as bilinears of Ψ. This is achieved by the insertion of Eq. (2.4a) and then Eq. (2.12) into Eq. (3.1). We find

$$N_j = \int_0^\pi \frac{dk_1 dk_2}{(2\pi)^2} \Psi^\dagger_{k_1} \mathbb{M}^j_{k_1 k_2} \Psi_{k_2}, \tag{3.5}$$

where for l_1, $l_2 = 1$, ..., N,

$$\begin{aligned} \left(\mathbb{M}^j_{k_1 k_2} \right)_{l_1 l_2} = \sum_{j_1 j_2} \mathbb{U}_{l_1, j_1, k_1} \mathbb{U}^*_{l_2, j_2, k_2} \Bigg[& \delta_{jj_1} \delta_{jj_2} \frac{1}{1 - e^{i(k_1 - k_2 + i0)}} + S^*_{jj_1} (k_1) \, \delta_{jj_2} \frac{1}{1 - e^{-i(k_1 + k_2 - i0)}} \\ & + \delta_{jj_1} S_{jj_2} (k_2) \frac{1}{1 - e^{i(k_1 + k_2 + i0)}} + S^*_{jj_1} (k_1) \, S_{jj_2} (k_2) \frac{1}{1 - e^{i(k_2 - k_1 + i0)}} \Bigg] . \end{aligned} \tag{3.6}$$

The matrix $\mathbb{M}$ obeys $\mathbb{M}^j_{k_1 k_2} = \left(\mathbb{M}^j_{k_2 k_1} \right)^\dagger$ which ensures N_j is Hermitian.

B. Disconnected part

We substitute Eq. (3.5) into Eq. (3.3). The disconnected part of the conductance is obtained by pairing up Ψ and $\Psi^\dagger$ operators to form two two-point Green's functions:

$$G'^{D}_{jj'}(\Omega) = -2i\int_0^\infty d\bar{t}e^{i\Omega^+\bar{t}}\int_0^\pi \frac{dk_1dk_2}{(2\pi)^2}\frac{dq_1dq_2}{(2\pi)^2}\,\mathrm{tr}\left[\mathbb{M}^{j}_{k_1k_2}\mathbb{G}^{>}_{k_2q_1}(\bar{t})\,\mathbb{M}^{j'}_{q_1q_2}\mathbb{G}^{<}_{q_2k_1}(-\bar{t}) - \mathbb{M}^{j'}_{q_1q_2}\mathbb{G}^{>}_{q_2k_1}(-\bar{t})\,\mathbb{M}^{j}_{k_1k_2}\mathbb{G}^{<}_{k_2q_1}(\bar{t})\right]. \tag{3.7}$$

Here the factor of 2 in the second line is due to the spin degeneracy. The greater and lesser Green's functions in the screening–non-screening basis are defined as

$$\mathbb{G}^{>}_{kq}(\bar{t}) \equiv -i\begin{pmatrix} \left\langle \psi_k(\bar{t})\,\psi^\dagger_q(0)\right\rangle & & & \\ & \left\langle \phi_{1,k}(\bar{t})\,\phi^\dagger_{1,q}(0)\right\rangle & & \\ & & \cdots & \\ & & & \left\langle \phi_{N-1,k}(\bar{t})\,\phi^\dagger_{N-1,q}(0)\right\rangle \end{pmatrix}, \tag{3.8a}$$

and

$$\mathbb{G}^{<}_{kq}(\bar{t}) \equiv +i\begin{pmatrix} \left\langle \psi^\dagger_q(0)\,\psi_k(\bar{t})\right\rangle & & & \\ & \left\langle \phi^\dagger_{1,q}(0)\,\phi_{1,k}(\bar{t})\right\rangle & & \\ & & \cdots & \\ & & & \left\langle \phi^\dagger_{N-1,q}(0)\,\phi_{N-1,k}(\bar{t})\right\rangle \end{pmatrix}. \tag{3.8b}$$

In equilibrium, fluctuation-dissipation theorem requires that $\mathbb{G}^{>}_{kq}(\omega) = 2i\left[1-f(\omega)\right]\mathrm{Im}\,\mathbb{G}^{R}_{kq}(\omega)$, and $\mathbb{G}^{<}_{kq}(\omega) = -2if(\omega)\,\mathrm{Im}\,\mathbb{G}^{R}_{kq}(\omega)$, where $f(\omega) = 1/\left(e^{\beta\omega}+1\right)$ is the Fermi function. These equilibrium relations result from the fact that $\mathbb{G}^{R}_{kq}(\omega) = \mathbb{G}^{R}_{qk}(\omega)$ for the Anderson model [see Eq. (3.12) below].[26] With these relations Eq. (3.7) becomes

$$G'^{D}_{jj'}(\Omega) = 8\int\frac{d\omega d\omega'}{(2\pi)^2}\frac{f(\omega)-f(\omega')}{\omega-\omega'+\Omega^+}\int_0^\pi\frac{dk_1dk_2}{(2\pi)^2}\frac{dq_1dq_2}{(2\pi)^2}\,\mathrm{tr}\left[\mathbb{M}^{j}_{k_1k_2}\,\mathrm{Im}\,\mathbb{G}^{R}_{k_2q_1}(\omega')\,\mathbb{M}^{j'}_{q_1q_2}\,\mathrm{Im}\,\mathbb{G}^{R}_{q_2k_1}(\omega)\right]. \tag{3.9}$$

We note that, in contrast to the case of Ref. 26, the momentum integral here is not necessarily real. Instead, its complex conjugate takes the same form but with ω and ω' interchanged:

$$\begin{aligned}&\int_0^\pi\frac{dk_1dk_2}{(2\pi)^2}\frac{dq_1dq_2}{(2\pi)^2}\,\mathrm{tr}\left[\mathbb{M}^{j}_{k_1k_2}\,\mathrm{Im}\,\mathbb{G}^{R}_{k_2q_1}(\omega')\,\mathbb{M}^{j'}_{q_1q_2}\,\mathrm{Im}\,\mathbb{G}^{R}_{q_2k_1}(\omega)\right]^*\\ &=\int_0^\pi\frac{dk_1dk_2}{(2\pi)^2}\frac{dq_1dq_2}{(2\pi)^2}\,\mathrm{tr}\left[\mathbb{M}^{j}_{k_1k_2}\,\mathrm{Im}\,\mathbb{G}^{R}_{k_2q_1}(\omega)\,\mathbb{M}^{j'}_{q_1q_2}\,\mathrm{Im}\,\mathbb{G}^{R}_{q_2k_1}(\omega')\right].\end{aligned} \tag{3.10}$$

Making use of this property, we can show that $\left[G'^{D}_{jj'}(-\Omega)\right]^* = G'^{D}_{jj'}(\Omega)$. Thus the disconnected contribution to the DC conductance can be written as

$$G^{D}_{jj'} = \frac{e^2}{h}\lim_{\Omega\to0}(-2\pi\Omega)\,\mathrm{Im}\,G'^{D}_{jj'}(\Omega). \tag{3.11}$$

We should realize, however, that taking the imaginary part of $G'^{D}_{jj'}$ is generally not equivalent to taking the δ-function part of $1/(\omega-\omega'+\Omega^+)$ in Eq. (3.9).

For the Anderson model, it is not difficult to find the Dyson's equation for the retarded Green's function by the equation-of-motion technique:

$$\mathbb{G}^{R}_{k_2q_1}(\omega) = 2\pi\delta(k_2-q_1)\,g^{R}_{k_2}(\omega) + \tau_\psi g^{R}_{k_2}(\omega)\,\mathrm{T}_{k_2q_1}(\omega)\,g^{R}_{q_1}(\omega), \tag{3.12}$$

where the free retarded Green's function for ψ and ϕ is

$$g^{R}_{k}(\omega) = \frac{1}{\omega^+-\epsilon_k}, \tag{3.13}$$

and τ_ψ is the projection operator onto the screening channel subspace. Again, only the Green's function of the screening channel is modified by coupling to the QD. The retarded T-matrix of the screening channel is related to the retarded two-point function of the QD by

$$\mathrm{T}_{k_2 q_1}(\omega) = V_{k_2} G^R_{dd}(\omega) V_{q_1}, \tag{3.14}$$

where $G^R_{dd}(\omega) \equiv -i\int_0^\infty d\bar{t} e^{i\omega^+\bar{t}} \left\langle \left\{ d(\bar{t}), d^\dagger(0) \right\} \right\rangle$.

From Eqs. (3.9) and (3.12) we may express the disconnected contribution to the linear DC conductance in the Landauer form:

$$G^D_{jj'} = \frac{2e^2}{h} \int_{-2t}^{2t} d\epsilon_p \left[-f'(\epsilon_p) \right] \mathcal{T}^D_{jj'}(\epsilon_p), \tag{3.15}$$

where the disconnected "transmission probability" $\mathcal{T}^D_{jj'}$ is written in terms of the absolute square of a "transmission amplitude",

$$\begin{aligned} \mathcal{T}^D_{jj'}(\epsilon_p) &= \delta_{jj'} - \left| \left\{ S(p) \left[1 - 2i\pi\nu_p \mathrm{T}_{pp}(\epsilon_p) \mathbb{U}^\dagger_p \tau_\psi \mathbb{U}_p \right] \right\}_{jj'} \right|^2 \\ &= \delta_{jj'} - \left| S_{jj'}(p) + \frac{2i}{V_p^2} \left[S(p) \Gamma^\dagger(p) \lambda \Gamma(p) \right]_{jj'} \left[-\pi\nu_p \mathrm{T}_{pp}(\epsilon_p) \right] \right|^2. \end{aligned} \tag{3.16}$$

Again λ is the QD coupling matrix defined in Eq. (2.8) and ν_p is the density of states per channel per spin for the tight-binding model

$$\nu_p = \frac{1}{4\pi t \sin p}. \tag{3.17}$$

The detailed derivation of Eq. (3.16) by contour methods is left for Appendix B. As a consistency check, we show in Appendix C that for a non-interacting QD, $U = 0$, Eq. (3.16) and solving the Schroedinger's equation yield the same transmission probability.

At zero temperature, when the screening channel T-matrix obeys the optical theorem and the inelastic part of the T-matrix vanishes,[6] there is no connected contribution and Eq. (3.15) yields the full linear DC conductance.[26] In this case a clear picture emerges from Eq. (3.16): the conductance is given by the Landauer formula with an effective single-particle S-matrix, which is obtained from the original S-matrix simply by imposing a phase shift on the screening channel, corresponding to the particle-hole symmetry breaking potential scattering and the elastic scattering by the Kondo singlet.[30,45]

Another useful representation of the disconnected probability, similar to that in Ref. 26, is obtained by expanding Eq. (3.16):

$$\begin{aligned} \mathcal{T}^D_{jj'}(\epsilon_p) = \mathcal{T}_{0,jj'}(\epsilon_p) &+ \mathcal{Z}_{R,jj'}(\epsilon_p) \mathrm{Re}\left[-\pi\nu_p \mathrm{T}_{pp}(\epsilon_p) \right] \\ &+ \mathcal{Z}_{I,jj'}(\epsilon_p) \mathrm{Im}\left[-\pi\nu_p \mathrm{T}_{pp}(\epsilon_p) \right] + \mathcal{Z}_{2,jj'}(\epsilon_p) \left| -\pi\nu_p \mathrm{T}_{pp}(\epsilon_p) \right|^2, \end{aligned} \tag{3.18a}$$

with a background transmission term

$$\mathcal{T}_{0,jj'}(\epsilon_p) = \delta_{jj'} - \left| S_{jj'}(p) \right|^2, \tag{3.18b}$$

a term linear in the real part of the T-matrix, proportional to

$$\mathcal{Z}_{R,jj'}(\epsilon_p) = \frac{4}{V_p^2} \mathrm{Im}\left\{ \left[S(p) \Gamma^\dagger(p) \lambda \Gamma(p) \right]_{jj'} S^*_{jj'}(p) \right\}, \tag{3.18c}$$

a term linear in the imaginary part, proportional to

$$\mathcal{Z}_{I,jj'}(\epsilon_p) = \frac{4}{V_p^2}\,\mathrm{Re}\left\{\left[S(p)\,\Gamma^\dagger(p)\,\lambda\Gamma(p)\right]_{jj'} S^*_{jj'}(p)\right\}, \tag{3.18d}$$

and a term quadratic in the T-matrix, proportional to

$$\mathcal{Z}_{2,jj'}(\epsilon_p) = -\frac{4}{V_p^4}\left|\left[S(p)\,\Gamma^\dagger(p)\,\lambda\Gamma(p)\right]_{jj'}\right|^2. \tag{3.18e}$$

In the DC limit, the total current flowing out of the junction is zero, and a uniform voltage applied to all leads does not result in any current; hence the linear DC conductance satisfies current and voltage Kirchhoff's laws $\sum_j G_{jj'} = \sum_{j'} G_{jj'} = 0$. As a comparison it is interesting to consider the sum of the disconnected transmission probability, Eq. (3.18a), over j or j'. Using the unitarity of S and Eq. (2.8) it is not difficult to find that

$$\sum_j \mathcal{T}^D_{jj'}(\epsilon_p) = \left\{\mathrm{Im}\left[-\pi\nu_p \mathrm{T}_{pp}(\epsilon_p)\right] - \left|-\pi\nu_p \mathrm{T}_{pp}(\epsilon_p)\right|^2\right\}\frac{4}{V_p^2}\left[\Gamma^\dagger(p)\,\lambda\Gamma(p)\right]_{j'j'}, \tag{3.19}$$

and

$$\sum_{j'} \mathcal{T}^D_{jj'}(\epsilon_p) = \left\{\mathrm{Im}\left[-\pi\nu_p \mathrm{T}_{pp}(\epsilon_p)\right] - \left|-\pi\nu_p \mathrm{T}_{pp}(\epsilon_p)\right|^2\right\}\frac{4}{V_p^2}\left[S(p)\,\Gamma^\dagger(p)\,\lambda\Gamma(p)\,S^\dagger(p)\right]_{jj}. \tag{3.20}$$

As mentioned in Ref. 26, the quantity in curly brackets in Eqs. (3.19) and (3.20) measures the deviation of the single-particle sector of the T-matrix from the optical theorem.[6] In the case of a non-interacting QD or the $T = 0$ Fermi liquid theory of the Kondo limit, where the connected contribution to the conductance vanishes, these row/column sum formulas conform to our expectations: the T-matrix obeys the optical theorem, leading to $\sum_j \mathcal{T}^D_{jj'} = \sum_{j'} \mathcal{T}^D_{jj'} = 0$, so that $\sum_j G_{jj'} = \sum_{j'} G_{jj'} = 0$ is ensured.

C. Connected part and its low-temperature elimination

In this subsection we show that the connected contribution to the conductance is again a Fermi surface contribution, and discuss how it can be approximately eliminated at low temperatures. Following Ref. 26 we construct a transmission probability for this contribution. After a partial insertion of Eq. (3.5) into Eq. (3.4), the connected part of the density-density correlation function can be written as

$$\mathcal{G}'^C_{jj'}(i\omega_p) = \int_0^\beta d\tau e^{i\omega_p\tau} P_{jj'}(\tau,\tau), \tag{3.21}$$

where the connected four-point function $P_{jj'}$ with two temporal arguments is

$$P_{jj'}(\tau_1,\tau_2) \equiv -\int_0^\pi \frac{dk_1 dk_2}{(2\pi)^2}\left(\mathbb{M}^j_{k_1k_2}\right)_{11}\sum_\sigma\left\langle T_\tau \psi^\dagger_{k_1\sigma}(\tau_1)\,\psi_{k_2\sigma}(\tau_2)\,N_{j'}(0)\right\rangle_C; \tag{3.22}$$

the subscript C denotes connected diagrams. Note that only the screening channel contributes to the connected part, as the non-screening channels are free fermions. Using the equation-of-motion technique, it is easy to relate $P_{jj'}$ to a partially amputated quantity:

$$P_{jj'}(\tau,\tau) = \int_0^\pi \frac{dk_1 dk_2}{(2\pi)^2}\left(\mathbb{M}^j_{k_1k_2}\right)_{11} V_{k_1}V_{k_2}\int d\tau_1 d\tau_2 g_{k_1}(\tau_1-\tau)\,g_{k_2}(\tau-\tau_2)\sum_\sigma\left\langle T_\tau d^\dagger_\sigma(\tau_1)\,d_\sigma(\tau_2)\,N_{j'}(0)\right\rangle_C, \tag{3.23}$$

where

$$g_k(\tau) \equiv [f(\tau) - \theta(\tau)] e^{-\epsilon_k \tau} \tag{3.24}$$

is the imaginary time free Green's function and $\theta(\tau)$ is the Heaviside unit-step function. With τ only appearing in free propagators, we can perform the Fourier transform explicitly,

$$\begin{aligned}
\mathcal{G}'^{C}_{jj'}(i\omega_p) &= \frac{1}{\beta}\sum_{\omega_m} P_{jj'}(i\omega_m, i\omega_m + i\omega_p) \\
&= \frac{1}{\beta}\sum_{\omega_m}\int_0^\pi \frac{dk_1 dk_2}{(2\pi)^2}\left(\mathbb{M}^j_{k_1k_2}\right)_{11} g_{k_1}(i\omega_m)\, g_{k_2}(i\omega_m + i\omega_p)\, V_{k_1} V_{k_2} \\
&\times \int d\tau_1 d\tau_2 e^{-i\omega_m\tau_1} e^{i(\omega_m+\omega_p)\tau_2} \sum_\sigma \left\langle T_\tau d^\dagger_\sigma(\tau_1)\, d_\sigma(\tau_2)\, N_{j'}(0)\right\rangle_C .
\end{aligned} \tag{3.25}$$

One may now use the contour integration argument in Ref. 26.[46] The final result is that the connected contribution to the DC conductance is expressed in terms of a transmission probability $\mathcal{T}^C$ related to $P_{jj'}$:

$$G^C_{jj'} = \frac{2e^2}{h}\int_{-2t}^{2t} d\omega\, [-f'(\omega)]\, \mathcal{T}^C_{jj'}(\omega), \tag{3.26}$$

where

$$\mathcal{T}^C_{jj'}(\omega) = \lim_{\Omega\to 0}\frac{\Omega^2}{8} P_{jj'}(\omega - i\eta_1, \omega + \Omega + i\eta_2) + \text{c.c.} \tag{3.27}$$

and

$$\begin{aligned}
&P_{jj'}(\omega - i\eta_1, \omega + \Omega + i\eta_2) \\
&= \int_0^\pi \frac{dk_1 dk_2}{(2\pi)^2}\left(\mathbb{M}^j_{k_1k_2}\right)_{11} g^A_{k_1}(\omega)\, g^R_{k_2}(\omega+\Omega)\, V_{k_1} V_{k_2} \int d\tau_1 d\tau_2 e^{-i\omega^-\tau_1} e^{i\left(\omega^+ + \Omega\right)\tau_2} \sum_\sigma \left\langle T_\tau d^\dagger_\sigma(\tau_1)\, d_\sigma(\tau_2)\, N_{j'}(0)\right\rangle_C .
\end{aligned} \tag{3.28}$$

It is in fact possible to do the k_1 and k_2 integrals. Using Eqs. (2.10), (3.6) and finally (B6), we obtain

$$\begin{aligned}
&\int_0^\pi \frac{dk_1 dk_2}{(2\pi)^2}\left(\mathbb{M}^j_{k_1k_2}\right)_{11} g^A_{k_1}(\epsilon_p)\, g^R_{k_2}(\epsilon_p+\Omega)\, V_{k_1} V_{k_2} \\
&= \sum_{r_1 r_2} t^*_{r_1} t_{r_2}\int_{-\pi}^\pi \frac{dk_1 dk_2}{(2\pi)^2} g^A_{k_1}(\epsilon_p)\, g^R_{k_2}(\epsilon_p+\Omega)\, \Gamma_{r_1 j}(k_1)\, \Gamma^*_{r_2 j}(k_2)\, \frac{1}{1 - e^{i(k_1 - k_2 + i0)}}.
\end{aligned} \tag{3.29}$$

Here domains of the momentum integrals are extended to $(-\pi, \pi)$ according to Eq. (B6), which facilitates the application of the residue method. As explained in Appendix B, the poles of $\Gamma(k_1)$ and $\Gamma^*(k_2)$ are not important in the DC limit $\Omega \to 0$. Therefore, the $O(1/\Omega)$ contribution is dominated by the poles of the free Green's functions, and is given by

$$\int_0^\pi \frac{dk_1 dk_2}{(2\pi)^2}\left(\mathbb{M}^j_{k_1k_2}\right)_{11} g^A_{k_1}(\epsilon_p)\, g^R_{k_2}(\epsilon_p+\Omega)\, V_{k_1} V_{k_2} = \frac{2\pi i}{\Omega}\nu_p \left[S(p')\,\Gamma^\dagger(p')\,\lambda\Gamma(p)\, S^\dagger(p)\right]_{jj} + O(1). \tag{3.30}$$

where $\epsilon_p + \Omega \equiv \epsilon_{p'}$, $0 \le p, p' \le \pi$. This leads to

$$\mathcal{T}^C_{jj'}(\epsilon_p) = \nu_p \left[S(p)\,\Gamma^\dagger(p)\,\lambda\Gamma(p)\, S^\dagger(p)\right]_{jj}\left[\frac{i\pi}{4}\lim_{\Omega\to 0}\Omega\int d\tau_1 d\tau_2 e^{-i\omega^-\tau_1} e^{i\left(\omega^+ + \Omega\right)\tau_2}\sum_\sigma \left\langle T_\tau d^\dagger_\sigma(\tau_1)\, d_\sigma(\tau_2)\, N_{j'}(0)\right\rangle_C + \text{c.c.}\right]. \tag{3.31}$$

A similar manipulation can be done for the $N_{j'}$ part of the correlation function.

One can again consider the row and column sums of the tensor $\mathcal{T}^C$. Tracing over j immediately yields

$$\sum_j \mathcal{T}^C_{jj'}(\epsilon_p) = \nu_p V_p^2 \left[\frac{i\pi}{4} \lim_{\Omega\to 0} \Omega \int d\tau_1 d\tau_2 e^{-i\omega^- \tau_1} e^{i(\omega^+ + \Omega)\tau_2} \sum_\sigma \left\langle T_\tau d^\dagger_\sigma(\tau_1)\, d_\sigma(\tau_2)\, N_{j'}(0)\right\rangle_C + \text{c.c.} \right]; \tag{3.32}$$

combining the last two equations, we have

$$\mathcal{T}^C_{jj'}(\epsilon_p) - \frac{1}{V_p^2}\left[S(p)\,\Gamma^\dagger(p)\,\lambda\Gamma(p)\,S^\dagger(p)\right]_{jj} \sum_{j''} \mathcal{T}^C_{j''j'}(\epsilon_p) = 0. \tag{3.33}$$

Let us now define E_{conn} as the characteristic energy scale below which both $S(p)$ and $\Gamma(p)$ vary slowly. By definition $E_{\text{conn}} \lesssim E_V$; while E_{conn} is not necessarily the same as E_V, for the two ABK ring geometries considered in this paper $E_V \sim E_{\text{conn}}$. For a mesoscopic structure with characteristic length scale L, E_{conn} is usually the Thouless energy, $E_{\text{conn}} \sim v_F/L$; however, this is again not always the case, and the open long ABK ring in Sec. VI provides a counterexample where E_{conn} is comparable to the bandwidth. Below E_{conn}, the function $\left[S(p)\,\Gamma^\dagger(p)\,\lambda\Gamma(p)\,S^\dagger(p)\right]_{jj}/V_p^2$ is only weakly dependent on p.

Eq. (3.33) suggests that we can approximately eliminate the connected part of $G_{jj'}$, provided the temperature is low compared to E_{conn}.[26] Consider the linear combination

$$G_{jj'} - \frac{1}{V_{k_F}^2}\left[S(k_F)\,\Gamma^\dagger(k_F)\,\lambda\Gamma(k_F)\,S^\dagger(k_F)\right]_{jj} \sum_{j''} G_{j''j'} \equiv G_{jj'}; \tag{3.34}$$

this corresponds to measuring the conductance by measuring the current in lead j, plus a constant times the total current in all leads. By Kirchhoff's law, this linear combination must equal $G_{jj'}$ itself. We write it as a sum of disconnected and connected contributions:

$$\begin{aligned} G_{jj'} = &\left(G^D_{jj'} - \frac{1}{V_{k_F}^2}\left[S(k_F)\,\Gamma^\dagger(k_F)\,\lambda\Gamma(k_F)\,S^\dagger(k_F)\right]_{jj} \sum_{j''} G^D_{j''j'} \right) \\ &+ \int d\epsilon_p \left[-f'(\epsilon_p)\right] \left\{ \mathcal{T}^C_{jj'}(\epsilon_p) - \frac{1}{V_{k_F}^2}\left[S(k_F)\,\Gamma^\dagger(k_F)\,\lambda\Gamma(k_F)\,S^\dagger(k_F)\right]_{jj} \sum_{j''} \mathcal{T}^C_{j''j'}(\epsilon_p) \right\}. \end{aligned} \tag{3.35}$$

For $T \ll E_{\text{conn}}$, by Eq. (3.33), the quantity in curly brackets approximately vanishes for $|\epsilon_p - \epsilon_{k_F}| \lesssim T$, whereas the Fermi factor approximately vanishes for $|\epsilon_p - \epsilon_{k_F}| \gg T$. Therefore

$$G_{jj'} \approx G^D_{jj'} - \frac{1}{V_{k_F}^2}\left[S(k_F)\,\Gamma^\dagger(k_F)\,\lambda\Gamma(k_F)\,S^\dagger(k_F)\right]_{jj} \sum_{j''} G^D_{j''j'}; \tag{3.36}$$

in other words, at $T \ll E_{\text{conn}}$ it is possible to write the conductance in terms of disconnected contributions alone.

Since Eq. (3.36) contains only the disconnected contribution, we may calculate it explicitly using Eqs. (3.18a) and (3.19). Since both $S(p)$ and $\Gamma(p)$ are slowly varying below the energy scale E_{conn}, we find the conductance is approximately linear in the T-matrix,

$$\begin{aligned} G_{jj'} \approx \frac{2e^2}{h} \int d\epsilon_p \left[-f'(\epsilon_p)\right] \{ &\mathcal{T}_{0,jj'}(\epsilon_{k_F}) + \mathcal{Z}_{R,jj'}(\epsilon_{k_F}) \,\mathrm{Re}\left[-\pi\nu_p \mathrm{T}_{pp}(\epsilon_p)\right] \\ &+ \left[\mathcal{Z}_{I,jj'}(\epsilon_{k_F}) + \mathcal{Z}_{2,jj'}(\epsilon_{k_F})\right] \mathrm{Im}\left[-\pi\nu_p \mathrm{T}_{pp}(\epsilon_p)\right] \}, \end{aligned} \tag{3.37}$$

provided $T \ll E_{\text{conn}}$. Eq. (3.37) can also be obtained by eliminating the connected part with the column sum Eq. (3.20) instead of the row sum,

$$G_{jj'} - \frac{1}{V_{k_F}^2}\left[\Gamma^\dagger\left(k_F\right)\lambda\Gamma\left(k_F\right)\right]_{j'j'}\sum_{j''}G_{jj''}, \tag{3.38}$$

which corresponds to measuring the conductance by applying a small uniform bias voltage in all leads, in addition to the small bias voltage in lead j'.

Eq. (3.37) is the first central result of this paper. It generalizes the result of the two-lead short ABK ring in Ref. 26 to an arbitrary ABK ring, and expresses the linear DC conductance as a linear function of the scattering channel T-matrix, as long as the temperature is low compared to the mesoscopic energy scale $E_{\rm conn}$ at which $S\left(p\right)$ and $\Gamma\left(p\right)$ varies significantly.

IV. PERTURBATION THEORIES

A. Weak-coupling perturbation theory

Although we now understand that the connected part of the conductance can be eliminated at low temperatures, this procedure may not be applicable in the weak-coupling regime $T \gg T_K$. In this subsection we calculate the linear DC conductance perturbatively in powers of V_k^2/U, again generalizing the short ring results of Ref. 26; we expect the result to be valid in both small and large Kondo cloud regimes as long as $T \gg T_K$ and the renormalized Kondo coupling constant remains weak.

1. Disconnected part

We first find the disconnected part; the result is already given in Ref. 26, but for completeness we reproduce it here. As implied by Eq. (3.16), our task amounts to calculating the retarded T-matrix of the screening channel, which is in turn achieved by calculating the two-point Green's function $-\left\langle T_\tau\psi_k\left(\tau\right)\psi_{k'}^\dagger\left(0\right)\right\rangle$. The pertinent Feynman diagrams to $O\left(J^2\right)$ and $O\left(K^2\right)$ are depicted in Fig. 3, and we find

$$\nu\mathrm{T}_{kk'}\left(\Omega\right) = \nu K_{kk'} + \nu^2\int d\epsilon_q \frac{1}{\Omega^+ - \epsilon_q}\left(K_{kq}K_{qk'} + \frac{3}{16}J_{kq}J_{qk'}\right), \tag{4.1}$$

where again $\nu = 1/\left(2\pi v_F\right)$ for the model with a reduced band. The factor of 3/16 results from time-ordering the impurity spin, where we have used the following identity

$$\left\langle T_\tau S_d^a\left(\tau_1\right)S_d^b\left(\tau_2\right)\right\rangle = \frac{1}{4}\delta^{ab}. \tag{4.2}$$

The $O\left(K\right)$ and $O\left(K^2\right)$ terms, accounting for the particle-hole symmetry breaking potential scattering due to the QD, clearly obey the optical theorem $\mathrm{Im}\left[-\pi\nu_p\mathrm{T}_{pp}\left(\epsilon_p\right)\right] = \left|-\pi\nu_p\mathrm{T}_{pp}\left(\epsilon_p\right)\right|^2$. If κ is comparable to the renormalized value of j then the $O\left(K\right)$ term dominates the T-matrix.

On the other hand, if we tune the QD to be particle-hole symmetric, $\epsilon_d = -U/2$ and $\kappa = 0$, both terms containing K will vanish, and the $O\left(J^2\right)$ term becomes the lowest order contribution to the T-matrix. For this term, one should also make a distinction between the real principal value part and the imaginary δ-function part. As noticed in Ref. 30 and reiterated in Ref. 26, the principal value part introduces non-universalities due to its dependence on all energies in the reduced band $(-D, D)$; nevertheless it is merely an elastic potential scattering term, and we neglect it in the following. Meanwhile, the δ-function part is an inelastic effect stemming from the Kondo physics, as can be seen from its violation of the optical theorem. Therefore, for a particle-hole symmetric QD, to $O\left(J^2\right)$ we have[26]

$$-\pi\nu\mathrm{T}_{pp}\left(\epsilon_p\right) = i\frac{3\pi^2}{16}\nu^2 J_{pp}^2. \tag{4.3}$$

The weak-coupling perturbation theory is famous for being infrared divergent at $O\left(J^3\right)$,[1,46] but as long as $T \gg T_K$, to logarithmic accuracy we can verify that the $O\left(J^3\right)$ corrections to the T-matrix can be absorbed into our $O\left(J^2\right)$

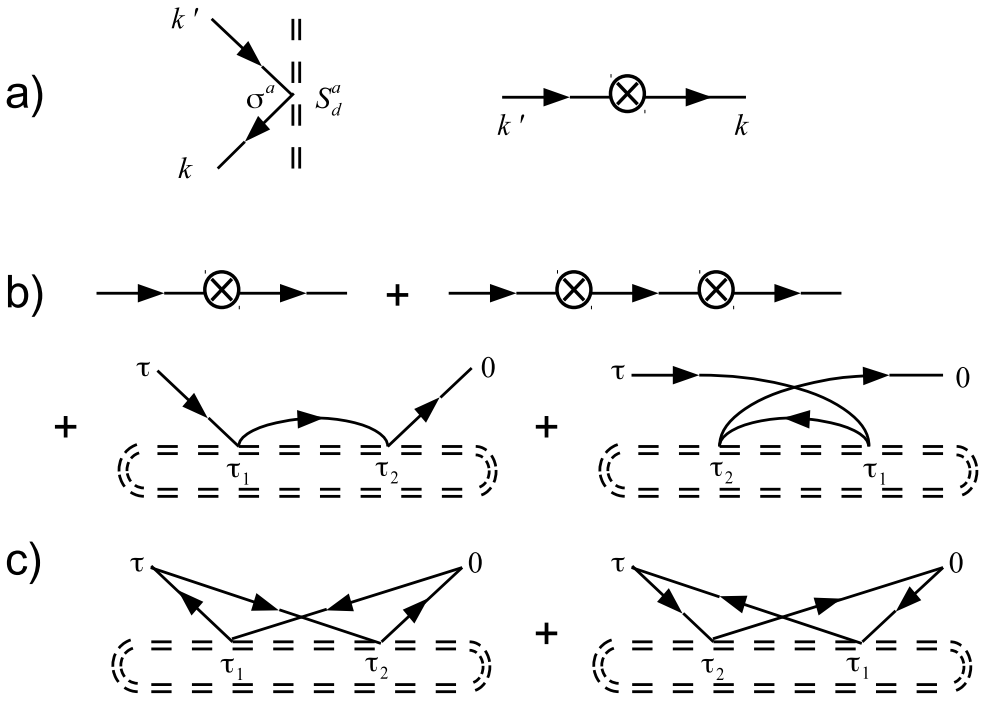

FIG. 3. Diagrammatics of weak-coupling perturbation theory. a) The vertices corresponding to the Kondo coupling and the potential scattering in Eq. (2.13a). b) Diagrams contributing to the T-matrix of the screening basis ψ electrons up to $O\left(J^2\right) \sim O\left(K^2\right)$. We have traced over the impurity spin, and arranged the internal time variables from left to right in increasing order. c) Connected diagrams contributing to the linear DC conductance up to $O\left(J^2\right)$.

result by reinterpreting the bare Kondo coupling constant J_{pp} as a renormalized one. The renormalization is governed by Eq. (2.14), and cut off at either the "electron energy" $|\epsilon_p|$ or the temperature T, whichever is larger. In other words, the Kondo coupling J_{pp} in Eq. (4.3) should be replaced by $J_{pp}\left(\max\left\{|\epsilon_p|, T\right\}\right)$, where the argument in round brackets stands for the energy cutoff D in Eq. (2.14) where the running coupling constant is evaluated.

2. Connected part

We now calculate the connected part to $O\left(J^2\right)$; the calculation follows Ref. 26 closely. Inserting Eq. (3.5) into Eq. (3.4), we write the connected part of the density-density correlation function in terms of a four-point correlation function of ψ:

$$\mathcal{G}'^{C}_{jj'}\left(i\omega_p\right) = \int_0^{\pi} \frac{dk_1 dk_2 dq_1 dq_2}{\left(2\pi\right)^4} \left(\mathbb{M}^{j}_{k_1 k_2}\right)_{11} \left(\mathbb{M}^{j'}_{q_1 q_2}\right)_{11} \mathcal{G}^{C}_{k_1 k_2 q_1 q_2}\left(i\omega_p\right), \tag{4.4}$$

where

$$\mathcal{G}^{C}_{k_1 k_2 q_1 q_2}\left(i\omega_p\right) \equiv -\int_0^{\beta} d\tau e^{i\omega_p \tau} \sum_{\sigma\sigma'} \left\langle T_\tau \psi^{\dagger}_{k_1\sigma}\left(\tau\right) \psi_{k_2\sigma}\left(\tau\right) \psi^{\dagger}_{q_1\sigma'}\left(0\right) \psi_{q_2\sigma'}\left(0\right)\right\rangle_C . \tag{4.5}$$

We insert Eqs. (2.10) and (3.6) into Eq. (4.4), and take the continuum limit, which is appropriate for the Kondo model. Because in the wide band limit the most divergent contribution to $G'^{C}_{jj'}\left(\Omega\right)$ is from $k_1 \approx k_2$ and $q_1 \approx q_2$, we can expand the integrand around these points,

$$
\begin{aligned}
&\mathcal{G}'^{C}_{jj'}\left(i\omega_p\right)\\
&=O\left(1\right)+\int\frac{dk_1dk_2dq_1dq_2}{\left(2\pi\right)^4}\frac{1}{V_{k_1}V_{k_2}V_{q_1}V_{q_2}}\mathcal{G}^{C}_{k_1k_2q_1q_2}\left(i\omega_p\right)\sum_{r_1r_2r_1'r_2'}t^*_{r_1}t_{r_2}t^*_{r_1'}t_{r_2'}\\
&\times\left\{\Gamma_{r_1j}\left(k_1\right)\Gamma^*_{r_2j}\left(k_2\right)\frac{1}{-i\left(k_1-k_2+i0\right)}+\left[\Gamma S^\dagger\left(k_1\right)\right]_{r_1j}\left[\Gamma S^\dagger\left(k_2\right)\right]^*_{r_2j}\frac{1}{-i\left(k_2-k_1+i0\right)}\right\}\\
&\times\left\{\Gamma_{r_1'j'}\left(q_1\right)\Gamma^*_{r_2'j'}\left(q_2\right)\frac{1}{-i\left(q_1-q_2+i0\right)}+\left[\Gamma S^\dagger\left(q_1\right)\right]_{r_1'j'}\left[\Gamma S^\dagger\left(q_2\right)\right]^*_{r_2'j'}\frac{1}{-i\left(q_2-q_1+i0\right)}\right\}.
\end{aligned}
\tag{4.6}
$$

The only non-vanishing diagrams at $O\left(J^2\right)$ are shown in panel c) of Fig. 3:

$$
\begin{aligned}
\mathcal{G}^{C}_{k_1k_2q_1q_2}\left(i\omega_p\right)&=\frac{3}{8}J_{q_2k_1}J_{k_2q_1}\int_0^\beta d\tau e^{i\omega_p\tau}\int_0^\beta d\tau_1d\tau_2g_{q_2}\left(-\tau_1\right)g_{k_1}\left(\tau_1-\tau\right)g_{k_2}\left(\tau-\tau_2\right)g_{q_1}\left(\tau_2\right)\\
&=\frac{3}{8}J_{q_2k_1}J_{k_2q_1}\frac{1}{\beta}\sum_{\omega_{n_1}}g_{q_2}\left(i\omega_{n_1}\right)g_{k_1}\left(i\omega_{n_1}\right)g_{k_2}\left(i\omega_{n_1}+i\omega_p\right)g_{q_1}\left(i\omega_{n_1}+i\omega_p\right);
\end{aligned}
\tag{4.7}
$$

we have again used Eq. (4.2). The frequency summation is performed by deforming the complex plane contour and wrapping it around the lines $\mathrm{Im}\, z=0$ and $\mathrm{Im}\, z=-\omega_p$. Analytic continuation yields

$$
\begin{aligned}
G^{C}_{k_1k_2q_1q_2}\left(\Omega\right)=-\frac{3J_{q_2k_1}J_{k_2q_1}}{16\pi i}\int d\omega f\left(\omega\right)\{&\left[g^R_{q_2}\left(\omega\right)g^R_{k_1}\left(\omega\right)-g^A_{q_2}\left(\omega\right)g^A_{k_1}\left(\omega\right)\right]g^R_{k_2}\left(\omega+\Omega\right)g^R_{q_1}\left(\omega+\Omega\right)\\
&+g^A_{q_2}\left(\omega-\Omega\right)g^A_{k_1}\left(\omega-\Omega\right)\left[g^R_{k_2}\left(\omega\right)g^R_{q_1}\left(\omega\right)-g^A_{k_2}\left(\omega\right)g^A_{q_1}\left(\omega\right)\right]\}.
\end{aligned}
\tag{4.8}
$$

Substituting Eqs. (4.8) and (2.13b) into Eq. (4.6), we are able to evaluate the momentum integrals in the $\Lambda\to\infty$ limit by contour methods. The $RRRR$ and $AAAA$ terms vanish, and the $AARR$ terms combine to produce a Fermi surface factor $f'\left(\omega\right)$:

$$
\begin{aligned}
&G'^{C}_{jj'}\left(\Omega\right)\\
&=O\left(1\right)-\frac{1}{\Omega}\int d\omega\left[-f'\left(\omega\right)\right]\frac{3\left(2j\right)^2}{16\pi i}\sum_{r_1r_2r_1'r_2'}t^*_{r_1}t_{r_2}t^*_{r_1'}t_{r_2'}\left[\Gamma S^\dagger\left(k_F+\frac{\omega}{v_F}\right)\right]_{r_1j}\\
&\times\left[\Gamma S^\dagger\left(k_F+\frac{\omega+\Omega}{v_F}\right)\right]^*_{r_2j}\Gamma_{r_1'j'}\left(k_F+\frac{\omega+\Omega}{v_F}\right)\Gamma^*_{r_2'j'}\left(k_F+\frac{\omega}{v_F}\right)\frac{1}{v_F^2}\\
&=O\left(1\right)+\frac{1}{i\pi\Omega}\int d\epsilon_p\left[-f'\left(\epsilon_p\right)\right]\frac{3\pi^2\nu^2J_{pp}^2}{16}\mathcal{Z}_{2,jj'}\left(\epsilon_p\right),
\end{aligned}
\tag{4.9}
$$

where we used Eq. (3.18e). The connected contribution to the conductance is now clearly a Fermi surface property:

$$
G^{C}_{jj'}=\frac{2e^2}{h}\int d\epsilon_p\left[-f'\left(\epsilon_p\right)\right]\mathcal{T}^{C(2)}_{jj'}\left(\epsilon_p\right),
\tag{4.10}
$$

where the connected transmission probability is

$$
\mathcal{T}^{C}_{jj'}\left(\epsilon_p\right)=\mathcal{Z}_{2,jj'}\left(\epsilon_p\right)\frac{3\pi^2}{16}\nu^2J_{pp}^2.
\tag{4.11}
$$

This is formally identical to the short ring result, and is of the same order of magnitude as the disconnected contribution for a particle-hole symmetric QD.[26]

Just as with the T-matrix, when we calculate the connected part further to $O\left(J^3\right)$ to logarithmic accuracy, the result can be absorbed into Eq. (4.11) if the coupling constant J is understood as fully renormalized according to Eq. (2.14), with its renormalization cut off by $|\epsilon_p|$ or T.

3. Total conductance

We write the total conductance at $T \gg T_K$ as a background term and a correction due to the QD:

$$G_{jj'} = \frac{2e^2}{h} \int d\epsilon_p \left[-f'\left(\epsilon_p\right)\right] \left[\mathcal{T}_{0,jj'}\left(\epsilon_p\right) + \delta\mathcal{T}_{jj'}\left(\epsilon_p\right)\right]. \tag{4.12}$$

If the QD is well away from particle-hole symmetry, κ can be of the same order of magnitude as $j\left(T\right)$ even when the latter is fully renormalized to the given temperature. In this case, the $T \gg T_K$ correction to the background conductance will be dominated by the potential scattering term; the connected contribution is negligible. The expression for $\delta\mathcal{T}$ is

$$\delta\mathcal{T}_{jj'}\left(\epsilon_p\right) \approx -\mathcal{Z}_{R,jj'}\left(\epsilon_p\right) \pi\nu K_{pp}. \tag{4.13}$$

If, however, the QD is particle-hole symmetric, the connected contribution becomes important. Inserting Eq. (4.3) into Eq. (3.18a) and combining with (4.11), we find the Kondo-type correction to $O\left(J^2\right)$ at $T \gg T_K$

$$\delta\mathcal{T}_{jj'}\left(\epsilon_p\right) = \left[\mathcal{Z}_{I,jj'}\left(\epsilon_p\right) + \mathcal{Z}_{2,jj'}\left(\epsilon_p\right)\right] \frac{3\pi^2}{16}\nu^2 J_{pp}^2. \tag{4.14}$$

Again, in the RG improved perturbation theory, J_{pp} in Eq. (4.14) should be replaced by $J_{pp}\left(\max\left(\left|\epsilon_p\right|, T\right)\right)$, indicating that J_{pp} is the renormalized value at the running energy cutoff $\max\left(\left|\epsilon_p\right|, T\right)$. This expression is valid as long as $T \gg T_K$, irrespective of whether the system is in small or large Kondo cloud regime.

Eq. (4.14) is formally similar to the previously obtained short ring result.[26] It should be noted, however, that the energy dependence of $\mathcal{Z}_I$, $\mathcal{Z}_2$ and J^2 is possibly much stronger than the short ring case, and the thermal averaging in Eq. (4.12) can lead to very different results in small and large Kondo cloud regimes. For instance, if $E_{\text{conn}} \ll T_K \ll T$ (which may happen in the small cloud regime), the Fermi factor in Eq. (4.12) averages over many peaks in $\mathcal{T}$, $\mathcal{Z}_I$, $\mathcal{Z}_2$ and V^2 that are associated with the underlying mesoscopic structure. In this case connected part elimination is not applicable. On the other hand, if $T_K \ll T \ll E_{\text{conn}}$, the variation of $\mathcal{T}$, $\mathcal{Z}_I$, $\mathcal{Z}_2$ or V^2 is negligible on the scale of T, and the Fermi factor in Eq. (4.12) may be approximated by a δ function. This leads to

$$G_{jj'} = \frac{2e^2}{h} \left\{ \mathcal{T}_{0,jj'}\left(\epsilon_{k_F}\right) + \left[\mathcal{Z}_{I,jj'}\left(\epsilon_{k_F}\right) + \mathcal{Z}_{2,jj'}\left(\epsilon_{k_F}\right)\right] \frac{3\pi^2}{16}\nu^2 J_{k_F k_F}^2 \right\}, \tag{4.15}$$

which agrees with our prescription of eliminating the connected part, Eq. (3.37).

B. Fermi liquid perturbation theory

It is also interesting to consider temperatures low compared to the Kondo temperature $T \ll T_K$. Since our formalism does not by itself provide a low-energy effective theory of the small cloud regime for $T_K \gg E_V$, we focus on the very large Kondo cloud regime $T_K \ll E_V$, where as explained in Sec. II the low-energy effective theory is simply a Fermi liquid theory. If we further assume $T \ll E_{\text{conn}}$, then we can simply eliminate the connected contribution to the conductance with Eq. (3.37).

To use Eq. (3.37) we need the low-energy T-matrix for the screening channel in the Fermi liquid regime, which is again well known.[44,47] As mentioned in Sec. I, the strong-coupling single particle wave function at zero temperature is obtained by imposing a phase shift on the weak-coupling wave function. This phase shift $\delta_{\psi\psi}$ results from both elastic scattering off the Kondo singlet and particle-hole symmetry breaking potential scattering:

$$\delta_{\psi\psi,\sigma} = \sigma\frac{\pi}{2} + \delta_P, \tag{4.16}$$

where $\sigma = \pm 1$ for spin-up/spin-down electrons. To the lowest order in potential scattering $O\left(K\right)$, we have[30]

$$\tan\delta_P = -\pi\nu K_{k_F k_F}. \tag{4.17}$$

Let us introduce the phase-shifted screening channel $\tilde{\psi}$, which is then related to the original screening channel ψ via a scattering basis transformation:

$$\psi_{k,\sigma} = \int_{k_F-\Lambda}^{k_F+\Lambda} \frac{dp}{2\pi} \left(\frac{i}{k-p+i0} - e^{2i\delta_{\psi\psi,\sigma}} \frac{i}{k-p-i0} \right) \tilde{\psi}_{p,\sigma}. \tag{4.18}$$

Using the definition of the T-matrix Eq. (3.12) and the transformation Eq. (4.18) one can show that retarded T-matrices for ψ and $\tilde{\psi}$ are related by

$$\mathrm{T}_\sigma(\omega) = \frac{i}{2\pi\nu} \left(e^{2i\delta_{\psi\psi,\sigma}} - 1 \right) + e^{2i\delta_{\psi\psi,\sigma}} \tilde{\mathrm{T}}_\sigma(\omega). \tag{4.19}$$

Since $\tilde{\psi}$ diagonalizes the strong-coupling fixed point Hamiltonian, by definition $\tilde{\mathrm{T}}(\omega=0)=0$ at zero temperature.

The leading irrelevant operator perturbing the strong-coupling fixed point is localized at the QD and quadratic in spin current.[13,44] It is most conveniently written in terms of $\tilde{\psi}$:

$$H_{int} = \frac{2\pi v_F^2}{T_K} : \tilde{\psi}_\alpha^\dagger \tilde{\psi}_\alpha \tilde{\psi}_\beta^\dagger \tilde{\psi}_\beta : (x=0) - i\frac{v_F^2}{T_K} \left[: \tilde{\psi}_\alpha^\dagger \frac{d}{dx} \tilde{\psi}_\alpha - \left(\frac{d}{dx} \tilde{\psi}_\alpha^\dagger \right) \tilde{\psi}_\alpha : \right] (x=0). \tag{4.20}$$

Here :: denotes normal ordering and sums over repeated spin indices α and β are implied. These two terms are illustrated in panel a) of Fig. 4 as a four-point vertex and a two-point one. Both terms share a single coupling constant of $O(1/T_K)$, because the leading irrelevant operator written in the $\tilde{\psi}$ basis must be particle-hole symmetric by definition. The T-matrix for $\tilde{\psi}$ is calculated to $O\left(1/T_K^2\right)$ in Ref. 44:

$$-\pi\nu\tilde{\mathrm{T}}(\omega) = \frac{\omega}{T_K} + i\frac{3\omega^2+\pi^2T^2}{2T_K^2}. \tag{4.21}$$

It is diagramatically represented by Fig. 4 panel b).

Substituting Eqs. (4.16), (4.19) and (4.21) into Eq. (3.37), we eliminate the connected contribution, and obtain the $T \ll T_K$ conductance in the very large Kondo cloud regime:

$$\begin{aligned} G_{jj'} \approx \frac{2e^2}{h} \Bigg\{ & \mathcal{T}_{0,jj'}(\epsilon_{k_F}) - \mathcal{Z}_{R,jj'}(\epsilon_{k_F}) \left(\frac{1}{2} - \frac{\pi^2T^2}{T_K^2} \right) \sin 2\delta_P \\ & + \left[\mathcal{Z}_{I,jj'}(\epsilon_{k_F}) + \mathcal{Z}_{2,jj'}(\epsilon_{k_F}) \right] \left(\cos^2\delta_P - \frac{\pi^2T^2}{T_K^2} \cos 2\delta_P \right) \Bigg\}. \end{aligned} \tag{4.22}$$

Predictions of the conductance at high temperatures [Eq. (4.12)] and at low temperatures [Eq. (4.22)] together constitute the second main result of this paper. We emphasize once more that, while Eq. (4.12) is valid as long as $T \gg T_K$, Eq. (4.22) is expected to be justified provided $T \ll T_K \ll E_V$, so that the Fermi liquid theory applies, and also $T \ll E_{\mathrm{conn}}$, so that the connected contribution can be eliminated.

For clarity we tabulate various regimes of energy scales discussed so far (Table I). Note again that the connected contribution to conductance can be eliminated when $T \ll E_{\mathrm{conn}}$. In general we have $E_{\mathrm{conn}} \lesssim E_V$, but we assume in this table that $E_{\mathrm{conn}} \sim E_V$, which is the case with the systems to be discussed in this paper.

V. CLOSED LONG ABK RINGS

In this section we apply our general formalism to the simplest model of a closed long ABK ring, studied in Ref. 24 (Fig. 5): the QD is coupled directly to the source and drain leads, and a long reference arm connects the two leads smoothly. A weak link with hopping t' splits the reference arm into two halves of equal length $d_{ref}/2$ where d_{ref} is an even integer. As opposed to Ref. 24, however, we use gauge invariance to assign the AB phase to the QD tunnel couplings rather than the weak link: $t_1 \equiv t_L e^{i\varphi/2}$ and $t_2 \equiv t_R e^{-i\varphi/2}$. We assume no additional non-interacting long arms connecting the QD with the source and drain leads, because multiple traversal processes in such long QD arms will lead to interference effects[48] independent of the AB phase, complicating the problem.[24] The Hamiltonian representing this model takes the form

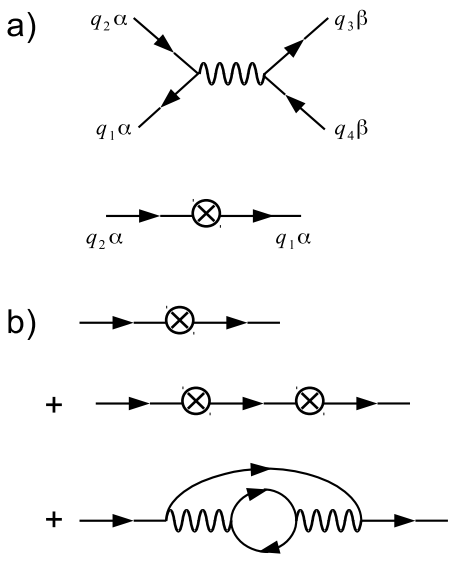

FIG. 4. Diagrammatics of Fermi liquid perturbation theory. a) The two vertices given by the leading irrelevant operator, Eq. (4.20). b) Diagrams contributing to the T-matrix of $\tilde{\psi}$ electrons up to $O\left(T^2/T_K^2\right)$. The propagators are those of the phase-shifted screening basis operators $\tilde{\psi}$.

$$
\begin{aligned}
H_{0,\text{junction}} = -t & \left[\left(\sum_{n=1}^{d_{ref}/2-1} + \sum_{n=d_{ref}/2+1}^{d_{ref}-1} \right) c^\dagger_{ref,n} c_{ref,n+1} + \text{h.c.} \right] \\
& -t \left(c^\dagger_{ref,1} c_{1,0} + c^\dagger_{ref,d_{ref}} c_{2,0} + \text{h.c.} \right) \\
& -t' \left(c^\dagger_{ref,d_{ref}/2} c_{ref,d_{ref}/2+1} + \text{h.c.} \right) ; \qquad (5.1)
\end{aligned}
$$

the coupling sites are $c_{C,r=1} \equiv c_{1,0}$ and $c_{C,r=2} \equiv c_{2,0}$.

We first repeat the Kondo temperature analysis in Ref. 24 in order to distinguish between small and large Kondo

TABLE I. Different regimes of energy scales discussed in this paper. T, T_K and E_V are respectively the temperature, the Kondo temperature, and the energy scale over which V_k^2 varies significantly. We also assume $E_{\text{conn}} \sim E_V$, where E_{conn} is the energy scale over which S and Γ vary significantly. For the low-temperature conductance in the small Kondo cloud regime, see discussion in Sec. VII.

	Weak-coupling perturbation theory applies	T_K depends on mesoscopic details	Connected part elimination possible
$T \gg T_K \gg E_V$	Yes	No	No
$T \gg E_V \gg T_K$	Yes	Yes	No
$E_V \gg T \gg T_K$	Yes	Yes	Yes
	Fermi liquid perturbation theory applies	**T_K depends on mesoscopic details**	**Connected part elimination possible**
$T \ll T_K \ll E_V$	Yes	Yes	Yes
$T \ll E_V \ll T_K$	?	No	Yes
$E_V \ll T \ll T_K$	?	No	No

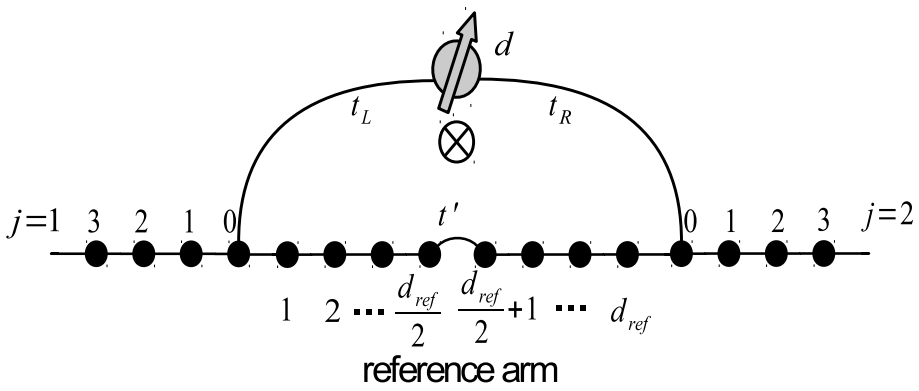

FIG. 5. Geometry of the long ABK ring with short upper arms and a pinched reference arm.

cloud regimes, then carefully study the conductance at high and low temperatures, taking into account the previously neglected connected contribution.

A. Kondo temperature

The background S-matrix for this model is identical to the short ABK ring[30] up to overall phases, due to the smooth connection between reference arm and leads:

$$S(k) = e^{ikd_{ref}} \begin{pmatrix} \tilde{r}(k) & \tilde{t}(k) \\ \tilde{t}(k) & \tilde{r}(k) \end{pmatrix}; \tag{5.2}$$

where the S-matrix elements $\tilde{r}$ and $\tilde{t}$ for the weak link are

$$\tilde{r}(k) = -\frac{1-\tilde{\tau}^2}{e^{-2ik}-\tilde{\tau}^2}, \tilde{t}(k) = -\frac{2i\tilde{\tau}\sin k}{e^{-2ik}-\tilde{\tau}^2}, \tag{5.3}$$

and we introduce the shorthand $\tilde{\tau} = t'/t$. The wave function is also straightforward to find:

$$\Gamma_{jj'}(k) = \delta_{jj'} + S_{jj'}(k). \tag{5.4}$$

In the wide band limit, $\tilde{r}$ and $\tilde{t}$ are approximately independent of k in the reduced band $k_F - \Lambda_0 < k < k_F + \Lambda_0$ where the momentum cutoff $\Lambda_0 \ll 1$. This allows us to approximate them by their Fermi surface values, $\tilde{r}(k) \approx \tilde{r} = |\tilde{r}| e^{i\theta}$ and $\tilde{t}(k) \approx \tilde{t} = \pm i |\tilde{t}| e^{i\theta}$ (the $\pm\pi/2$ phase difference is required by unitarity of S); without loss of generality we focus on the $\tilde{t} = i|\tilde{t}| e^{i\theta}$ case.

From Eq. (5.4) one conveniently obtains the normalization factor

$$\begin{aligned} V_k^2 &= 2\left(t_L^2 + t_R^2\right)\left[1 + |\tilde{r}|\cos(kd_{ref}+\theta) - \gamma|\tilde{t}|\cos\varphi\sin(kd_{ref}+\theta)\right] \\ &= 2\left(t_L^2 + t_R^2\right)\left[1 + \sqrt{1-|\tilde{t}|^2(1-\gamma^2\cos^2\varphi)}\cos(kd_{ref}+\theta')\right], \end{aligned} \tag{5.5}$$

where $\gamma = 2t_L t_R/\left(t_L^2 + t_R^2\right)$ measures the degree of symmetry of coupling to the QD. In the second line we have used $|\tilde{t}|^2 + |\tilde{r}|^2 = 1$ and introduced another phase θ', where $\theta' - \theta$ is a function of γ, $|\tilde{t}|$ and φ but independent of k. We note that this expression is also applicable in the continuum limit, where the lattice constant $a \to 0$ (we have previously set $a = 1$) but the arm length $d_{ref}a$ is fixed. In that case d_{ref} should be understood as the arm length $d_{ref}a$.

For long rings and filling factors not too small $k_F d_{ref} \gg 1$, V_k^2 oscillates around $2\left(t_L^2+t_R^2\right)$ as a function of k, and has its extrema at $k_n = \left(n\pi - \theta'\right)/d_{ref}$ where n takes integer values. The only characteristic energy scale for V_k^2 is therefore the peak/valley spacing $\Delta = v_F\pi/d_{ref}$, and $E_V \sim E_{\text{conn}} \sim \Delta$. As in Ref. 24 we define the reduced band such that $\Delta \ll D_0 \equiv v_F\Lambda_0$, and the reduced band initially contains many oscillations.

In the small Kondo cloud regime $T_K \gg \Delta$, one may assume the oscillations of V_k^2 are smeared out when the energy cutoff is being reduced from D_0, which is still well above T_K: $V_k^2 \simeq \overline{V_k^2} = 2\left(t_L^2+t_R^2\right)$. This means T_K in this regime is approximately the background Kondo temperature T_K^0 defined in Eq. (2.17), independent of the position of the Fermi level at the energy scale Δ, and also independent of the magnetic flux.

On the other hand, in the large cloud regime $T_K \lesssim \Delta$, now that the Kondo temperature is largely determined by the value of V_k^2 in a very narrow range of energies around the Fermi level, the mesoscopic k oscillations become much more important. When the running energy cutoff D is above the peak/valley spacing Δ, the renormalization of j is controlled by $\overline{V_k^2}$ as in Eq. (2.16). Once D is reduced below Δ, we may approximate the renormalization of j as being dominated by $V_{k_F}^2$. This leads to the following estimation of the Kondo temperature:

$$T_K \simeq \Delta \exp\left[-\frac{1}{2V_{k_F}^2 \nu j\left(\Delta\right)}\right] = \Delta\left(\frac{T_K^0}{\Delta}\right)^{\left[1+\sqrt{1-\left|\tilde{t}\right|^2\left(1-\gamma^2\cos^2\varphi\right)}\cos\left(k_F d_{ref}+\theta'\right)\right]^{-1}}. \tag{5.6}$$

It is clear that T_K can be significantly dependent on the AB phase φ in this regime. In particular, T_K varies from $\sim\sqrt{T_K^0\Delta}$ ("on resonance") to practically 0 ("off resonance") as φ is tuned between 0 and π, when the Fermi energy is located on a peak or in a valley $k_F = k_n$, the background transmission is perfect $\left|\tilde{t}\right| = 1$, and coupling to the QD is symmetric $\gamma = 1$; see Fig. 6.[24] (The special case $V_{k_F}^2 = 0$ corresponds to a pseudogap problem $\nu V_k^2 \propto \left(k-k_F\right)^2$, and the stable RG fixed point can be the local moment fixed point or the asymmetric strong coupling fixed point, depending on the degree of particle-hole symmetry.[49]) As a general rule, stronger transmission through the pinch $\left|\tilde{t}\right|$ and greater symmetry of coupling γ result in stronger interference between the two tunneling paths through the device, and hence increases the tunability of the Kondo temperature by the magnetic flux.

B. High-temperature conductance

We now calculate the conductance at $T \gg T_K$ by perturbation theory. Following the discussion in Ref. 24, we consider the case of a particle-hole symmetric QD $\kappa = 0$ and $K_{kk'} = 0$, and also ignore the elastic real part of the potential scattering generated at $O\left(J^2\right)$.[26] These assumptions allow us to adopt Eq. (4.14) for the $O\left(J^2\right)$ correction to the transmission probability:

$$\delta\mathcal{T}_{jj'}\left(\epsilon_k\right) = 3\pi^2\nu^2 j^2\left(V_k^2\,\text{Re}\left\{\left[S\left(k\right)\Gamma^\dagger\left(k\right)\lambda\Gamma\left(k\right)\right]_{jj'} S_{jj'}^*\left(k\right)\right\} - \left|\left[S\left(k\right)\Gamma^\dagger\left(k\right)\lambda\Gamma\left(k\right)\right]_{jj'}\right|^2\right), \tag{5.7}$$

where we have used Eqs. (3.18d) and (3.18e).

Note that Eq. (5.7) does not depend on details of the non-interacting part of the ring Hamiltonian $H_{0,\text{junction}}$. For a parity-symmetric geometry with two leads and two coupling sites ($N = M = 2$), when coupling to the QD is also symmetric ($t_L = t_R$) and time-reversal symmetry is present ($\varphi = 0$ or π), we can further show that the sign of the $O\left(J^2\right)$ transmission probability correction is determined by the sign of $1 - 2\left|\mathcal{T}_{0,12}\right|$, a property discussed in Ref. 26 at the end of Sec. IV C. Indeed, parity symmetry implies that $S_{11} = S_{22}$, $S_{12} = S_{21}$, $\Gamma_{11} = \Gamma_{22}$, $\Gamma_{12} = \Gamma_{21}$; hence it is not difficult to find from Eq. (5.7) that

$$\frac{1}{4}\left[\delta\mathcal{T}_{11}\left(\epsilon_k\right) + \delta\mathcal{T}_{22}\left(\epsilon_k\right) - \delta\mathcal{T}_{12}\left(\epsilon_k\right) - \delta\mathcal{T}_{21}\left(\epsilon_k\right)\right] = \frac{3}{8}\pi^2\nu^2 J_{kk}^2\left[1 - 2\left|S_{12}\left(k\right)\right|^2\right]. \tag{5.8}$$

The left-hand side correspond to a particular way to measure the conductance, namely parity-symmetric bias voltage and parity-symmetric current probes, or $y = 1/2$ in Sec. V of Ref. 26.

We now return to the long ring geometry without assumptions about t_L, t_R and φ. Plugging Eqs. (5.2) and (5.4) into Eq. (5.7) we find

$$\delta\mathcal{T}_{11}\left(\epsilon_k\right) = -3\pi^2\nu^2 j^2\left[C_0\left(k\right) + C_1\left(k\right)\cos\varphi + C_2\left(k\right)\cos 2\varphi\right], \tag{5.9}$$

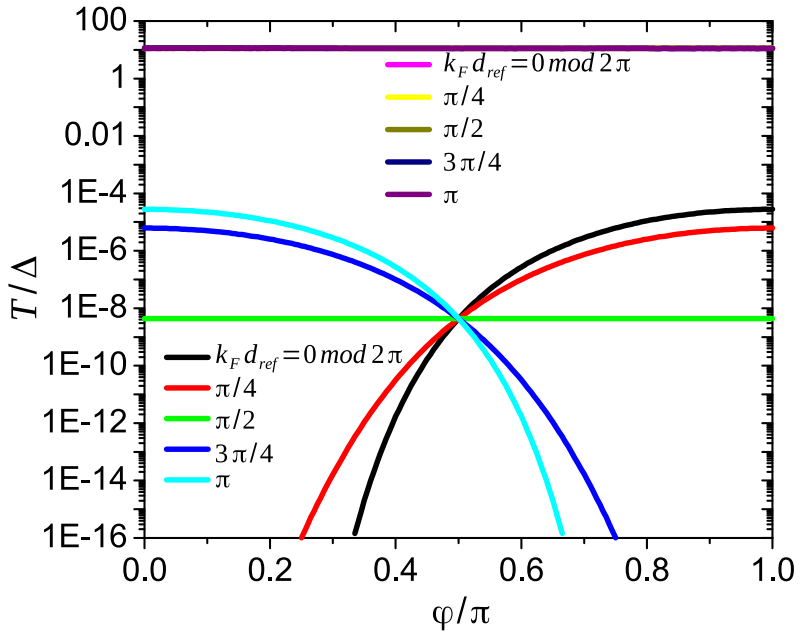

FIG. 6. Kondo temperature T_K for the closed long ABK ring, calculated by numerical integration of the weak coupling RG equation Eq. (2.15), plotted against the AB phase φ. $T_K(\varphi)$ is an even function of φ and has a period of 2π, so only $0 \leq \varphi \leq \pi$ is shown. System parameters are: $d_{ref} = 60$, $\theta = \pi/2$, $|\tilde{r}| = 0$, $t_L = t_R$, $D_0 = 10$. The curves with $T_K \gg \Delta$ (small Kondo cloud regime) have a large bare Kondo coupling $\left(t_L^2 + t_R^2\right) j_0/\pi = 0.15$, whereas the curves with $T_K \ll \Delta$ (large Kondo cloud regime) have a much smaller bare Kondo coupling $\left(t_L^2 + t_R^2\right) j_0/\pi = 0.02$. In the small cloud regime T_K is almost independent of φ and k_F, as the curves are flat and overlapping with each other. In the large cloud regime, however, T_K highly sensitive to both φ and k_F.

where the coefficients $C_0(k)$, $C_1(k)$ and $C_2(k)$ are independent of φ but are usually complicated functions of k:

$$\begin{aligned} C_0(k) = {} & \left(t_L^4 + t_R^4\right) \left|\tilde{t}\right|^2 \left[1 + 2\left|\tilde{r}\right| \cos\left(kd_{ref} + \theta\right) + \left|\tilde{r}\right|^2 \cos 2\left(kd_{ref} + \theta\right)\right] \\ & - 2t_L^2 t_R^2 \left[3 - 4\left|\tilde{t}\right|^2 + 4\left|\tilde{r}\right|^3 \cos\left(kd_{ref} + \theta\right) + \left(\left|\tilde{r}\right|^4 + \left|\tilde{t}\right|^4\right) \cos 2\left(kd_{ref} + \theta\right)\right], \end{aligned} \tag{5.10a}$$

$$\begin{aligned} C_1(k) = {} & 4\left|\tilde{t}\right| t_L t_R \left(t_L^2 + t_R^2\right) \sin\left(kd_{ref} + \theta\right) \\ & \times \left[\left|\tilde{r}\right|^2 \cos 2\left(kd_{ref} + \theta\right) + \left|\tilde{r}\right| \left(\left|\tilde{r}\right|^2 - \left|\tilde{t}\right|^2\right) \cos\left(kd_{ref} + \theta\right) - \left|\tilde{t}\right|^2\right], \end{aligned} \tag{5.10b}$$

$$C_2(k) = 2\left|\tilde{t}\right|^2 t_L^2 t_R^2 \left\{1 + 2\left|\tilde{r}\right| \cos\left(kd_{ref} + \theta\right) + \left|\tilde{r}\right|^2 \cos 2\left(kd_{ref} + \theta\right)\right\}. \tag{5.10c}$$

In the special case of a smooth reference arm $|\tilde{r}| = 0$ and $\left|\tilde{t}\right| = 1$, the Kondo-type correction becomes especially simple:

$$\begin{aligned} \delta\mathcal{T}_{11}(\epsilon_k) = {} & -3\pi^2 \nu^2 j^2 \left[t_L^2 + t_R^2 - 2t_L t_R \sin\left(kd_{ref} + \theta + \varphi\right)\right] \\ & \times \left[t_L^2 + t_R^2 - 2t_L t_R \sin\left(kd_{ref} + \theta - \varphi\right)\right]. \end{aligned} \tag{5.11}$$

As in Refs. 24 and 26, only the first and the second harmonics of the AB phase φ appear in the correction to the transmission probability $\delta\mathcal{T}_{11}$.

We may perform the thermal averaging in Eq. (4.12) at this stage. The Fermi factor $-f'(\epsilon_k)$ ensures only the energy range $|\epsilon_k| \lesssim T$ contributes significantly to the conductance; in this energy range the renormalization of j is cut off by T.

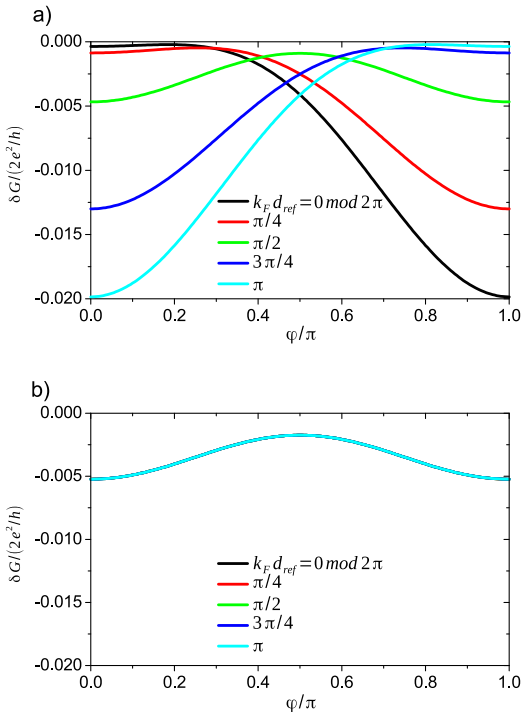

FIG. 7. Kondo-type correction to the conductance δG at $T \gg T_K$ for the closed long ABK ring with a particle-hole symmetric QD, calculated by RG improved perturbation theory Eq. (5.9), plotted against the AB phase φ. Again only $0 \leq \varphi \leq \pi$ is shown. System parameters are: $d_{ref} = 60$, $\theta = \pi/2$, $|\tilde{r}| = 0$, $t_L = t_R$, $\left(t_L^2 + t_R^2\right) j_0/\pi = 0.02$ at $D_0 = 10$ (i.e. the system is in the large cloud regime). $T/\Delta = 0.0955$ in panel a) and $T/\Delta = 19.1$ in panel b). For $T \ll \Delta$ the conductance shows considerable k_F dependence, while for $T \gg \Delta$ such dependence essentially vanishes and curves at different k_F overlap. Also, for $T \gg \Delta$ the first harmonic $\cos\varphi$ drops out as predicted by Eq. (5.12), and $\delta G(\varphi)$ has a period of π.

In the small Kondo cloud regime, $T \gg T_K$ means $T \gg \Delta$ so that we can average over many peaks of $\delta\mathcal{T}_{jj'}(\epsilon_k)$, so we may drop all rapidly oscillating Fourier components in Eq. (5.9). This leads to

$$\delta G \approx -\frac{2e^2}{h} 3\pi^2 \nu^2 \left[j(T)\right]^2 \left[\left(t_L^4 + t_R^4\right)\left|\tilde{t}\right|^2 - 2t_L^2 t_R^2 \left(3 - 4\left|\tilde{t}\right|^2\right) + 2\left|\tilde{t}\right|^2 t_L^2 t_R^2 \cos 2\varphi\right]. \tag{5.12}$$

We see that the first harmonic in φ approximately drops out upon thermal averaging.

On the other hand, in the large Kondo cloud regime, for $T \gg T_K$ it is possible to have either $T \gg \Delta$ or $T \ll \Delta$. In the former case Eq. (5.12) continues to hold. In the latter case $\delta\mathcal{T}_{jj'}(\epsilon_k)$ has little variation in the energy range $|\epsilon_k| \lesssim T$, so it is appropriate to replace $-f'(\epsilon_k)$ with a δ function at the Fermi level; thus

$$\delta G \approx -\frac{2e^2}{h} 3\pi^2 \nu^2 \left[j(T)\right]^2 \left[C_0(k_F) + C_1(k_F)\cos\varphi + C_2(k_F)\cos 2\varphi\right]. \tag{5.13}$$

Fig. 7 illustrates these two different cases for the large Kondo cloud regime. We note that our $T \gg T_K$ results, Eq. (5.12) for $T \gg \Delta$ and Eq. (5.13) for $T \ll \Delta$, are different from those of Ref. 24. We believe the discrepancy is due to the fact that only single-particle scattering processes are taken into consideration by Ref. 24; the connected contribution to the conductance is omitted, despite being of comparable magnitude with the disconnected contribution.

C. Fermi liquid conductance

It is also interesting to calculate the conductance in the $T \ll T_K$ limit in the very large Kondo cloud regime, starting from Eq. (4.22). We make the assumption that the particle-hole symmetry breaking potential scattering is negligible,

$\delta_P = 0$, as in Ref. 24. Inserting Eqs. (5.2) and (5.4) into Eqs. (3.18d) and (3.18e), we find the total conductance has the form

$$G = \frac{2e^2}{h}\left[T_s + \left(\left|\tilde{t}\right|^2 - T_s\right)\left(\frac{\pi T}{T_K}\right)^2\right], \tag{5.14}$$

where the $T = 0$ transmission probability is

$$\begin{aligned} T_s = \Bigg| & e^{ik_F d_{ref}}\tilde{t} - \frac{2}{V_{k_F}^2}\left[t_L e^{i\frac{\varphi}{2}}\left(e^{ik_F d_{ref}}\tilde{r}+1\right) + t_R e^{-i\frac{\varphi}{2}} e^{ik_F d_{ref}}\tilde{t}\right] \\ & \times\left[t_L e^{-i\frac{\varphi}{2}} e^{ik_F d_{ref}}\tilde{t} + t_R e^{i\frac{\varphi}{2}}\left(1 + e^{ik_F d_{ref}}\tilde{r}\right)\right]\Bigg|^2 . \end{aligned} \tag{5.15}$$

While Eq. (5.14) is ostensibly in agreement with Eq. (69) of Ref. 24, we suspect that there are two oversights in the derivation of the latter: at finite temperature, Ref. 24 neglects the connected contribution to the conductance, and also replaces the thermal factor $-f'(\epsilon_p)$ with a δ function in Eq. (3.37). These two discrepancies cancel each other, leading to the same $T \ll T_K$ result as ours.

VI. OPEN LONG ABK RINGS

We turn to the open long ABK ring, with strong electron leakage due to side leads coupled to the arms of the ring, where our multi-terminal formalism shows its full capacity.

In our geometry shown in Fig. 8, the source lead branches into two paths at the left Y-junction, a QD path of length $d_L + d_R$ and a reference path of length d_{ref}. These two paths converge at the right Y-junction at the end of the drain lead. An embedded QD in the Kondo regime separates the QD path into two arms of lengths d_L and d_R. To open up the ring we attach additional non-interacting side leads to all sites inside the ring other than the two central sites in the Y-junctions and QD.[23,39–41] The side leads, numbering $d_L + d_R + d_{ref}$ in total, are assumed to be identical to the main leads (source and drain), except that the first link on every side lead (connecting site 0 of the side lead to its base site in the ring) is assumed to have a hopping strength t_x which is generally different than the bulk hopping t. The Hamiltonian representing this model is therefore

$$\begin{aligned} H_{0,\text{junction}} = & -t\left(\sum_{n=0}^{d_L-2} c_{L,n}^\dagger c_{L,n+1} + \sum_{n=0}^{d_R-2} c_{R,n}^\dagger c_{R,n+1} + \sum_{n=1}^{d_{ref}-1} c_{ref,n}^\dagger c_{ref,n+1} + \text{h.c.}\right) \\ & - \left[\left(t_{JL}^L c_{1,0}^\dagger + t_{JQ}^L c_{L,d_L-1}^\dagger + t_{JR}^L c_{ref,1}^\dagger\right) c_{JL} + \text{h.c.}\right] \\ & - \left[\left(t_{JL}^R c_{2,0}^\dagger + t_{JQ}^R c_{R,d_R-1}^\dagger + t_{JR}^R c_{ref,d_{ref}}^\dagger\right) c_{JR} + \text{h.c.}\right] \\ & - t_x\left(\sum_{n=0}^{d_L-1} c_{L,n}^\dagger c_{n,0}^{(L)} + \sum_{n=0}^{d_R-1} c_{R,n}^\dagger c_{n,0}^{(R)} + \sum_{n=1}^{d_{ref}} c_{ref,n}^\dagger c_{n,0}^{(ref)} + \text{h.c.}\right), \end{aligned} \tag{6.1}$$

where $c_{JL(R)}$ is the annihilation operator on the central site of the left (right) Y-junction, and $c_{n,0}^{(\alpha)}$ is the annihilation operator on site 0 of the side lead attached to the nth site on arm α, $\alpha = L$, R and ref. The coupling sites are $c_{C,r=1} \equiv c_{L,0}$ and $c_{C,r=2} \equiv c_{R,0}$, and again we let the couplings to the QD be $t_1 = t_L e^{i\frac{\varphi}{2}}$ and $t_2 = t_R e^{-i\frac{\varphi}{2}}$.

Our hope is that in certain parameter regimes the open long ring provides a realization of the two-path interferometer, where the two-slit interference formula applys:

$$G_{sd} = G_{ref} + G_d + 2\sqrt{\eta_v}\sqrt{G_{ref}G_d}\cos\left(\varphi + \varphi_t\right), \tag{6.2}$$

where G_{ref} is the conductance through the reference arm with the QD arm sealed off, and G_d is the conductance through the QD with the reference arm sealed off. φ is as before the AB phase, and φ_t is the accumulated non-magnetic phase difference of the two paths (*including* the $\pi/2$ transmission phase through the QD). η_v is the unit-normalized

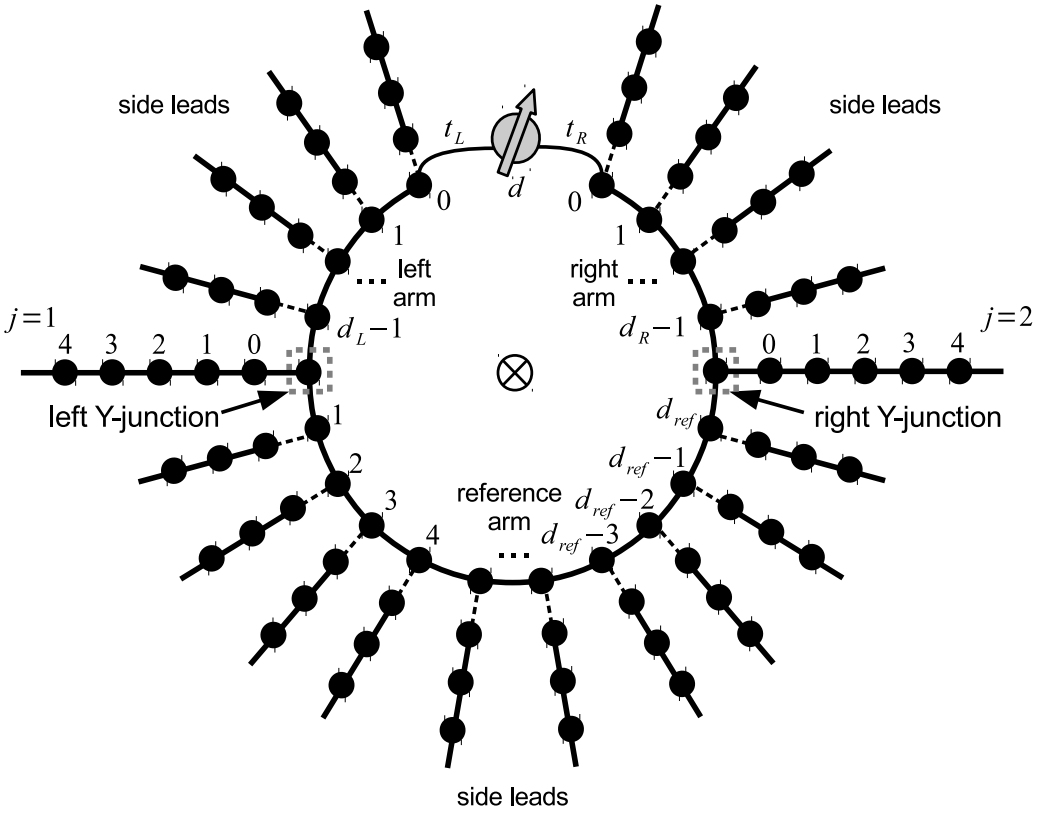

FIG. 8. Geometry of the open long ABK ring. Side leads are appended to the QD arms and the reference arms, which are all of comparable lengths.

visibility of the AB oscillations; $\eta_v = 1$ at zero temperature if all transport processes are coherent.[39] In the two-path interferometer regime, φ_t reflects the intrinsic transmission phase through the QD, provided that the geometric phases of the two paths are the same (e.g. identical path lengths in a continuum model), no external magnetic field is applied to the QD, and the particle-hole symmetry breaking phase shift is zero.

For non-interacting embedded QDs well outside of the Kondo regime, small transmission through the lossy arms is known to suppress multiple traversals of the ring and ensure that the transmission amplitudes in two paths are mutually independent.[40] We show below that in our interferometer with a Kondo QD, the same criterion renders the mesoscopic fluctuations of the normalization factor V_k^2 negligible, and paves the way to the two-slit condition $t_{sd} = t_{ref} + t_d e^{i\varphi}$. If we additionally have small reflection by the lossy arms, then both the Kondo temperature of the system and the intrinsic transmission amplitude through the QD are the same as their counterparts for a QD directly embedded between the source and the drain. At finite temperature $T \ll T_K$, we recover and generalize the single-channel Kondo results of Ref. 39 for the normalized visibility η_v and the transmission phase φ_t.

A. Wave function on a single lossy arm

To solve for the background S-matrix S and the wave function matrix Γ of the open ring, we first analyze a single lossy arm attached to side leads, depicted in Fig. 9.[40]

Consider an arbitrary site labeled n on this arm; let the wave function on this site be ϕ_n, and let incident and scattered amplitudes on the side lead attached to this site be A_n^s and B_n^s. The wave function on site l ($l \geq 0$) on the side lead is then written as $A_n^s e^{-ikl} + B_n^s e^{ikl}$. The Schroedinger's equations are

$$t\left(A_n^s e^{ik} + B_n^s e^{-ik}\right) = t_x \phi_n, \tag{6.3a}$$

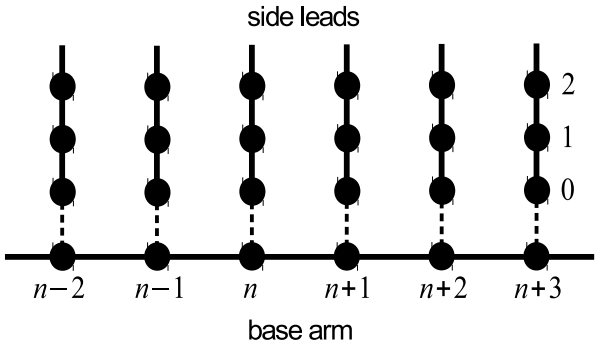

FIG. 9. A single lossy arm attached to side leads.

$$(-2t\cos k)\,\phi_n = -t\phi_{n-1} - t\phi_{n+1} - t_x\,(A_n^s + B_n^s)\,. \tag{6.3b}$$

Eliminating B_n^s, we find

$$\left(-2\cos k + \frac{t_x^2}{t^2}e^{ik}\right)\phi_n = -\phi_{n-1} - \phi_{n+1} + e^{ik}\,(2i\sin k)\,\frac{t_x}{t}A_n^s. \tag{6.4}$$

This means if $A_n^s = 0$, i.e. no electron is incident from the side lead n, we can write the wave function on the nth site on the arm as

$$\phi_n = C_L\eta_1^n + C_R\eta_2^n, \tag{6.5}$$

where $C_{L,R}$ are constants independent of n and k. $\eta_{1,2}$ are roots of the characteristic equation

$$\eta^2 + \left(-2\cos k + \frac{t_x^2}{t^2}e^{ik}\right)\eta + 1 = 0, \tag{6.6}$$

so that $\eta_1\eta_2 = 1$. Hereafter we choose the convention $|\eta_1| < 1$. When $t_x/t \ll \sin k$, to the lowest nontrivial order in t_x/t,

$$\eta_1 \approx e^{ik}\left(1 - \frac{t_x^2}{t^2}\frac{e^{ik}}{2i\sin k}\right), \tag{6.7}$$

and thus $|\eta_1|^2 \approx 1 - t_x^2/t^2$.

Eq. (6.5) bypasses the difficulty of solving for each ϕ_n individually: on the same arm the constants C_L and C_R only change where the side lead incident amplitude $A_n^s \neq 0$.

Let us now quantify the conditions of small transmission and small reflection. Connecting external leads smoothly to both ends of a lossy arm of length $d_A \gg 1$, we may write the scattering state wave function incident from one end as

$$\begin{cases} e^{-ikn} + \tilde{R}e^{ikn}\ (\text{left lead},\ n = 0, 1, 2, \cdots) \\ C_L\eta_1^n + C_R\eta_1^{-n}\ (\text{lossy arm},\ n = 1, \cdots, d_A)\ \ ; \\ \tilde{T}e^{ikn}\ (\text{right lead},\ n = 0, 1, 2, \cdots) \end{cases} \tag{6.8}$$

the Schroedinger's equation then yields

$$1+\tilde{R}=C_L+C_R, \tag{6.9a}$$

$$e^{ik}+\tilde{R}e^{-ik}=C_L\eta_1+C_R\eta_1^{-1}, \tag{6.9b}$$

$$\tilde{T}=C_L\eta_1^{d_A+1}+C_R\eta_1^{-d_A-1}, \tag{6.9c}$$

$$\tilde{T}e^{-ik}=C_L\eta_1^{d_A}+C_R\eta_1^{-d_A}. \tag{6.9d}$$

It is now straightforward to find the transmission and reflection coefficients:

$$\tilde{T}=\frac{e^{ik}\left(e^{2ik}-1\right)\eta_1^{d_A}\left(\eta_1^2-1\right)}{1-\eta_1^{2d_A+2}+2e^{ik}\eta_1\left(\eta_1^{2d_A}-1\right)+e^{2ik}\left(\eta_1^2-\eta_1^{2d_A}\right)}, \tag{6.10a}$$

$$\tilde{R}=\frac{e^{ik}\left(\eta_1^{2d_A}-1\right)\left[e^{ik}\left(1+\eta_1^2\right)-\left(e^{2ik}+1\right)\eta_1\right]}{1-\eta_1^{2d_A+2}+2e^{ik}\eta_1\left(\eta_1^{2d_A}-1\right)+e^{2ik}\left(\eta_1^2-\eta_1^{2d_A}\right)}. \tag{6.10b}$$

At $k=0$ or π we always have trivially $\left|\tilde{R}\right|=1$ and $\left|\tilde{T}\right|=0$; we therefore focus on energies that are not too close to the band edges, so that $\sin k$ is not too small. In this case, under the long arm assumption $d_A\gg 1$, the small transmission condition $\left|\tilde{T}\right|\ll 1$ is satisfied if and only if $|\eta_1|^{d_A}\ll 1$, and the small reflection condition $\left|\tilde{R}\right|\ll 1$ is satisfied if and only if $t_x\ll t$.[40]

B. Background S-matrix and coupling site wave functions

We now return to the open long ring model to solve for S and Γ with the aid of Eq. (6.5). Let us denote the incident amplitude vector by

$$\left(A_1,A_2,A_0^{(L)},\cdots,A_{d_L-1}^{(L)},A_1^{(ref)},\cdots,A_{d_L}^{(ref)},A_0^{(R)},\cdots,A_{d_R-1}^{(R)}\right)^T; \tag{6.11}$$

here $A_n^{(\alpha)}$ is the incident amplitude in the side lead attached to the nth site on arm α. We are interested in the normalization factor V_k^2 and the source-lead component of the conductance tensor G_{12}; for this purpose, according to Eqs. (2.7) and (4.22), the first two rows of the S-matrix S and the full coupling site wave function matrix Γ must be found. In other words, we need to express the scattered amplitudes in the main leads B_1, B_2, as well as the wave functions at the coupling sites Γ_1 and Γ_2, in terms of incident amplitudes. Because the Schroedinger equation is linear and all incident amplitudes are independent, we can let all but one of the incident amplitudes be zero at a time, and obtain the full solution by means of linear superposition.

When the incident amplitudes from the side leads are all zero $A_n^{(\alpha)}=0$, according to Eq. (6.5) the wave function at wave vector k takes the form

$$\begin{cases} A_je^{-ikn}+B_je^{ikn}\,(\text{main lead } j=1,2,\ n=0,1,2,\cdots) \\ D_L^{(L)}\eta_1^n+D_R^{(L)}\eta_1^{-n}\,(\text{left QD arm},\ n=0,1,\cdots,d_L-1) \\ D_L^{(ref)}\eta_1^n+D_R^{(ref)}\eta_1^{-n}\,(\text{reference arm},\ n=1,2,\cdots,d_{ref}) \\ D_L^{(R)}\eta_1^n+D_R^{(R)}\eta_1^{-n}\,(\text{right QD arm},\ n=0,1,\cdots,d_R-1) \end{cases}. \tag{6.12}$$

To characterize the two Y-junctions in the AB ring, it is convenient to introduce the auxiliary objects S'_L and S'_R:

$$\begin{pmatrix} B_1 \\ D_R^{(L)}\eta_1^{-d_L+1} \\ D_L^{(ref)}\eta_1 \end{pmatrix} = S'_L \begin{pmatrix} A_1 \\ D_L^{(L)}\eta_1^{d_L-1} \\ D_R^{(ref)}\eta_1^{-1} \end{pmatrix}, \tag{6.13}$$

$$\begin{pmatrix} B_2 \\ D_R^{(R)}\eta_1^{-d_R+1} \\ D_R^{(ref)}\eta_1^{-d_{ref}} \end{pmatrix} = S'_R \begin{pmatrix} A_2 \\ D_L^{(R)}\eta_1^{d_R-1} \\ D_L^{(ref)}\eta_1^{d_{ref}} \end{pmatrix}. \tag{6.14}$$

The 3×3 matrices S'_L and S'_R are generally not unitary. They are properties of the Y-junctions, and are independent of the amplitudes (A, B etc.) and arm lengths (d_L, d_R and d_{ref}). In the limit $t_x/t \to 0$, $\eta_1 \to e^{ik}$, and S'_L and S'_R turn into the usual unitary S-matrices, which we denote as $S_{L,R} \equiv S'_{L,R}\,(t_x \to 0)$. For our model we can find S'_L and S'_R explicitly by solving the Schroedinger's equations below:

$$t_{JL}^L \phi_L = t\left(A_1 e^{ik} + B_1 e^{-ik}\right), \tag{6.15a}$$

$$t_{JQ}^L \phi_L = t\left(D_L^{(L)}\eta_1^{d_L} + D_R^{(L)}\eta_1^{-d_L}\right), \tag{6.15b}$$

$$t_{JR}^L \phi_L = t\left(D_L^{(ref)} + D_R^{(ref)}\right), \tag{6.15c}$$

$$\begin{aligned}(-2t\cos k)\,\phi_L = &-t_{JL}^L\,(A_1+B_1) - t_{JQ}^L\left(D_L^{(L)}\eta_1^{d_L-1} + D_R^{(L)}\eta_1^{-d_L+1}\right) \\ &- t_{JR}^L\left(D_L^{(ref)}\eta_1 + D_R^{(ref)}\eta_1^{-1}\right),\end{aligned} \tag{6.15d}$$

where ϕ_L is the wave function on the central site of the left Y-junction. We can solve for S'_R in a similar fashion.

For given A_1 and A_2, Eq. (6.12) has 8 unknowns. Now that S'_L and S'_R are known, Eqs. (6.13) and (6.14) provide us with 6 equations. The remaining two equations are the open boundary conditions at the ends of the two QD arms, appropriate when the QD is decoupled:

$$D_L^{(L)}\eta_1^{-1} + D_R^{(L)}\eta_1 = 0, \tag{6.16}$$

$$D_L^{(R)}\eta_1^{-1} + D_R^{(R)}\eta_1 = 0. \tag{6.17}$$

It is straightforward to solve the closed set of equations.

On the other hand, when we let one of the incident amplitudes in the side leads be nonzero, there are two additional amplitudes in the wave function. For instance, if $A_m^{(L)} \neq 0$ for a given m, we need to effectuate the following changes to the wave function on the left QD arm in Eq. (6.12):

$$\begin{cases} D_L^{(L1)}\eta_1^n + D_R^{(L1)}\eta_1^{-n}\ (\text{left QD arm},\ n = 0, 1, \cdots, m) \\ D_L^{(L2)}\eta_1^n + D_R^{(L2)}\eta_1^{-n}\ (\text{left QD arm},\ n = m, m+1, \cdots, d_L - 1) \end{cases}; \tag{6.18}$$

$D_{L,R}^{(L)}$ should be replaced by $D_{L,R}^{(L1)}$ in Eq. (6.16) and by $D_{L,R}^{(L2)}$ in Eq. (6.13). Furthermore, we should have two boundary conditions at site m:

$$D_L^{(L1)}\eta_1^m + D_R^{(L1)}\eta_1^{-m} = D_L^{(L2)}\eta_1^m + D_R^{(L2)}\eta_1^{-m}, \tag{6.19}$$

$$
\begin{aligned}
&-\left(\eta_1+\frac{1}{\eta_1}\right)\left(D_L^{(L1)}\eta_1^m+D_R^{(L1)}\eta_1^{-m}\right)\\
&=-\left(D_L^{(L1)}\eta_1^{m-1}+D_R^{(L1)}\eta_1^{-m+1}\right)-\left(D_L^{(L2)}\eta_1^{m+1}+D_R^{(L2)}\eta_1^{-(m+1)}\right)+e^{ik}\left(2i\sin k\right)\frac{t_x}{t}A_m^{(L)},
\end{aligned}
\tag{6.20}
$$

thus closing the set of equations. The last equation is none other than Eq. (6.4).

We are now in a position to present the solutions for B_1, B_2 and Γ_1, Γ_2 in terms of incident amplitudes. If we assume $d_L\sim d_R\sim d_{ref}/2\gg 1$ (comparable arm lengths and path lengths in the long ring) and $|\eta_1|^{d_L}\ll 1$ (small transmission criterion), we have to $O\left(|\eta_1|^{d_L}\right)$

$$
\begin{aligned}
B_1=&S'_{L11}A_1+S'_{L13}S'_{R31}\eta_1^{d_{ref}-1}A_2-\sum_{n=0}^{d_L-1}e^{ik}\left(2i\sin k\right)\frac{t_x}{t}\frac{\eta_1^{n+1}-\eta_1^{-n-1}}{\eta_1-\eta_1^{-1}}S'_{L12}\eta_1^{d_L}A_n^{(L)}\\
&+\sum_{n=1}^{d_{ref}}e^{ik}\left(2i\sin k\right)\frac{t_x}{t}\frac{S'_{R33}\eta_1^{d_{ref}-n}+\eta_1^{-d_{ref}+n}}{\eta_1-\eta_1^{-1}}S'_{L13}\eta_1^{d_{ref}-1}A_n^{(ref)},
\end{aligned}
\tag{6.21a}
$$

$$
\begin{aligned}
B_2=&S'_{L31}S'_{R13}\eta_1^{d_{ref}-1}A_1+S'_{R11}A_2+\sum_{n=1}^{d_{ref}}e^{ik}\left(2i\sin k\right)\frac{t_x}{t}\frac{\eta_1^{-n+1}+S'_{L33}\eta_1^{n-1}}{\eta_1-\eta_1^{-1}}S'_{R13}\eta_1^{d_{ref}-1}A_n^{(ref)}\\
&-\sum_{n=0}^{d_R-1}e^{ik}\left(2i\sin k\right)\frac{t_x}{t}\frac{\eta_1^{n+1}-\eta_1^{-n-1}}{\eta_1-\eta_1^{-1}}S'_{R12}\eta_1^{d_R}A_n^{(R)},
\end{aligned}
\tag{6.21b}
$$

$$
\begin{aligned}
\Gamma_1=&S'_{L21}\eta_1^{(d_L-1)}\left(1-\eta_1^2\right)A_1-\sum_{n=0}^{d_L-1}e^{ik}\left(2i\sin k\right)\frac{t_x}{t}\left(\eta_1^{-d_L+n+1}+S'_{L22}\eta_1^{d_L-n-1}\right)\eta_1^{d_L}A_n^{(L)}\\
&-\sum_{n=1}^{d_{ref}}e^{ik}\left(2i\sin k\right)\frac{t_x}{t}\left(S'_{R33}\eta_1^{d_{ref}-n}+\eta_1^{-d_{ref}+n}\right)S'_{L23}\eta_1^{d_L}\eta_1^{d_{ref}-1}A_n^{(ref)},
\end{aligned}
\tag{6.21c}
$$

$$
\begin{aligned}
\Gamma_2=&S'_{R21}\eta_1^{(d_R-1)}\left(1-\eta_1^2\right)A_2-\sum_{n=1}^{d_{ref}}e^{ik}\left(2i\sin k\right)\frac{t_x}{t}\left(\eta_1^{-n+1}+S'_{L33}\eta_1^{n-1}\right)S'_{R23}\eta_1^{d_R}\eta_1^{d_{ref}-1}A_n^{(ref)}\\
&-\sum_{n=0}^{d_R-1}e^{ik}\left(2i\sin k\right)\frac{t_x}{t}\left(\eta_1^{-d_R+n+1}+S'_{R22}\eta_1^{d_R-n-1}\right)\eta_1^{d_R}A_n^{(R)}.
\end{aligned}
\tag{6.21d}
$$

C. Kondo temperature and conductance

To the lowest nontrivial order in $|\eta|^{d_L}$, Eq. (6.21) leads to the following simple results after some algebra:

$$
V_k^2=-\left(\eta_1-\eta_1^*\right)\left(2i\sin k\right)\left(t_L^2+t_R^2\right),
\tag{6.22}
$$

$$
S_{12}\left(k\right)=S'_{L13}S'_{R31}\eta_1^{d_{ref}-1},
\tag{6.23}
$$

$$
\left[S\left(k\right)\Gamma^\dagger\left(k\right)\lambda\Gamma\left(k\right)\right]_{12}=t_Lt_Re^{i\varphi}\left(2i\sin k\right)\left(\eta_1-\eta_1^{-1}\right)S'_{L12}S'_{R21}\eta_1^{d_L+d_R}.
\tag{6.24}
$$

In obtaining Eq. (6.24) we have used the algebraic identity

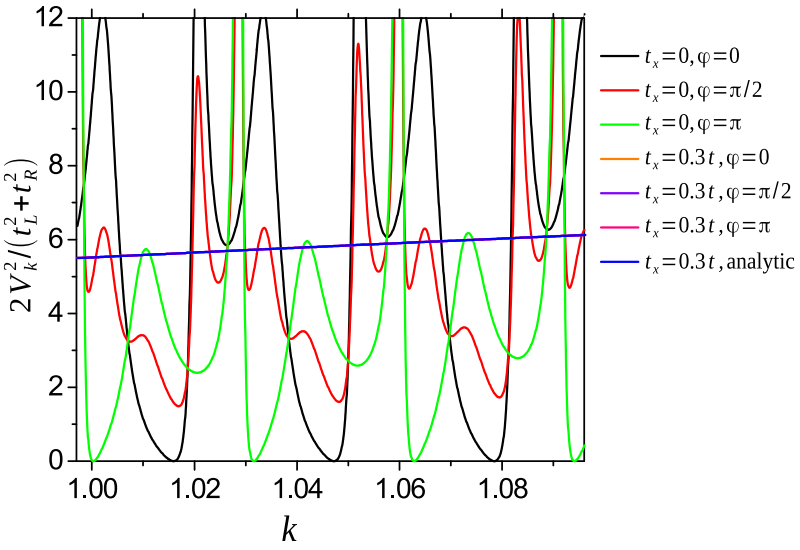

FIG. 10. Normalization factor V_k^2 from Eq. (2.7) as a function of k for different AB phases φ in the open long ABK ring, obtained by solving the full tight-binding model. We focus on a small slice of momentum $|k-\pi/3|<0.05$. Two values of t_x are considered: $t_x=0$ corresponding to the closed ring without electron leakage, and $t_x=0.3t$ corresponding to strong leakage along and small transmission across the arms. System parameters are: $d_L=d_R=d_{ref}/2=100$, $t_{JL}^{L,R}=t_{JQ}^{L,R}=t_{JR}^{L,R}=t$, and symmetric QD coupling $t_L=t_R$. For comparison we have also plotted the analytic prediction Eq. (6.22) for $t_x=0.3t$, which agrees quantitatively with the full tight-binding solution. While V_k^2 for the closed ring is extremely sensitive to k_F and φ, the sensitivity is strongly suppressed by electron leakage, and curves for different φ overlap when $t_x=0.3t$. Since V_k^2 controls the renormalization of the Kondo coupling, the Kondo temperature of the open long ABK ring is not sensitive to mesoscopic details in the small transmission limit.

$$S'^{*}_{L21}S'_{L11}\left|\left(1-\eta_1^2\right)\right|^2=\left(4\sin^2 k\right)\left(\frac{t_x}{t}\right)^2\left[\frac{|\eta_1|^2\eta_1^* S'_{L12}}{\eta_1-\eta_1^*}-\frac{|\eta_1|^2}{1-|\eta_1|^2}\left(S'^{*}_{L22}S'_{L12}+S'^{*}_{L23}S'_{L13}\right)\right]; \tag{6.25}$$

in the limit $t_x\to 0$ this is just a statement of the S-matrix unitarity.

Eq. (6.22) tells us that, in the small transmission limit, the normalization factor V_k^2 exhibits little mesoscopic fluctuation, so that $E_V\sim t$; furthermore, it does not depend on the AB phase φ at all (see Fig. 10). When we also impose the small reflection condition $t_x\ll t$, $\eta_1\approx e^{ik}$ and we find $V_k^2\approx\left(4\sin^2 k\right)\left(t_L^2+t_R^2\right)$; this is precisely the normalization factor for a QD embedded between source and drain leads. We recall from Eq. (2.15) that the normalization of Kondo coupling is governed by V_k^2. Therefore, at least for our simple model of an interacting QD, the conditions of small transmission and small reflection combine to reduce the Kondo temperature of the open long ABK ring to that of the simple embedded geometry, independent of the details of the ring or the AB flux.

Proceeding with the small transmission assumption, we observe that since $E_V\sim t$, the distinction between small and large Kondo cloud regimes is no longer applicable. This is presumably because the Kondo cloud leaks into the side leads in the open ring, and is no longer confined in a mesoscopic region as in the closed ring. The low-energy theory of our model is therefore the usual local Fermi liquid. At zero temperature, the connected contribution to the conductance vanishes, and the conductance G_{12} is proportional to the disconnected transmission probability Eq. (3.16) at the Fermi energy:

$$-\mathcal{T}_{12}^{D}\left(\epsilon_{k_F}\right)=\left|S'_{L13}S'_{R31}\eta_1^{d_{ref}-1}+\frac{2t_Lt_R}{t_L^2+t_R^2}e^{i\varphi}\frac{\eta_1-\eta_1^{-1}}{\eta_1-\eta_1^*}S'_{L12}S'_{R21}\eta_1^{d_L+d_R}\frac{1}{2}\left(e^{2i\delta_P}+1\right)\right|^2, \tag{6.26}$$

where η_1, S'_L and S'_R are all evaluated at the Fermi surface, and we have used Eqs. (4.16) and (4.19). In the small reflection case, Eq. (6.26) becomes

$$-\mathcal{T}_{12}^{D}\left(\epsilon_{k_F}\right)=\left|S_{L13}S_{R31}\eta_1^{d_{ref}-1}+e^{i\varphi}S_{L12}S_{R21}\eta_1^{d_L+d_R-2}t_{QD}\right|^2, \tag{6.27}$$

where $S_{L,R} \equiv S'_{L,R}(t_x \to 0)$ as previously defined, and

$$t_{QD} \equiv e^{2ik} \frac{2t_L t_R}{t_L^2 + t_R^2} \frac{1}{2} \left(e^{2i\delta_P} + 1\right) \tag{6.28}$$

is the transmission amplitude through an embedded QD in the Kondo limit [see Eq. (A4)].

It is clear from Eq. (6.26) that the two-slit condition $t_{sd} = t_{ref} + t_d e^{i\varphi}$ is satisfied at zero temperature. Furthermore, under the small reflection condition, both $t_{ref} = S_{L13} S_{R31} \eta_1^{d_{ref}-1}$ and $t_d = S_{L12} S_{R21} \eta_1^{d_L + d_R - 2} t_{QD}$ have straightforward physical interpretations; in particular t_d can be factorized into a part t_{QD} which is the intrinsic transmission amplitude through QD, and a part due completely to the rest of the QD arm and the two Y-junctions.

We now consider the finite temperature conductance, assuming realistically that $T \ll t$ and $T_K \ll t$. If we further assume that the two Y-junctions are non-resonant, so that S'_L and S'_R change significantly as functions of energy only on the scale of the bandwidth $4t$, then mesoscopic fluctuations are entirely absent from Eq. (6.24), i.e. $E_{\text{conn}} \sim t$. (It is worth mentioning that E_{conn} can be much less than t if the Y-junctions allow resonances, e.g. when the central site of each Y-junction is weakly coupled to all three legs; however, $E_V \sim t$ even in this case.) Since $T \ll E_{\text{conn}}$, we can comfortably eliminate the connected contribution and use Eq. (4.22). At $T \ll T_K$ the total Fermi liquid regime conductance $G(T, \varphi) \equiv -G_{12}$ is found to $O(T/T_K)^2$:

$$G(T,\varphi) \equiv G_{ref} + G_d + 2\sqrt{G_{ref} G_d} \left\{ \cos(\varphi + \theta + \delta_P) - \left(\frac{\pi T}{T_K}\right)^2 \right.$$
$$\left. \times \left[\frac{\cos(\varphi + \theta + \delta_P)}{2\cos^2 \delta_P} - \tan\delta_P \sin(\varphi + \theta + \delta_P) \right] \right\}. \tag{6.29a}$$

Here the conductance through the reference path is defined as

$$G_{ref} \equiv \frac{2e^2}{h} \left| S'_{L13} S'_{R31} \eta_1^{d_{ref}-1} \right|^2, \tag{6.29b}$$

the conductance through the QD path is defined as

$$G_d(T) \equiv G_d^{(0)} \left[\cos^2 \delta_P - \left(\frac{\pi T}{T_K}\right)^2 \cos 2\delta_P \right] \tag{6.29c}$$

with its $T = 0$ and $\delta_P = 0$ value

$$G_d^{(0)} \equiv \frac{2e^2}{h} \frac{4t_L^2 t_R^2}{(t_L^2 + t_R^2)^2} \left| \frac{\eta_1 - \eta_1^{-1}}{\eta_1 - \eta_1^*} S'_{L12} S'_{R21} \eta_1^{d_L + d_R} \right|^2, \tag{6.29d}$$

and finally the non-magnetic phase difference between the QD path and the reference path (*including* the QD) in the absence of δ_P is

$$\theta = \arg\left(\frac{\eta_1 - \eta_1^{-1}}{\eta_1 - \eta_1^*} \eta_1^{d_L + d_R - d_{ref} + 1} \frac{S'_{L12} S'_{R21}}{S'_{L13} S'_{R31}} \right). \tag{6.29e}$$

Once again, η_1, S'_L and S'_R are all evaluated at the Fermi surface.

For $T \gg T_K$, on the other hand, we consider the case of relatively strong particle-hole asymmetry $\kappa \sim j(T)$, so as to demonstrate the $\pi/2$ phase shift due to Kondo physics. The leading contribution to the conductance from potential scattering is $O(K)$, and the leading contribution from the Kondo coupling is $O(J^2)$; therefore, $\kappa \sim j(T)$ indicates that we may neglect the Kondo coupling altogether at this temperature. To the lowest order in potential scattering $O(K)$, Eq. (4.13) applies; also, since $T \ll t$, the thermal averging in Eq. (4.12) becomes trivial. Using the relation between K and δ_P, Eq. (4.17), we finally obtain

$$G(T,\varphi) = G_{ref} + 2\sqrt{G_{ref} G_d^{(0)}} \tan\delta_P \sin(\varphi + \theta). \tag{6.30}$$

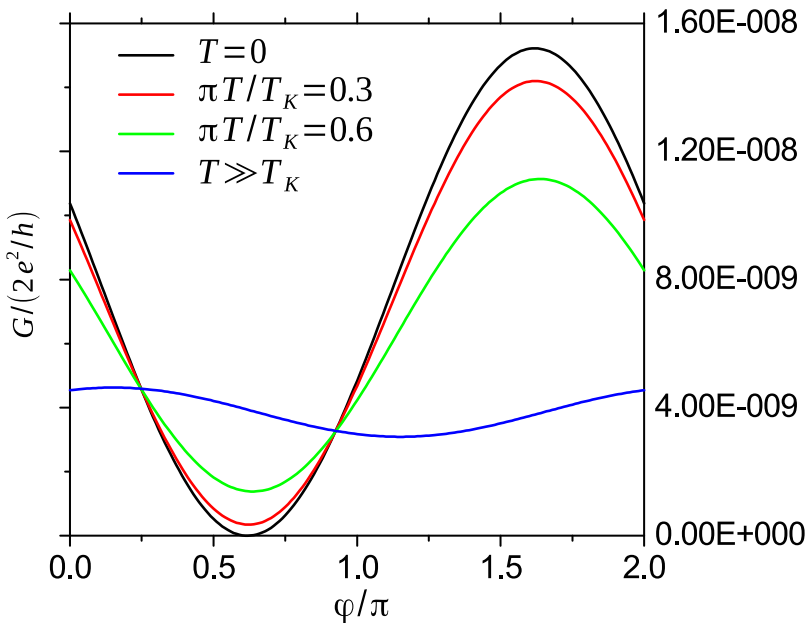

FIG. 11. Low-temperature and high-temperature conductances G as functions of AB phase φ in the open long ABK ring, calculated with Eqs. (6.29a) and (6.30). We assume $T_K \ll t$ so that the thermal averaging in the high temperature case is trivial. System parameters are: $t_x = 0.3t$, $k_F = \pi/3$, $d_L = d_R = d_{ref}/2 = 100$, $t_{JL}^{L,R} = t_{JQ}^{L,R} = t_{JR}^{L,R} = t$, and particle-hole symmetry breaking phase shift $\delta_P = 0.1$. A phase shift of approximately $\pi/2$ is clearly visible as the temperature is lowered and Kondo correlations become important.

Comparing Eqs. (6.29a) and (6.30), it becomes evident that transmission through the QD undergoes a $\pi/2+\delta_P$ phase shift from $T \gg T_K$ to $T \ll T_K$ as the Kondo correlations are switched on; see Fig. 11.

We can also make a direct comparison with Eq. (6.2). While θ itself is not necessarily $\pi/2$, φ_t is experimentally observed with respect to its value with Kondo correlations turned off, so we should define the reference value $\varphi_t^{(0)}$ by e.g. comparing with Eq. (6.30):

$$\varphi_t^{(0)} = \theta - \frac{\pi}{2}. \tag{6.31}$$

Therefore, to $O\left(T/T_K\right)^2$ we readily obtain the following results for the transmission phase and the normalized visibility:

$$\varphi_t - \varphi_t^{(0)} = \frac{\pi}{2} + \delta_P - \left(\frac{\pi T}{T_K}\right)^2 \tan\delta_P, \tag{6.32}$$

$$\eta_v = 1 - \left(\frac{\pi T}{T_K}\right)^2 \frac{1}{\cos^2\delta_P}. \tag{6.33}$$

These are in agreement with the $|\delta_P| \ll 1$, $T = 0$ and $\delta_P = 0$, $T \ll T_K$ results of Ref. 39, which assumes $\varphi_t^{(0)} = 0$, i.e. the non-magnetic phase difference between the two paths is zero without Kondo correlations. Note that in obtaining the T dependence in Eq. (6.33) it is crucial to include the connected contribution to conductance.

We stress that our $O\left(T/T_K\right)^2$ results for the transmission phase across the QD and the normalized visibility, Eqs. (6.32) and (6.33), are both exact in δ_P, which is non-universal and encompasses the effects of all particle-hole symmetry breaking perturbation. In particular, the $(T/T_K)^2$ coefficients were not reported previously.

VII. CONCLUSION AND OPEN QUESTIONS

In this paper, we generalized the method developed in Ref. 26 to calculate the linear DC conductance tensor of a generic multi-terminal Anderson model with an interacting QD. The linear DC conductance of the system has a disconnected contribution of the Landauer form, and a connected contribution which is also a Fermi surface property. At temperatures low compared to the mesoscopic energy scale below which the background S-matrix and the coupling site wave functions vary slowly, $T \ll E_{\text{conn}}$, the connected contribution can be approximately eliminated using properties of the conductance tensor; the elimination procedure physically corresponds to probing the current response or applying the bias voltages in a particular manner. At temperatures high compared to the Kondo temperature $T \gg T_K$ this connected part is computed explicitly to $O\left(J^2\right)$, and found to be of the same order of magnitude as the disconnected part in the case of a particle-hole symmetric QD.

With this method we scrutinize both closed and open long ABK ring models. We find modifications to early results on the closed ring with a long reference arm of length L: the high-temperature conductance at $T \gg T_K$ should have qualitatively distinct behaviors for $T \gg v_F/L$ and $T \ll v_F/L$. In the open ring we conclude that the two-path interferometer is realized when the arms on the ring have weak transmission and weak reflection, and demonstrate the possibility to observe in this device the $\pi/2$ phase shift due to Kondo physics, and the suppression of AB oscillation visibility due to inelastic scattering.

One question we have not so far addressed is the low-energy physics in the small Kondo cloud regime, $T \ll T_K$ and $E_V \ll T_K$; here E_V is the energy scale below which the normalization factor V_k^2 controlling the Kondo temperature varies slowly, and $E_V \gtrsim E_{\text{conn}}$. We assume E_V and E_{conn} are of the same order of magnitude, a condition satisfied by both the closed ring ($E_V \sim E_{\text{conn}} \sim v_F/L$) and the open ring with non-resonant Y-junctions ($E_V \sim E_{\text{conn}} \sim t$). For temperatures above the mesoscopic energy scale $E_V \ll T \ll T_K$, we are no longer able to eliminate the connected contribution. However, because $T \gg E_V$ one can argue that physics associated with the energy scale E_V is smeared out by thermal fluctuations, and the mesoscopic system behaves as a bulk system with parameters showing no mesoscopic fluctuations.[22] On the other hand, below the mesoscopic energy scale $T \ll E_V \ll T_K$, since for $T \ll E_{\text{conn}}$ our formalism predicts that the connected part can be eliminated, the knowledge of the screening channel T-matrix alone is adequate for us to predict the conductance. Ref. 22 again offers an appealing hypothesis: the low-energy effective theory is again a Fermi liquid theory, with the T-matrix governed by Kondo physics at short range $\sim O\left(L_K\right) = O\left(v_F/T_K\right)$ and modulated by mesoscopic fluctuations at long range $\sim O\left(L\right)$. This scenario leads to a quasiparticle spectrum which is in qualitative agreement with slave boson mean field theory.[22] The Fermi liquid picture is often analyzed by a renormalized perturbation theory of the quasiparticles, where the bare parameters of the QD are replaced by renormalized values; in particular the large U between bare electrons is replaced by a small renormalized $\tilde{U}$ between quasiparticles.[2] In the small Kondo cloud regime, we expect that the real space geometry in the renormalized perturbation theory resembles that of the bare theory;[15] thus a perturbation theory calculation in U in our formalism is potentially useful in understanding the low-energy physics, as long as U is interpreted as the effective $\tilde{U}$. It will be interesting to test this $E_V \ll T_K$ picture, along with our perturbative predictions on conductance in other parameter regimes in this paper, against results obtained from the numerical RG algorithm.[47,50,51]

There is also an issue regarding the assumption of a single-level QD in the Kondo regime. To experimentally detect the $\pi/2$ phase shift in an AB interferometer, one typically sweeps the plunger gate voltage on the QD, and monitors the phase shift between consecutive Coulomb blockade peaks. A $\pi/2$ plateau should be observed at $T \lesssim T_K$ near the center of each Coulomb valley deep in the local moment regime, with an odd number of electrons on the QD.[38,50] However, one needs to adopt a multi-level QD model to quantitatively reproduce the experimental results, in particular the phase shift lineshape asymmetry relative to the center of a valley, and also possibly a phase lapse inside the valley.[38,52] A generalization of the current formalism to the multi-level case is necessary in order to quantify the influence of the interferometer on the measured transmission phase shift through a realistic QD.

Another natural open problem is the extension to the multi-channel Kondo physics. In our generalized Anderson model, separation of screening and non-screening channels is achieved in a single-level QD, and there is only one effective screening channel. Exotic physics emerges in the presence of two or more screening channels, realizable in e.g. a many-QD system.[44,53,54] In the 2-channel Kondo effect with identical couplings to two channels, for example, the low-energy physics is governed by a non-Fermi liquid RG fixed point: at zero temperature a single particle scattered by the impurity can only enter a many-body state, and there are no elastic single-particle scattering events.[6] Ref. 39 discusses the manifestations of the 2-channel Kondo physics in the two-path interferometer, but again makes the two-slit assumption without examining its validity. Therefore an extension of our approach to the multi-channel case will be useful to justify the two-slit assumption in the open long ring and thus the 2-channel predictions of Ref. 39.

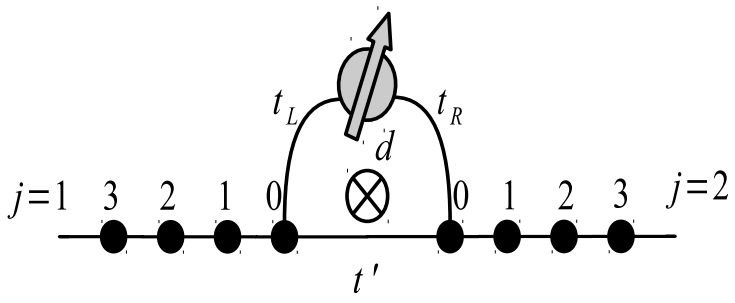

FIG. 12. The short ABK ring studied in Refs. 26 and 30.

ACKNOWLEDGMENTS

This work was supported in part by NSERC of Canada, Discovery Grant 36318-2009 (ZS). ZS is grateful to Prof. Ian Affleck for initiating the project, extensive discussions and proofreading the manuscript. YK gratefully acknowledges the kind hospitality of UBC Department of Physics and Astronomy during his visit. The authors would also like to acknowledge fruitful discussions with Prof. L. I. Glazman.

Appendix A: Comparison with early results

1. Short ABK ring

Our formalism can be applied to the short ABK ring[26,30] shown in Fig. 12. There are two leads ($N = 2$) and two coupling sites ($M = 2$); $H_{0,\text{junction}} = -t' \left(c^{\dagger}_{1,0} c_{2,0} + \text{h.c.} \right)$. The coupling sites coincide with the 0th sites of the leads, $c_{C,r=1} \equiv c_{1,0}$, $c_{C,r=2} \equiv c_{2,0}$; also the AB phase is on the couplings to the QD, $t_1 = t_L e^{i\frac{\varphi}{2}}$ and $t_2 = t_R e^{-i\frac{\varphi}{2}}$. We again let $\tilde{\tau} = t'/t$.

It is straightforward to obtain the background S-matrix and coupling site wave function matrix:

$$S(k) = -\frac{1}{1-\tilde{\tau}^2 e^{2ik}} \begin{pmatrix} e^{2ik}\left(1-\tilde{\tau}^2\right) & e^{ik}\tilde{\tau}\left(e^{2ik}-1\right) \\ e^{ik}\tilde{\tau}\left(e^{2ik}-1\right) & e^{2ik}\left(1-\tilde{\tau}^2\right) \end{pmatrix}, \tag{A1}$$

$$\Gamma(k) = -\frac{1}{1-\tilde{\tau}^2 e^{2ik}} \begin{pmatrix} e^{2ik}-1 & 2ie^{2ik}\tilde{\tau}\sin k \\ 2ie^{2ik}\tilde{\tau}\sin k & e^{2ik}-1 \end{pmatrix}. \tag{A2}$$

With Eqs. (2.15), (4.14) and (4.22), one reproduces all analytic results in Refs. 26 and 30, including the Kondo temperature, the high- and low-temperature conductance, and the elimination of connected contribution at low temperatures.

The limit $t' = 0$ is useful as a benchmark against long ring geometries so we study it in some more detail. In this limit we recover the simplest geometry where a QD is embedded between source and drain leads. The normalization factor is

$$V_k^2 = 4\left(t_L^2 + t_R^2\right)\sin^2 k, \tag{A3}$$

and the zero-temperature transmission amplitude through the QD is given by Eqs. (3.16), (4.16), (4.19) and (4.21):

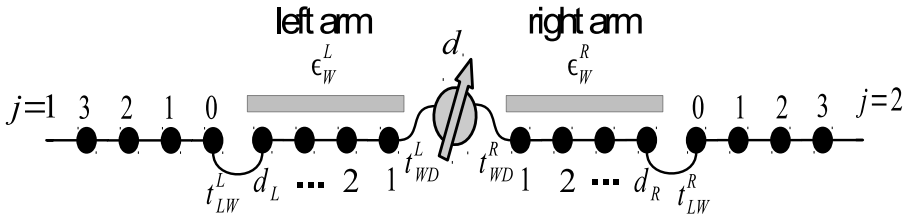

FIG. 13. The finite quantum wire geometry studied in Ref. 15.

$$t_{QD} \equiv \frac{2i}{V_k^2}\left[S\left(k\right)\Gamma^{\dagger}\left(k\right)\lambda\Gamma\left(k\right)\right]_{12}\left[-\pi\nu \mathrm{T}_{kk}\left(\epsilon_k\right)\right]$$
$$= e^{2ik}\frac{2t_L t_R}{t_L^2+t_R^2}\frac{1}{2}\left(e^{2i\delta_P}+1\right). \tag{A4}$$

2. Finite quantum wire

Another special case is the finite wire (or semi-transparent Kondo box) geometry in Fig. 13 where the reference arm is absent;[15] again $N = M = 2$. The left and right QD arms and coupling sites are subject to gate voltages:

$$H_{0,\text{junction}} = -t\left(\sum_{n=1}^{d_L-1} c_{L,n}^{\dagger}c_{L,n+1} + \sum_{n=1}^{d_R-1} c_{R,n}^{\dagger}c_{R,n+1} + \text{h.c.}\right)$$
$$+\left(\epsilon_W^L\sum_{n=1}^{d_L} c_{L,n}^{\dagger}c_{L,n} + \epsilon_W^R\sum_{n=1}^{d_R} c_{R,n}^{\dagger}c_{R,n}\right)$$
$$-\left(t_{LW}^L c_{L,d_L}^{\dagger}c_{1,0} + t_{LW}^R c_{R,d_R}^{\dagger}c_{2,0} + \text{h.c.}\right). \tag{A5}$$

The coupling sites are the first sites of the QD arms, $c_{C,r=1} \equiv c_{L,1}$, $c_{C,r=2} \equiv c_{R,1}$; $t_1 = t_{WD}^L$ and $t_2 = t_{WD}^R$.

The two leads are decoupled without the QD, so S and Γ are both diagonal. In this system we have

$$S_{11}\left(k\right) = -\frac{e^{ik}\sin k_L\left(d_L+1\right) - \gamma_L^2\sin k_L d_L}{e^{-ik}\sin k_L\left(d_L+1\right) - \gamma_L^2\sin k_L d_L}, \tag{A6}$$

and

$$\Gamma_{11}\left(k\right) = -\frac{2i\gamma_L\sin k\sin k_L}{e^{-ik}\sin k_L\left(d_L+1\right) - \gamma_L^2\sin k_L d_L}, \tag{A7}$$

where k_L is determined by the gate voltage ϵ_W^L,

$$-2t\cos k_L + \epsilon_W^L = -2t\cos k, \tag{A8}$$

and $\gamma_L = t_{LW}^L/t$. S_{22} and Γ_{22} can be obtained simply by substituting L with R. Again, these results allow us to reproduce the (weak coupling) Kondo temperature, the high-temperature conductance, as well as the low-temperature conductance in the large Kondo cloud regime. (We did not quantitatively discuss the low-temperature conductance in the small cloud regime in this paper; see Sec. VII.)

Appendix B: Details of the disconnected contribution

In this appendix we present the detailed derivation of Eq. (3.16) [or equivalently Eq. (3.18a)] from Eq. (3.9). The calculations are similar to those in Appendix B of Ref. 26, but an important difference is that here we cannot simply take the δ-function part and neglect the principal value part in Eq. (3.9). Instead, most of the momentum integrals are evaluated by means of contour integration.

From Eq. (3.12)

$$\begin{aligned}-2\,\mathrm{Im}\,\mathbb{G}^{R}_{k_2q_1}(\omega) &= (2\pi)^2\,\delta(k_2-q_1)\,\delta(\omega-\epsilon_{k_2})+i\tau_\psi \\ &\quad\times\left[g^{R}_{k_2}(\omega)\,V_{k_2}G^{R}_{dd}(\omega)\,V_{q_1}g^{R}_{q_1}(\omega)-g^{A}_{k_2}(\omega)\,V_{k_2}G^{A}_{dd}(\omega)\,V_{q_1}g^{A}_{q_1}(\omega)\right].\end{aligned} \tag{B1}$$

We denote the three terms above as 0, R and A respectively. Inserting into Eq. (3.9), we find 3 types of contributions to the disconnected part:

$$\begin{aligned}G'^{D}_{jj'}(\Omega) &= G'^{D}_{jj',00}(\Omega)+\left[G'^{D}_{jj',0R}(\Omega)+G'^{D}_{jj',0A}(\Omega)+G'^{D}_{jj',R0}(\Omega)+G'^{D}_{jj',A0}(\Omega)\right] \\ &\quad+\left[G'^{D}_{jj',RA}(\Omega)+G'^{D}_{jj',RR}(\Omega)+G'^{D}_{jj',AR}(\Omega)+G'^{D}_{jj',AA}(\Omega)\right];\end{aligned} \tag{B2}$$

The 00 term is the background transmission, the first pair of square brackets is linear in the T-matrix of the screening channel, and the second pair of square brackets is quadratic in the T-matrix.

Due to the multiplying factor of Ω in Eq. (3.2), $O(1/\Omega)$ terms in $G'^{D}_{jj'}$ contribute to the linear DC conductance, while $O(1)$ and other terms which are regular in the DC limit $\Omega\to 0$ do not contribute. (We can check explicitly that there are no $O\left(1/\Omega^2\right)$ or higher-order divergences.) Therefore, in the DC limit we are only interested in the $O(1/\Omega)$ part of $G'^{D}_{jj'}$.

1. Properties of the S-matrix and the wave functions

Before actually doing the calculations it is useful to examine the properties of the background S-matrix and the wave functions in our tight-binding model, since we rely on these properties to transform the momentum integrals into contour integrals and evaluate them.

First consider the analytic continuation $k\to -k$. The wave function "incident" from lead j at momentum $-k$ takes the following form on lead j' [cf. Eq. (2.3a)],

$$\chi_{j,-k}(j',n)=\delta_{jj'}e^{ikn}+S_{j'j}(-k)\,e^{-ikn}; \tag{B3}$$

and on coupling site r,

$$\chi_{j,-k}(r)=\Gamma_{rj}(-k).$$

This wave function should be a linear combination of the scattering state wave functions at momentum k which form a complete basis. The linear coefficients are obtained from S-matrix unitarity:

$$\chi_{j,-k}(j',n)=\sum_{j''}S^{*}_{jj''}(k)\,\chi_{j'',k}(j',n)=\delta_{jj'}e^{ikn}+S^{*}_{jj'}(k)\,e^{-ikn}, \tag{B4}$$

and the same coefficients apply to the coupling sites:

$$\chi_{j,-k}(r)=\sum_{j''}S^{*}_{jj''}(k)\,\Gamma_{rj''}(k).$$

Hence

$$S(-k)=S^{\dagger}(k), \tag{B5}$$

$$\Gamma(-k) = \Gamma(k) S^{\dagger}(k). \tag{B6}$$

Eq. (B5) is known as the Hermitian analyticity of the S-matrix.[55]

Another useful property is the location of poles of $S(k) \equiv S\left(z = e^{ik}\right)$ on the z complex plane. Our analysis closely follows Ref. 56 which deals with the case of quadratic dispersion.

Consider one pole of the S-matrix $k \equiv k_1 + ik_2$, where for certain values of j and j', $|S_{j'j}(k)| \to \infty$. In the scattering state $|q_{j,k}\rangle \equiv q^{\dagger}_{j,k}|0\rangle$, where $|0\rangle$ is the Fermi sea ground state, the incident component of the wave function at momentum k becomes negligible relative to the scattered component. Therefore, the time-dependent wave function on lead j' at site n reads

$$\chi_{j,k}(j', n, \bar{t}) \approx S_{j'j}(k) e^{ikn} e^{-i\epsilon_k \bar{t}} = S_{j'j}(k) e^{ikn} e^{2it\bar{t}\cos k_1 \cosh k_2} e^{2t\bar{t}\sin k_1 \sinh k_2}. \tag{B7}$$

This expression is valid for any j' where $|S_{j'j}(k)|$ is divergent; for other j' the wave function is negligible.

We define the "junction area" to include any tight-binding site that is not part of a lead, together with the 0th site of each lead. The total probability of the electron being inside the junction area, $N(\bar{t})$, obeys the probability continuity equation

$$\frac{d}{d\bar{t}} N(\bar{t}) = it \sum_{j'} \left(c^{\dagger}_{j',0} c_{j',1} - c^{\dagger}_{j',1} c_{j',0} \right)(\bar{t}), \tag{B8}$$

where the right-hand side is the current operator between site 0 and site 1 of lead j', summed over all leads. Taking the expectation value in the state $|q_{j,k}\rangle$, we find

$$-(4t \sin k_1 \sinh k_2) C_j(k) e^{4t\bar{t}\sin k_1 \sinh k_2} = \sum_{j'} (2t \sin k_1) e^{-k_2} |S_{j'j}(k)|^2 e^{4t\bar{t}\sin k_1 \sinh k_2}. \tag{B9}$$

For the left-hand side we have used the form of the time evolution $e^{-i\epsilon_k \bar{t}}$, and $C_j(k)$ is a positive time-independent constant proportional to the total probability in the junction area; $C_j(k)$ is divergent whenever $|S_{j'j}(k)|$ is divergent. For the right-hand side, we have used Eq. (B7) at $n = 0$ and $n = 1$; the summation is over any j' where $|S_{j'j}(k)|$ is divergent.

Eq. (B9) implies that either $\sin k_1 = 0$, in which case $k_1 = 0$ or π; or $\sinh k_2 < 0$, in which case $\left|e^{i(k_1 + ik_2)}\right| > 1$. The poles of $S(k)$ on the $z = e^{ik}$ plane are therefore either outside the unit circle or located on the real axis. For the models we study in this paper, the poles of $S(k)$ and those of $\Gamma(k)/(\sin k)$ coincide (see also Sec. C); in other words, the poles of $S(k)$ and $\Gamma(k)/(\sin k)$ on the $z = e^{ik}$ plane are either outside the unit circle or on the real axis.

We mention that similar results apply in the theory with a reduced bandwidth and a linearized dispersion in the leads. Eqs. (B5) and (B6) continue to hold; on the other hand, the probability current is proportional to v_F instead of $2t \sin k_1$, and all poles of $S(k)$ and $\Gamma(k)/(\sin k)$ are located in the lower half of the k plane.

2. Background transmission

This part is independent of the QD and the result should be the famous Landauer formula:

$$G'^{D}_{jj',00}(\Omega) = 2 \int_0^{\pi} \frac{dk_1 dk_2}{(2\pi)^2} \frac{f(\epsilon_{k_1}) - f(\epsilon_{k_2})}{\epsilon_{k_1} - \epsilon_{k_2} + \Omega^+} \operatorname{tr}\left(\mathbb{M}^{j}_{k_1 k_2} \mathbb{M}^{j'}_{k_2 k_1} \right). \tag{B10}$$

Inserting Eq. (3.6), taking advantage of Eq. (B5) and the unitarity of the $\mathbb{U}$ matrix, we find

$$\begin{aligned} G'^{D}_{jj',00}(\Omega) = 2 \int_{-\pi}^{\pi} & \frac{dk_1 dk_2}{(2\pi)^2} \frac{f(\epsilon_{k_1}) - f(\epsilon_{k_2})}{\epsilon_{k_1} - \epsilon_{k_2} + \Omega^+} \\ & \times \left\{ \delta_{jj'} \frac{1}{1 - e^{i(k_1 - k_2 + i0)}} \frac{1}{1 - e^{i(k_2 - k_1 + i0)}} + S^{*}_{jj'}(k_1) \delta_{jj'} \frac{1}{1 - e^{-i(k_1 + k_2 - i0)}} \frac{1}{1 - e^{i(k_2 - k_1 + i0)}} \right. \\ & \left. + \delta_{jj'} S_{jj'}(k_2) \frac{1}{1 - e^{i(k_1 + k_2 + i0)}} \frac{1}{1 - e^{i(k_2 - k_1 + i0)}} + S^{*}_{jj'}(k_1) S_{jj'}(k_2) \frac{1}{\left[1 - e^{i(k_2 - k_1 + i0)}\right]^2} \right\}. \end{aligned} \tag{B11}$$

By residue theorem we can perform the k_2 integral in the part proportional to $f(\epsilon_{k_1})$ and the k_1 integral in the part proportional to $f(\epsilon_{k_2})$. In the following we assume $\Omega > 0$; the case $\Omega < 0$ can be dealt with similarly.

We begin from the first term in curly brackets, which is proportional to $\delta_{jj'}$. For the part proportional to $f(\epsilon_{k_1})$, making the substitution $z_2 = e^{ik_2}$, and calculating the contour integral on the counterclockwise unit circle, we find

$$\begin{aligned}&\int_{-\pi}^{\pi} \frac{dk_2}{2\pi} \frac{f(\epsilon_{k_1})}{\epsilon_{k_1} - \epsilon_{k_2} + \Omega^+} \frac{1}{1 - e^{i(k_1 - k_2 + i\eta)}} \frac{1}{1 - e^{i(k_2 - k_1 + i\eta)}} \\ &= \frac{f(\epsilon_{k_1})}{2it \sin p_1} \frac{1}{1 - e^{i(k_1 - p_1)}} \frac{1}{1 - e^{i(p_1 - k_1)}} + \frac{f(\epsilon_{k_1})}{\Omega} \frac{1}{1 - e^{-2\eta}},\end{aligned} \tag{B12a}$$

where $\eta \to 0^+$. (η corresponds to the rate of switching on the bias voltage in Kubo formalism, so the limit $\eta \to 0$ should be taken before the DC limit $\Omega \to 0$.) We have assumed $\epsilon_{k_1} + \Omega \equiv \epsilon_{p_1}$ where $0 \le p_1 \le \pi$ if p_1 is real; the poles of the integrand inside the unit circle are then $z_2 = e^{i(p_1 + i0)}$ and $z_2 = e^{i(k_1 + i\eta)}$. At the band edges, $2t - \Omega < \epsilon_{k_1} < 2t$, and p_1 is purely imaginary; we can choose it to have a positive imaginary part so the above expression remains valid. Similarly

$$\begin{aligned}&\int_{-\pi}^{\pi} \frac{dk_1}{2\pi} \frac{f(\epsilon_{k_2})}{\epsilon_{k_1} - \epsilon_{k_2} + \Omega^+} \frac{1}{1 - e^{i(k_1 - k_2 + i\eta)}} \frac{1}{1 - e^{i(k_2 - k_1 + i\eta)}} \\ &= \frac{f(\epsilon_{k_2})}{2it \sin p_2} \frac{1}{1 - e^{i(-p_2 - k_2)}} \frac{1}{1 - e^{i(p_2 + k_2)}} + \frac{f(\epsilon_{k_2})}{\Omega} \frac{1}{1 - e^{-2\eta}},\end{aligned} \tag{B12b}$$

where $\epsilon_{k_2} - \Omega = \epsilon_{p_2}$, $0 \le p_2 \le \pi$ if p_2 is real, or $p_2 = -i|p_2|$ if p_2 is purely imaginary. Now combine the two parts. In the $\Omega \to 0$ limit, $p_1 \to k_1$ only for p_1 real and $k_1 > 0$, and $p_2 \to -k_2$ only for p_2 real and $k_2 < 0$; the most divergent contribution is therefore

$$\begin{aligned}&\int_{-\pi}^{\pi} \frac{dk_1 dk_2}{(2\pi)^2} \frac{f(\epsilon_{k_1}) - f(\epsilon_{k_2})}{\epsilon_{k_1} - \epsilon_{k_2} + \Omega^+} \frac{1}{1 - e^{i(k_1 - k_2 + i0)}} \frac{1}{1 - e^{i(k_2 - k_1 + i0)}} \\ &= \int_{-2t}^{2t-\Omega} \frac{d\epsilon_{k_1}}{2\pi i} \left[f(\epsilon_{k_1}) - f(\epsilon_{k_1} + \Omega)\right] \frac{1}{(2t \sin k_1)(2t \sin p_1)} \frac{1}{1 - e^{i(k_1 - p_1)}} \frac{1}{1 - e^{i(p_1 - k_1)}} + O(1).\end{aligned} \tag{B13}$$

We have substituted the dummy variables $k_2 \to p_1$, $p_2 \to k_1$, and noted that $\epsilon_{p_1} = \epsilon_{k_1} + \Omega$. Expanding various parts of the integrand in $\Omega \to 0$ limit, we find

$$\begin{aligned}&\int_{-\pi}^{\pi} \frac{dk_1 dk_2}{(2\pi)^2} \frac{f(\epsilon_{k_1}) - f(\epsilon_{k_2})}{\epsilon_{k_1} - \epsilon_{k_2} + \Omega^+} \frac{1}{1 - e^{i(k_1 - k_2 + i0)}} \frac{1}{1 - e^{i(k_2 - k_1 + i0)}} \\ &= \frac{1}{2\pi i \Omega} \int_{-2t}^{2t-\Omega} d\epsilon_{k_1} \left[-f'(\epsilon_{k_1})\right] + O(1).\end{aligned} \tag{B14}$$

The two terms in $G'^D_{jj',00}(\Omega)$ which are linear in the S-matrix do not contribute any terms of $O(1/\Omega)$ to $G'^D_{jj'}$: the difference of Fermi functions is proportional to Ω, but the denominators are also $O(\Omega)$, unlike the case for the $\delta_{jj'}$ terms whose denominators are $O(\Omega^2)$. This leaves us with the term quadratic in the S-matrix, which can be similarly evaluated. For the part proportional to $f(\epsilon_{k_1})$,

$$\begin{aligned}&\int_{-\pi}^{\pi} \frac{dk_2}{2\pi} \frac{f(\epsilon_{k_1})}{\epsilon_{k_1} - \epsilon_{k_2} + \Omega^+} S^*_{jj'}(k_1) S_{jj'}(k_2) \frac{1}{\left[1 - e^{i(k_2 - k_1 + i0)}\right]^2} \\ &= \frac{f(\epsilon_{k_1})}{2it \sin p_1} S^*_{jj'}(k_1) S_{jj'}(p_1) \frac{1}{\left[1 - e^{i(p_1 - k_1)}\right]^2} + (\text{contribution of poles of } S_{jj'});\end{aligned} \tag{B15a}$$

the poles of $S_{jj'}$ inside the unit circle (on the real axis) may contribute to the contour integral, but these terms are regular in the $\Omega \to 0$ limit and do not contribute to the DC conductance. Similarly

$$\int_{-\pi}^{\pi}\frac{dk_1}{2\pi}\frac{f\left(\epsilon_{k_2}\right)}{\epsilon_{k_1}-\epsilon_{k_2}+\Omega^{+}}S_{jj'}^{*}\left(k_1\right)S_{jj'}\left(k_2\right)\frac{1}{\left[1-e^{i(k_2-k_1+i0)}\right]^2}$$
$$=\frac{f\left(\epsilon_{k_2}\right)}{2it\sin p_2}S_{jj'}^{*}\left(p_2\right)S_{jj'}\left(k_2\right)\frac{1}{\left[1-e^{i(k_2-p_2)}\right]^2}+\left(\text{contribution of poles of } S_{jj'}^{*}\right), \tag{B15b}$$

Therefore

$$\int_{-\pi}^{\pi}\frac{dk_1dk_2}{\left(2\pi\right)^2}\frac{f\left(\epsilon_{k_1}\right)-f\left(\epsilon_{k_2}\right)}{\epsilon_{k_1}-\epsilon_{k_2}+\Omega^{+}}S_{jj'}^{*}\left(k_1\right)S_{jj'}\left(k_2\right)\frac{1}{\left[1-e^{i(k_2-k_1+i0)}\right]^2}$$
$$=\int_{-2t}^{2t-\Omega}\frac{d\epsilon_{k_1}}{2\pi i}\frac{f\left(\epsilon_{k_1}\right)-f\left(\epsilon_{k_1}+\Omega\right)}{\left(2t\sin k_1\right)\left(2t\sin p_1\right)}S_{jj'}^{*}\left(k_1\right)S_{jj'}\left(p_1\right)\frac{1}{\left[1-e^{i(p_1-k_1)}\right]^2}+O\left(1\right)$$
$$=-\frac{1}{2\pi i\Omega}\int_{-2t}^{2t-\Omega}d\epsilon_{k_1}\left[-f'\left(\epsilon_{k_1}\right)\right]S_{jj'}^{*}\left(k_1\right)S_{jj'}\left(p_1\right)+O\left(1\right). \tag{B16}$$

From Eqs. (B14) and (B16), we conclude that

$$G_{jj',00}'^{D}\left(\Omega\right)=\frac{1}{\pi i\Omega}\int_{-2t}^{2t-\Omega}d\epsilon_{k_1}\left[-f'\left(\epsilon_{k_1}\right)\right]\left[\delta_{jj'}-S_{jj'}^{*}\left(k_1\right)S_{jj'}\left(p_1\right)\right]+O\left(1\right); \tag{B17}$$

taking the $\Omega\to 0$ limit, noting that $p_1\to k_1$, we recover the Landauer formula, Eq. (3.18b).

3. Terms linear in T-matrix

We focus on $G_{jj',0R}'^{D}+G_{jj',0A}'^{D}$; the calculation of $G_{jj',R0}'^{D}+G_{jj',A0}'^{D}$ is analogous.

$$G_{jj',0R}'^{D}\left(\Omega\right)+G_{jj',0A}'^{D}\left(\Omega\right)$$
$$=2\int_{0}^{\pi}\frac{dk_1}{\left(2\pi\right)^2}\frac{dq_1dq_2}{\left(2\pi\right)^2}\int d\omega\frac{f\left(\omega\right)-f\left(\epsilon_{q_1}\right)}{\omega-\epsilon_{q_1}+\Omega^{+}}\operatorname{tr}\left\{\mathbb{M}_{k_1q_1}^{j}\mathbb{M}_{q_1q_2}^{j'}\left(i\tau_{\psi}\right)\right.$$
$$\left.\times\left[g_{q_2}^{R}\left(\omega\right)V_{q_2}G_{dd}^{R}\left(\omega\right)V_{k_1}g_{k_1}^{R}\left(\omega\right)-g_{q_2}^{A}\left(\omega\right)V_{q_2}G_{dd}^{A}\left(\omega\right)V_{k_1}g_{k_1}^{A}\left(\omega\right)\right]\right\}. \tag{B18}$$

Using Eqs. (2.10), (3.6), (B5) and (B6), a huge simplification takes place:

$$G_{jj',0R}'^{D}\left(\Omega\right)$$
$$=2\int_{-\pi}^{\pi}\frac{dk_1dq_1dq_2}{\left(2\pi\right)^4}\int d\omega\frac{f\left(\omega\right)-f\left(\epsilon_{q_1}\right)}{\omega-\epsilon_{q_1}+\Omega^{+}}ig_{q_2}^{R}\left(\omega\right)G_{dd}^{R}\left(\omega\right)g_{k_1}^{R}\left(\omega\right)\sum_{r_1r_2}t_{r_1}^{*}t_{r_2}$$
$$\times\Gamma_{r_1j}\left(k_1\right)\left[\delta_{jj'}\frac{1}{1-e^{i(k_1-q_1+i0)}}+S_{jj'}\left(q_1\right)\frac{1}{1-e^{i(k_1+q_1+i0)}}\right]\Gamma_{r_2j'}^{*}\left(q_2\right)\frac{1}{1-e^{i(q_1-q_2+i0)}}, \tag{B19a}$$

$$G_{jj',0A}'^{D}\left(\Omega\right)$$
$$=2\int_{-\pi}^{\pi}\frac{dk_1dq_1dq_2}{\left(2\pi\right)^4}\int d\omega\frac{f\left(\omega\right)-f\left(\epsilon_{q_1}\right)}{\omega-\epsilon_{q_1}+\Omega^{+}}\left(-i\right)g_{q_2}^{A}\left(\omega\right)G_{dd}^{A}\left(\omega\right)g_{k_1}^{A}\left(\omega\right)\sum_{r_1r_2}t_{r_1}^{*}t_{r_2}$$
$$\times\Gamma_{r_1j}\left(k_1\right)\left[\delta_{jj'}\frac{1}{1-e^{i(k_1-q_1+i0)}}+S_{jj'}\left(q_1\right)\frac{1}{1-e^{i(k_1+q_1+i0)}}\right]\Gamma_{r_2j'}^{*}\left(q_2\right)\frac{1}{1-e^{i(q_1-q_2+i0)}}. \tag{B19b}$$

Writing $\omega = \epsilon_k$, where $0 \le k \le \pi$ or $k = i\,|k|$, we are now free to do the k_1 and q_2 integrals. The poles of $\Gamma(k_1)$ and $\Gamma^*(q_2)$ are again not important in the DC limit:

$$\begin{aligned}
&G'^{D}_{jj',0R}(\Omega) \\
&= 2\int_{-\pi}^{\pi}\frac{dq_1}{(2\pi)^2}\int d\epsilon_k \frac{f(\epsilon_k)-f(\epsilon_{q_1})}{\epsilon_k-\epsilon_{q_1}+\Omega^+} i\sum_{r_1r_2} t^*_{r_1}t_{r_2}\frac{1}{2it\sin k}G^R_{dd}(\epsilon_k)\frac{1}{2it\sin k} \\
&\times \Gamma_{r_1j}(k)\left[\delta_{jj'}\frac{1}{1-e^{i(k-q_1+i0)}}+S_{jj'}(q_1)\frac{1}{1-e^{i(k+q_1+i0)}}\right]\Gamma^*_{r_2j'}(-k)\frac{1}{1-e^{i(q_1+k+i0)}}+O(1),
\end{aligned} \tag{B20a}$$

$$\begin{aligned}
&G'^{D}_{jj',0A}(\Omega) \\
&= 2\int_{-\pi}^{\pi}\frac{dq_1}{(2\pi)^2}\int d\epsilon_k \frac{f(\epsilon_k)-f(\epsilon_{q_1})}{\epsilon_k-\epsilon_{q_1}+\Omega^+}(-i)\sum_{r_1r_2} t^*_{r_1}t_{r_2}\frac{1}{-2it\sin k}G^A_{dd}(\epsilon_k)\frac{1}{-2it\sin k} \\
&\times \Gamma_{r_1j}(-k)\left[\delta_{jj'}\frac{1}{1-e^{i(-k-q_1+i0)}}+S_{jj'}(q_1)\frac{1}{1-e^{i(-k+q_1+i0)}}\right]\Gamma^*_{r_2j'}(k)\frac{1}{1-e^{i(q_1-k+i0)}}+O(1).
\end{aligned} \tag{B20b}$$

Now do the ϵ_k and q_1 integrals. The $\delta_{jj'}$ terms are regular in the DC limit, so we only need to keep the $S_{jj'}$ terms. In the $0R$ term, while the q_1 integral in the $f(\epsilon_k)$ part is straightforward, the ϵ_k integral in the $f(\epsilon_{q_1})$ part can be simplified by expanding around $k+q_1=0$:

$$\begin{aligned}
&G'^{D}_{jj',0R}(\Omega) \\
&= 2\frac{1}{2\pi}\int_{-2t}^{2t-\Omega} d\epsilon_k \frac{f(\epsilon_k)}{2it\sin p} i\sum_{r_1r_2} t^*_{r_1}t_{r_2}\frac{1}{2it\sin k}G^R_{dd}(\epsilon_k)\frac{\Gamma_{r_1j}(k)\Gamma^*_{r_2j'}(-k)}{2it\sin k}S_{jj'}(p) \\
&\times \frac{1}{\left[1-e^{i(k+p+i0)}\right]^2} - 2\int_{-\pi}^{0}\frac{dq_1}{(2\pi)^2}(2t\sin q_1)S_{jj'}(q_1)\int_{-\infty}^{\infty}d\epsilon_k\frac{f(\epsilon_{q_1})}{(\epsilon_k-\epsilon_{q_1}+\Omega^+)} \\
&\times i\sum_{r_1r_2} t^*_{r_1}t_{r_2}G^R_{dd}(\epsilon_k)\frac{\Gamma_{r_1j}(k)\Gamma^*_{r_2j'}(-k)}{2t\sin k}\frac{1}{(\epsilon_k-\epsilon_{-q_1}+i0)^2}+O(1) \\
&= O(1).
\end{aligned} \tag{B21a}$$

Here, in the $f(\epsilon_k)$ part, we have written $\epsilon_k+\Omega \equiv \epsilon_p$ $(0 \le p \le \pi)$ assuming $\Omega > 0$, integrated over q_1 using the complex variable e^{iq_1}, and again neglected $O(1)$ contributions from the poles of $S(q_1)$. Because $k+p$ is always positive and never close to 0, the denominator for the $f(\epsilon_k)$ part is $O(1)$; thus the $f(\epsilon_k)$ part is itself $O(1)$. Meanwhile, in the $f(\epsilon_{q_1})$ part, we have used $(2t\sin k)(k+q_1+i0) \approx (2t\sin q_1)(k+q_1+i0) \approx \epsilon_k-\epsilon_{-q_1}+i0$ for $|k+q_1| \ll 1$. We then extend the ϵ_k domain of integration back to the entire real axis. Both $G^R_{dd}(\epsilon_k)$ and $\Gamma_{r_1j}(k)\Gamma^*_{r_2j'}(-k)/(\sin k)$ are analytic in the upper ϵ_k half plane; thus, closing the ϵ_k contour above the real axis, the ϵ_k integral in the $f(\epsilon_{q_1})$ part sees no pole and vanishes. Similarly, in the $0A$ term,

$$\begin{aligned}
&G'^{D}_{jj',0A}(\Omega) \\
&= 2\frac{1}{2\pi i}\int_{-2t}^{2t-\Omega} d\epsilon_k f(\epsilon_k)(-i)\sum_{r_1r_2} t^*_{r_1}t_{r_2}G^A_{dd}(\epsilon_k)\frac{\Gamma_{r_1j}(-k)\Gamma^*_{r_2j'}(k)}{2t\sin k}S_{jj'}(p)\frac{1}{\Omega^2} \\
&- 2\int_{-2t+\Omega}^{2t}\frac{d\epsilon_{q_1}}{2\pi i}S_{jj'}(q_1)f(\epsilon_{q_1})(-i)\sum_{r_1r_2} t^*_{r_1}t_{r_2}G^A_{dd}(\epsilon_{p_1})\frac{\Gamma_{r_1j}(-p_1)\Gamma^*_{r_2j'}(p_1)}{2t\sin p_1}\frac{1}{\Omega^2}+O(1) \\
&= -2\frac{1}{\pi\Omega}\int_{-2t}^{2t-\Omega} d\epsilon_k\left[-f'(\epsilon_k)\right]\sum_{r_1r_2} t^*_{r_1}t_{r_2}\Gamma_{r_1j}(-k)\Gamma^*_{r_2j'}(k)\pi\nu_k G^A_{dd}(\epsilon_k)S_{jj'}(p)+O(1).
\end{aligned} \tag{B21b}$$

We have adopted the shorthand $\epsilon_{q_1}-\Omega \equiv \epsilon_{p_1}$ $(0 \le p_1 \le \pi)$ and identified k with p_1 and p with q_1. This result, together with $G'^{D}_{jj',R0}+G'^{D}_{jj',A0}$ which yields its complex conjugate, leads to Eqs. (3.18c) and (3.18d).

4. Terms quadratic in T-matrix

We focus on $G'^{D}_{jj',RR}(\Omega)+G'^{D}_{jj',RA}(\Omega)$ first.

$$\begin{aligned}
&G'^{D}_{jj',RR}(\Omega)+G'^{D}_{jj',RA}(\Omega)\\
&=2\int\frac{d\omega d\omega'}{(2\pi)^2}\frac{f(\omega)-f(\omega')}{\omega-\omega'+\Omega^+}\int_0^\pi\frac{dk_1dk_2}{(2\pi)^2}\frac{dq_1dq_2}{(2\pi)^2}\,\mathrm{tr}\left\{\mathbb{M}^{j}_{k_1k_2}(i\tau_\psi)\,g^R_{k_2}(\omega')\,V_{k_2}G^R_{dd}(\omega')\,V_{q_1}g^R_{q_1}(\omega')\right.\\
&\left.\times\,\mathbb{M}^{j'}_{q_1q_2}(i\tau_\psi)\left[g^R_{q_2}(\omega)\,V_{q_2}G^R_{dd}(\omega)\,V_{k_1}g^R_{k_1}(\omega)-g^A_{q_2}(\omega)\,V_{q_2}G^A_{dd}(\omega)\,V_{k_1}g^A_{k_1}(\omega)\right]\right\}.
\end{aligned}\tag{B22}$$

Inserting Eqs. (2.10), (3.6) and using Eq. (B6) again, we find

$$\begin{aligned}
&G'^{D}_{jj',RR}(\Omega)+G'^{D}_{jj',RA}(\Omega)\\
&=2\int\frac{d\omega d\omega'}{(2\pi)^2}\frac{f(\omega)-f(\omega')}{\omega-\omega'+\Omega^+}\int_{-\pi}^{\pi}\frac{dk_1dk_2}{(2\pi)^2}\frac{dq_1dq_2}{(2\pi)^2}\sum_{r_1r_2r_1'r_2'}t^*_{r_1}t_{r_2}t^*_{r_1'}t_{r_2'}\Gamma_{r_1j}(k_1)\\
&\times\Gamma^*_{r_2j}(k_2)\frac{1}{1-e^{i(k_1-k_2+i0)}}ig^R_{k_2}(\omega')\,G^R_{dd}(\omega')\,g^R_{q_1}(\omega')\,\Gamma_{r_1'j'}(q_1)\,\Gamma^*_{r_2'j'}(q_2)\\
&\times\frac{1}{1-e^{i(q_1-q_2+i0)}}i\left[g^R_{q_2}(\omega)\,G^R_{dd}(\omega)\,g^R_{k_1}(\omega)-g^A_{q_2}(\omega)\,G^A_{dd}(\omega)\,g^A_{k_1}(\omega)\right].
\end{aligned}\tag{B23}$$

We can integrate over all four momenta. Let $\omega=\epsilon_k$ where $0\le k\le\pi$ or $k=i|k|$, and $\omega'=\epsilon_{k'}$ where $0\le k'\le\pi$ or $k'=-i|k'|$; integrating over k_2 and q_1,

$$\begin{aligned}
&G'^{D}_{jj',RR}(\Omega)+G'^{D}_{jj',RA}(\Omega)\\
&=2\int\frac{d\epsilon_kd\epsilon_{k'}}{(2\pi)^2}\frac{f(\epsilon_k)-f(\epsilon_{k'})}{\epsilon_k-\epsilon_{k'}+\Omega^+}\int_{-\pi}^{\pi}\frac{dk_1dq_2}{(2\pi)^2}\sum_{r_1r_2r_1'r_2'}t^*_{r_1}t_{r_2}t^*_{r_1'}t_{r_2'}\Gamma_{r_1j}(k_1)\\
&\times\Gamma^*_{r_2j}(-k')\frac{1}{1-e^{i(k_1+k'+i0)}}i\frac{1}{2it\sin k'}G^R_{dd}(\epsilon_{k'})\frac{1}{2it\sin k'}\Gamma_{r_1'j'}(k')\,\Gamma^*_{r_2'j'}(q_2)\\
&\times\frac{1}{1-e^{i(k'-q_2+i0)}}i\left[g^R_{q_2}(\epsilon_k)\,G^R_{dd}(\epsilon_k)\,g^R_{k_1}(\epsilon_k)-g^A_{q_2}(\epsilon_k)\,G^A_{dd}(\epsilon_k)\,g^A_{k_1}(\epsilon_k)\right];
\end{aligned}\tag{B24}$$

finally, integrating over k_1 and q_2, we find

$$G'^{D}_{jj',RR}(\Omega)=O(1),\tag{B25a}$$

$$\begin{aligned}
&G'^{D}_{jj',RA}(\Omega)\\
&=2\int\frac{d\epsilon_kd\epsilon_{k'}}{(2\pi)^2}\frac{f(\epsilon_k)-f(\epsilon_{k'})}{\epsilon_k-\epsilon_{k'}+\Omega^+}\sum_{r_1r_2r_1'r_2'}t^*_{r_1}t_{r_2}t^*_{r_1'}t_{r_2'}\Gamma_{r_1j}(-k)\,\Gamma^*_{r_2j}(-k')\,\Gamma_{r_1'j'}(k')\\
&\times\Gamma^*_{r_2'j'}(k)\frac{1}{(2t\sin k')^2}\frac{1}{(2t\sin k)^2}\frac{1}{\left[1-e^{i(k'-k+i0)}\right]^2}G^R_{dd}(\epsilon_{k'})\,G^A_{dd}(\epsilon_k).
\end{aligned}\tag{B25b}$$

Expanding around $k=k'$ and integrating over ϵ_k and $\epsilon_{k'}$, assuming $\Omega>0$, we obtain

$$\begin{aligned}
&G'^{D}_{jj',RA}(\Omega)\\
&=2\int_{-2t}^{2t-\Omega}\frac{d\epsilon_k}{2\pi i}\Omega\left[-f'(\epsilon_k)\right]\sum_{r_1r_2r_1'r_2'}t^*_{r_1}t_{r_2}t^*_{r_1'}t_{r_2'}\frac{\Gamma_{r_1j}(-k)\,\Gamma^*_{r_2'j'}(k)}{2t\sin k}\\
&\times\frac{\Gamma^*_{r_2j}(-p)\,\Gamma_{r_1'j'}(p)}{2t\sin p}\frac{1}{-\Omega^2}G^R_{dd}(\epsilon_p)\,G^A_{dd}(\epsilon_k)+O(1),
\end{aligned}\tag{B26}$$

where we have written $\epsilon_k + \Omega \equiv \epsilon_p$. A similar calculation can be performed on $G'^D_{jj',AR}(\Omega)$ and $G'^D_{jj',AA}(\Omega)$; both are $O(1)$ for the same reason that $G'^D_{jj',RR}(\Omega)$ is $O(1)$. Therefore, $G'^D_{jj',RA}$ is the only term quadratic in the T-matrix which contributes to the linear DC conductance. Note that this is not the case in Ref. 26, where the RA term and the AR term are complex conjugates as a result of taking the δ-function part in Eq. (3.9). It is easy to see that Eq. (B26) reproduces Eq. (3.18e).

We mention in passing that Eq. (3.18a) can be derived in the wide band limit with essentially the same method, although the pole structure is much simpler in that case.

Appendix C: Non-interacting QD

In this appendix we verify Eq. (3.16) in the case of a non-interacting QD with $U = 0$ as a consistency check on our formalism. The connected part must vanish completely in this case; thus the disconnected contribution to the conductance should coincide with the Landauer formula, with an S-matrix modified by the presence of the non-interacting QD.

1. Relation between $S(k)$ and $\Gamma(k)$

First let us quantify the relation between the background S-matrix $S(k)$ and the coupling site wave function matrix $\Gamma(k)$. $S(k)$ and $\Gamma(k)$ are both determined by the non-interacting part of the system H_0 with the QD decoupled, and are usually intimately related: for instance they often have the same poles on the complex momentum plane, and have resonances (sharp changes in amplitude and phase) over the same range of real momenta. To characterize this relation, we attach to each of the M coupling sites an additional "phantom" lead. These phantom leads have the same nearest neighbor hopping t as the N pre-existing leads. The coupling site is designated as site 0 of its phantom lead. We let S^0 be the S-matrix of the resulting non-interacting system with $(N+M)$ leads; that is, for the scattering state incident from lead m with momentum k, the wave function on lead m' should be

$$\chi_{m,k}(m',n) = \delta_{mm'}e^{-ikn} + S^0_{m'm}(k)\,e^{ikn}. \tag{C1}$$

m and m' can be $j = 1, \cdots, N$ or $r = 1, \cdots, M$, so that S^0 is an $(N+M)\times(N+M)$ unitary matrix. For future convenience we partition S^0 as follows,

$$S^0 \equiv \begin{pmatrix} S^0_{LL} & S^0_{LD} \\ S^0_{DL} & S^0_{DD} \end{pmatrix}, \tag{C2}$$

where L and D are shorthands for lead and dot respectively; S^0_{LL} is $N\times N$ and S^0_{DD} is $M\times M$. Note that S^0_{LL} and S^0_{DD} are not usually unitary, although all four blocks are constrained by the overall unitarity of S^0. Also, our argument for $S(-k)$ in Sec. B applies to $S^0(-k)$:

$$S^0(-k) = \left[S^0(k)\right]^\dagger. \tag{C3}$$

Due to the non-interacting nature of the system, we can conveniently express S and Γ in terms of the auxiliary object S^0. With the QD decoupled, the phantom leads should be terminated by open boundary conditions. The wave function on phantom lead r should be

$$\chi_{j,k}(r,n) = \frac{\Gamma_{rj}(k)}{2i\sin k}\left(e^{ik}e^{-ikn} - e^{-ik}e^{ikn}\right), \tag{C4}$$

so that $\chi_{j,k}(r,1) = 0$ and $\chi_{j,k}(r,0) = \Gamma_{rj}(k)$. The incident amplitude and reflected amplitude in lead r are respectively $\pm e^{\pm ik}\Gamma_{rj}(k)/(2i\sin k)$. We then see, from the definition of S^0, that $\Gamma_{rj}(k)$ and S obey the following relations:

$$S^0_{rj}(k) + \sum_{r'=1}^{M} S^0_{rr'}(k)\,\frac{\Gamma_{r'j}(k)\,e^{ik}}{2i\sin k} = -\frac{\Gamma_{rj}(k)\,e^{-ik}}{2i\sin k}, \tag{C5a}$$

$$S_{j'j}(k) = S^0_{j'j}(k) + \sum_{r'=1}^{M} S^0_{j'r'}(k) \frac{\Gamma_{r'j}(k) e^{ik}}{2i \sin k}. \tag{C5b}$$

Therefore,

$$\Gamma(k) = -(2i \sin k) \left[e^{ik} S^0_{DD}(k) + e^{-ik}\right]^{-1} S^0_{DL}(k), \tag{C6}$$

and

$$S(k) = S^0_{LL}(k) - S^0_{LD}(k) \left[e^{ik} S^0_{DD}(k) + e^{-ik}\right]^{-1} S^0_{DL}(k) e^{ik}. \tag{C7}$$

It is straightforward to check the unitarity of $S(k)$.

2. Green's function of the QD

We now find the retarded T-matrix of the non-interacting QD. As is standard for the non-interacting Anderson model in Eq. (2.5),[46] the retarded Green's function for the QD is

$$G^R_{dd}(\omega) = \frac{1}{\omega^+ - \epsilon_d - \Sigma^R_{dd}(\omega)}, \tag{C8}$$

where $\omega^+ \equiv \omega + i0$, and the retarded self-energy is

$$\Sigma^R_{dd}(\omega) = \int_0^\pi \frac{dq}{2\pi} \frac{V_q^2}{\omega^+ - \epsilon_q} = \int_0^\pi \frac{dq}{2\pi} \frac{\mathrm{tr}\left(\lambda \Gamma_q \Gamma_q^\dagger\right)}{\omega^+ - \epsilon_q}. \tag{C9}$$

We have used Eq. (2.7). Inserting Eq. (C6), using the unitarity of S^0 and Eq. (C3), we obtain

$$\begin{aligned}
&\int_0^\pi \frac{dq}{2\pi} \frac{\Gamma_q \Gamma_q^\dagger}{\omega^+ - \epsilon_q} \\
&= \int_0^\pi \frac{dq}{2\pi} \frac{4 \sin^2 q}{\omega^+ - \epsilon_q} \left[e^{2iq} S^0_{DD}(q) + 1\right]^{-1} \left[1 - S^0_{DD}(q) \left(S^0_{DD}(q)\right)^\dagger\right] \left\{\left[e^{2iq} S^0_{DD}(q) + 1\right]^{-1}\right\}^\dagger \\
&= \int_0^\pi \frac{dq}{2\pi} \frac{4 \sin^2 q}{\omega^+ - \epsilon_q} \left(\left[e^{2iq} S^0_{DD}(q) + 1\right]^{-1} + \left\{\left[e^{2iq} S^0_{DD}(q) + 1\right]^{-1}\right\}^\dagger - 1\right) \\
&= \int_{-\pi}^\pi \frac{dq}{2\pi} \frac{4 \sin^2 q}{\omega^+ - \epsilon_q} \left\{\left[e^{2iq} S^0_{DD}(q) + 1\right]^{-1} - \frac{1}{2}\right\}.
\end{aligned} \tag{C10}$$

With contour methods it is straightforward to show, for $0 < p < \pi$ and integer n, that

$$\int_{-\pi}^\pi \frac{dq}{2\pi} \frac{e^{inq}}{\epsilon_p - \epsilon_q + i0} = \frac{e^{i|n|p}}{2it \sin p}. \tag{C11}$$

We now make the assumption that $S^0_{DD}\left(z = e^{iq}\right) \equiv S^0_{DD}(q)$ is analytic at the origin of the complex plane. This appears to be a reasonable assumption, because a singularity at the origin would imply an infinite energy feature, which should decouple completely from any properties of system probed at finite energies. Thus $S^0_{DD}(z)$ can be expanded around the origin in a Taylor series of z, and we may integrate term by term to find

$$\int_{-\pi}^\pi \frac{dq}{2\pi} \frac{e^{in_1 q} \left[S^0_{DD}(q)\right]^{n_2}}{\epsilon_p - \epsilon_q + i0} = \frac{e^{in_1 p} \left[S^0_{DD}(p)\right]^{n_2}}{2it \sin p}, \tag{C12}$$

where n_1 and n_2 are non-negative integers.

Expanding $4\sin^2 q\left\{\left[e^{2iq}S^0_{DD}(q)+1\right]^{-1}-1/2\right\}$ in powers of e^{iq} and $S^0_{DD}(q)$, the only negative power term in the series is $-(1/2)\,e^{-2iq}$; therefore, by Eq. (C11),

$$\int_0^\pi \frac{dq}{2\pi}\frac{\Gamma_q\Gamma_q^\dagger}{\epsilon_p-\epsilon_q+i0}=\frac{1}{2it\sin p}\left(4\sin^2 p\left\{\left[e^{2ip}S^0_{DD}(p)+1\right]^{-1}-\frac{1}{2}\right\}+\frac{1}{2}e^{-2ip}-\frac{1}{2}e^{2ip}\right), \tag{C13}$$

and hence

$$\Sigma^R_{dd}(\epsilon_p)=-\frac{1}{t}\,\mathrm{tr}\left(\lambda\left\{e^{-ip}+2i\sin p\left[e^{2ip}S^0_{DD}(p)+1\right]^{-1}\right\}\right). \tag{C14}$$

Eqs. (C8) and (C14) give the retarded T-matrix $\mathrm{T}_{pp}(\epsilon_p)=V_p^2G^R_{dd}(\epsilon_p)$. One can easily verify that the optical theorem $\mathrm{Im}\left[-\pi\nu_p\mathrm{T}_{pp}(\epsilon_p)\right]=\left|-\pi\nu_p\mathrm{T}_{pp}(\epsilon_p)\right|^2$ is obeyed, which must be the case for a non-interacting system. Inserting Eqs. (C7), (C6), (C8), and (C14) into Eq. (3.16), we find

$$\mathcal{T}^D_{jj'}(\epsilon_p)=\delta_{jj'}-\left|S^{\mathrm{NI}}_{jj'}(p)\right|^2, \tag{C15}$$

where

$$\begin{aligned}S^{\mathrm{NI}}(p)=S^0_{LL}(p)+S^0_{LD}(p)\Bigg\{&\frac{(2i\sin p)\,e^{-2ip}\left[S^0_{DD}(p)+e^{-2ip}\right]^{-1}\bar\lambda_p\left[S^0_{DD}(p)+e^{-2ip}\right]^{-1}}{1+\mathrm{tr}\left(\bar\lambda_p\left\{e^{-ip}+2i\sin p\left[e^{2ip}S^0_{DD}(p)+1\right]^{-1}\right\}\right)}\\&-\left[S^0_{DD}(p)+e^{-2ip}\right]^{-1}\Bigg\}S^0_{DL}(p).\end{aligned} \tag{C16}$$

Here we have defined the dimensionless coupling matrix

$$\bar\lambda_p\equiv\frac{\lambda}{t(\epsilon_p-\epsilon_d)}. \tag{C17}$$

3. Landauer formula

We turn to the alternative method of scattering state wave functions to find the S-matrix S^{NI} in the presence of the QD.

By definition, for the scattering state incident from j, the wave function on lead j' is

$$\chi_{j,k}(j',n)=\delta_{jj'}e^{-ikn}+S^{\mathrm{NI}}_{j'j}(k)\,e^{ikn}. \tag{C18}$$

The coupling sites are now attached to the QD. We imagine that the QD and the coupling sites are separated by "phantom leads" of zero length, so that the wave function on phantom lead r takes the form

$$\chi_{j,k}(r,n)=A_{r,j,k}e^{-ikn}+B_{r,j,k}e^{ikn}, \tag{C19}$$

where $n=0$ only. Since the phantom leads are also attached to the QD, the Schroedinger equation on coupling site r is

$$t\left(A_{r,j,k}e^{-ik}+B_{r,j,k}e^{ik}\right)=t_r\phi_j(k), \tag{C20}$$

where $\phi_j(k)$ is the wave function on the QD. Meanwhile, the Schroedinger equation on the QD itself is

$$\epsilon_k \phi_j(k) = \epsilon_d \phi_j(k) - \sum_r t_r^* \left(A_{r,j,k} + B_{r,j,k}\right). \tag{C21}$$

Eqs. (C20) and (C21) allow us to express $B_{r,j,k}$ in terms of $A_{r,j,k}$, i.e. to find the S-matrix for the non-interacting QD:

$$t\left(A_{r,j,k}e^{-ik} + B_{r,j,k}e^{ik}\right) = -\frac{t_r}{\epsilon_k - \epsilon_d}\sum_{r'} t_{r'}^* \left(A_{r',j,k} + B_{r',j,k}\right), \tag{C22}$$

or more compactly

$$e^{-ik}A_k + e^{ik}B_k = -\bar{\lambda}_k\left(A_k + B_k\right), \tag{C23}$$

$$B_k = -\left(e^{ik} + \bar{\lambda}_k\right)^{-1}\left(e^{-ik} + \bar{\lambda}_k\right)A_k. \tag{C24}$$

On the other hand, the amplitudes A_k and B_k are also related to each other and to S^{NI} by the phantom-lead S-matrix S^0:

$$S^0_{rj}(k) + \sum_{r'} S^0_{rr'}(k)\, A_{r',j,k} = B_{r,j,k}, \tag{C25}$$

and

$$S^{\mathrm{NI}}_{j'j}(k) = S^0_{j'j}(k) + \sum_{r'} S^0_{j'r'}(k)\, A_{r',j,k}. \tag{C26}$$

Eliminating A_k and B_k from Eqs. (C24), (C25) and (C26) finally yields

$$S^{\mathrm{NI}}(k) = S^0_{LL}(k) - S^0_{LD}(k)\left[S^0_{DD}(k) + \left(e^{ik} + \bar{\lambda}_k\right)^{-1}\left(e^{-ik} + \bar{\lambda}_k\right)\right]^{-1} S^0_{DL}(k). \tag{C27}$$

Using Eqs. (2.8) and (C17), it is a lengthy but straightforward task to prove the equivalence of Eqs. (C16) and (C27). Therefore the disconnected contribution to the conductance recovers the Landauer formula in the case of a non-interacting QD.

Appendix D: Connected contribution in Fermi liquid theory

In this appendix, as another consistency check on our formalism, we directly compute the $O\left(T^2/T_K^2\right)$ connected contribution to the DC conductance in the very large Kondo cloud Fermi liquid regime $T \ll T_K \ll v_F/L$, and show that Eq. (3.33) is indeed satisfied.

Inserting Eqs. (4.5) and (4.18) into Eq. (4.6), and performing the k_1, k_2, q_1 and q_2 integrals, we obtain

$$\begin{aligned}\mathcal{G}'^{C}_{jj'}(i\omega_p) = \int \frac{dp_1 dp_2 dp_3 dp_4}{(2\pi)^4}\tilde{\mathcal{G}}^{C}_{p_1p_2p_3p_4}(i\omega_p)\sum_{j_1j_2}\sum_{j'_1j'_2}\mathbb{U}_{1,j_1}\mathbb{U}^*_{1,j_2}\mathbb{U}_{1,j'_1}\mathbb{U}^*_{1,j'_2}\\ \times\left(\delta_{jj_1}\delta_{jj_2}\frac{i}{p_1 - p_2 + i0} + S^*_{jj_1}S_{jj_2}\frac{i}{p_2 - p_1 + i0}\right)\\ \times\left(\delta_{j'j'_1}\delta_{j'j'_2}\frac{i}{p_3 - p_4 + i0} + S^*_{j'j'_1}S_{j'j'_2}\frac{i}{p_4 - p_3 + i0}\right);\end{aligned} \tag{D1}$$

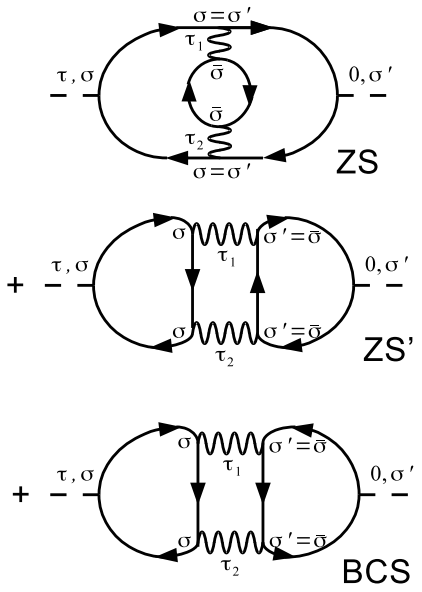

FIG. 14. The three connected diagrams at $O\left(T^2/T_K^2\right)$ contributing to the conductance. ZS, ZS' and BCS label only the topology of the diagrams and not necessarily the physics.

we have ignored the momentum dependence of $\mathbb{U}$ and S in the Fermi liquid regime. Here the δ_P-independent connected four-point correlation function for $\tilde{\psi}$ is defined as

$$\tilde{\mathcal{G}}^C_{p_1p_2p_3p_4}\left(i\omega_p\right) \equiv -\int_0^\beta d\tau e^{i\omega_p\tau} \sum_{\sigma\sigma'} \left\langle T_\tau \tilde{\psi}^\dagger_{p_1\sigma}\left(\tau\right) \tilde{\psi}_{p_2\sigma}\left(\tau\right) \tilde{\psi}^\dagger_{p_3\sigma'}\left(0\right) \tilde{\psi}_{p_4\sigma'}\left(0\right) \right\rangle_C . \tag{D2}$$

We observe that $\delta_{\psi\psi}$ drops out of $\mathcal{G}'^C_{jj'}$ completely, which reflects the inelastic nature of the connected contribution.

In momentum space, the leading irrelevant operator Eq. (4.20) takes the form

$$H_{int} = \frac{2\pi v_F^2}{T_K} \int \frac{dq_1 dq_2 dq_3 dq_4}{\left(2\pi\right)^4} : \tilde{\psi}^\dagger_{q_1\alpha} \tilde{\psi}_{q_2\alpha} \tilde{\psi}^\dagger_{q_3\beta} \tilde{\psi}_{q_4\beta} : - \frac{v_F^2}{T_K} \int \frac{dq_1 dq_2}{\left(2\pi\right)^2} \left(q_1 + q_2\right) : \tilde{\psi}^\dagger_{q_1\alpha} \tilde{\psi}_{q_2\alpha} : ; \tag{D3}$$

only the first term plays a role in the connected contribution.

To $O\left(T^2/T_K^2\right)$, there are three diagrams resulting in nonzero contributions to the linear DC conductance, depicted in Fig. 14. The corresponding 4-point functions read

$$\begin{aligned} \tilde{\mathcal{G}}^{C,\mathrm{BCS}}_{p_1p_2p_3p_4}\left(i\omega_p\right) = -4 \left(\frac{2\pi v_F^2}{T_K}\right)^2 \int_0^\beta d\tau e^{i\omega_p\tau} \int_0^\beta d\tau_1 d\tau_2 \sum_{\sigma\sigma'} \delta_{\sigma\bar{\sigma}'} \int \frac{dq_1 dq_3}{\left(2\pi\right)^2} \\ \times g_{p_1}\left(\tau_1 - \tau\right) g_{p_2}\left(\tau - \tau_2\right) g_{p_3}\left(\tau_1\right) g_{p_4}\left(-\tau_2\right) g_{q_1}\left(\tau_2 - \tau_1\right) g_{q_3}\left(\tau_2 - \tau_1\right) , \end{aligned} \tag{D4a}$$

$$\begin{aligned} \tilde{\mathcal{G}}^{C,\mathrm{ZS}}_{p_1p_2p_3p_4}\left(i\omega_p\right) = -4 \left(\frac{2\pi v_F^2}{T_K}\right)^2 \int_0^\beta d\tau e^{i\omega_p\tau} \int_0^\beta d\tau_1 d\tau_2 \sum_{\sigma\sigma'} \delta_{\sigma\sigma'} \int \frac{dq_3 dq_4}{\left(2\pi\right)^2} \\ \times g_{p_1}\left(\tau_1 - \tau\right) g_{p_2}\left(\tau - \tau_2\right) g_{p_3}\left(\tau_2\right) g_{p_4}\left(-\tau_1\right) g_{q_3}\left(\tau_2 - \tau_1\right) g_{q_4}\left(\tau_1 - \tau_2\right) , \end{aligned} \tag{D4b}$$

$$\tilde{\mathcal{G}}^{C,\mathrm{ZS'}}_{p_1p_2p_3p_4}(i\omega_p) = -4\left(\frac{2\pi v_F^2}{T_K}\right)^2 \int_0^\beta d\tau e^{i\omega_p\tau}\int_0^\beta d\tau_1 d\tau_2 \sum_{\sigma\sigma'}\delta_{\sigma\bar{\sigma}'}\int\frac{dq_1dq_4}{(2\pi)^2}$$
$$\times g_{p_1}(\tau_1-\tau)\, g_{p_2}(\tau-\tau_2)\, g_{p_3}(\tau_2)\, g_{p_4}(-\tau_1)\, g_{q_1}(\tau_2-\tau_1)\, g_{q_4}(\tau_1-\tau_2). \tag{D4c}$$

Here the terminology of BCS, ZS and ZS′ is borrowed from Ref. 57 and refers only to the topology of the diagrams.

We illustrate the calculation with the BCS diagram; ZS and ZS' again turn out to be completely analogous. Going to the Fourier space,

$$\tilde{\mathcal{G}}^{C,\mathrm{BCS}}_{p_1p_2p_3p_4}(i\omega_p)$$
$$= -\left(\frac{2\pi v_F^2}{T_K}\right)^2 8\int\frac{dq_1dq_3}{(2\pi)^2}\frac{1}{\beta}\sum_{\omega_{n_1}}\frac{1}{\beta}\sum_{\omega_{n_3}}\frac{1}{\beta}\sum_{\omega_{n_5}}$$
$$\times g_{p_1}(i\omega_{n_1})\, g_{p_2}(i\omega_{n_1}+i\omega_p)\, g_{p_3}(i\omega_{n_3})\, g_{p_4}(i\omega_{n_3}-i\omega_p)\, g_{q_1}(i\omega_{n_5})\, g_{q_3}(i\omega_{n_1}+i\omega_{n_3}-i\omega_{n_5}); \tag{D5}$$

the ω_{n_5} summation is standard,[46] whereas the ω_{n_1} and ω_{n_3} summations require the following identities:

$$\frac{1}{\beta}\sum_{\omega_{n_3}}\frac{1}{i\omega_{n_3}-\epsilon_{p_3}}\frac{1}{i\omega_{n_3}-i\omega_p-\epsilon_{p_4}}\frac{1}{i\omega_{n_1}+i\omega_{n_3}-\epsilon_{q_1}-\epsilon_{q_3}}$$
$$= f(\epsilon_{p_3})\frac{1}{\epsilon_{p_3}-i\omega_p-\epsilon_{p_4}}\frac{1}{i\omega_{n_1}+\epsilon_{p_3}-\epsilon_{q_1}-\epsilon_{q_3}} + f(\epsilon_{p_4})\frac{1}{i\omega_p+\epsilon_{p_4}-\epsilon_{p_3}}\frac{1}{i\omega_{n_1}+i\omega_p+\epsilon_{p_4}-\epsilon_{q_1}-\epsilon_{q_3}}$$
$$- f_B(\epsilon_{q_1}+\epsilon_{q_3})\frac{1}{\epsilon_{q_1}+\epsilon_{q_3}-i\omega_{n_1}-\epsilon_{p_3}}\frac{1}{\epsilon_{q_1}+\epsilon_{q_3}-i\omega_{n_1}-i\omega_p-\epsilon_{p_4}}, \tag{D6a}$$

where $f_B(\omega) = 1/\left(e^{\beta\omega}-1\right)$ is the Bose function, and

$$-\frac{1}{\beta}\sum_{\omega_{n_1}}\frac{1}{i\omega_{n_1}-\epsilon_{p_1}}\frac{1}{i\omega_{n_1}+i\omega_p-\epsilon_{p_2}}\frac{1}{i\omega_{n_1}+i\omega_p+\epsilon_{p_4}-\epsilon_{q_1}-\epsilon_{q_3}}$$
$$= \int_{-\infty}^{\infty}\frac{d\epsilon}{2\pi i}f(\epsilon)\frac{1}{\epsilon-i\omega_p-\epsilon_{p_1}}\left(\frac{1}{\epsilon^+-\epsilon_{p_2}}\frac{1}{\epsilon^+-\epsilon_{p_4}-\epsilon_{q_1}-\epsilon_{q_3}}\right.$$
$$\left.-\frac{1}{\epsilon^--\epsilon_{p_2}}\frac{1}{\epsilon^-+\epsilon_{p_4}-\epsilon_{q_1}-\epsilon_{q_3}}\right) - f(\epsilon_{p_1})\frac{1}{\epsilon_{p_1}+i\omega_p-\epsilon_{p_2}}\frac{1}{\epsilon_{p_1}+i\omega_p+\epsilon_{p_4}-\epsilon_{q_1}-\epsilon_{q_3}}, \tag{D6b}$$

where $\epsilon^\pm \equiv \epsilon \pm i0^+$. The second identity can be derived by allowing the complex plane contour to wrap around the line $\mathrm{Im}\, z = \omega_p$.[46] Also useful is the identity

$$f_B(\epsilon_{q_1}+\epsilon_{q_3})\left[f(-\epsilon_{q_1})-f(\epsilon_{q_3})\right] = f(\epsilon_{q_1})\, f(\epsilon_{q_3}). \tag{D7}$$

After applying the identities above, performing analytic continuation $i\omega_p \to \Omega^+$, and performing all p integrals that are approachable by residue methods in Eq. (D1), we find

$$G'^{C,\mathrm{BCS}}_{jj'}(\Omega)$$
$$= -\left(\frac{2\pi v_F^2}{T_K}\right)^2 8\sum_{j_1j_2}\mathbb{U}_{1,j_1}\mathbb{U}^*_{1,j_2}\mathbb{U}_{1,j'}\mathbb{U}^*_{1,j'}S^*_{jj_1}S_{jj_2}\frac{1}{\Omega}$$
$$\times\left(\int\frac{dp_1dp_4dq_1dq_3}{(2\pi)^4}\left\{f(\epsilon_{p_4})\left[f(-\epsilon_{q_1})-f(\epsilon_{q_3})\right]+f(\epsilon_{q_1})\, f(\epsilon_{q_3})\right\}\frac{f(\epsilon_{p_1}+\Omega)-f(\epsilon_{p_1})}{\Omega}\frac{1}{\epsilon_{p_1}+\Omega^+ +\epsilon_{p_4}-\epsilon_{q_1}-\epsilon_{q_3}}\right.$$
$$\left.-\int\frac{dp_2dp_3dq_1dq_3}{(2\pi)^4}\left\{f(\epsilon_{p_3})\left[f(-\epsilon_{q_1})-f(\epsilon_{q_3})\right]+f(\epsilon_{q_1})\, f(\epsilon_{q_3})\right\}\frac{f(\epsilon_{p_2}-\Omega)-f(\epsilon_{p_2})}{-\Omega}\frac{1}{\epsilon_{p_2}-\Omega^+ +\epsilon_{p_3}-\epsilon_{q_1}-\epsilon_{q_3}}\right). \tag{D8}$$

In the DC limit, the principal value parts of the integrands cancel to $O(1/\Omega)$, while the δ-function parts remain:

$$G'^{C,\mathrm{BCS}}_{jj'}(\Omega) = -\frac{(2\pi)^2}{T_K^2} 8 \sum_{j_1 j_2} \mathbb{U}_{1,j_1} \mathbb{U}^*_{1,j_2} \mathbb{U}_{1,j'} \mathbb{U}^*_{1,j'} S^*_{jj_1} S_{jj_2} \frac{1}{\Omega} \frac{2i\pi}{(2\pi)^4} \int d\epsilon_{p_1} \left[-f'(\epsilon_{p_1})\right]$$
$$\times \int d\epsilon_{p_4} d\epsilon_{q_1} d\epsilon_{q_3} \left\{ f(\epsilon_{p_4}) \left[f(-\epsilon_{q_1}) - f(\epsilon_{q_3}) \right] + f(\epsilon_{q_1}) f(\epsilon_{q_3}) \right\} \delta(\epsilon_{p_1} + \epsilon_{p_4} - \epsilon_{q_1} - \epsilon_{q_3}) + O(1). \tag{D9}$$

The integral on the second line has been evaluated by Ref. 5 in the context of an inelastic scattering collision integral:

$$\int_{-\infty}^{\infty} d\epsilon_{p_4} d\epsilon_{q_1} d\epsilon_{q_3} \left\{ f(\epsilon_{p_4}) \left[f(-\epsilon_{q_1}) - f(\epsilon_{q_3}) \right] + f(\epsilon_{q_1}) f(\epsilon_{q_3}) \right\} \delta(\epsilon_{p_1} + \epsilon_{p_4} - \epsilon_{q_1} - \epsilon_{q_3}) = \frac{1}{2} \left(\pi^2 T^2 + \epsilon_{p_1}^2 \right); \tag{D10}$$

hence

$$G'^{C,\mathrm{BCS}}_{jj'}(\Omega) = -\frac{4}{T_K^2} \sum_{j_1 j_2} \mathbb{U}_{1,j_1} \mathbb{U}^*_{1,j_2} \mathbb{U}_{1,j'} \mathbb{U}^*_{1,j'} S^*_{jj_1} S_{jj_2} \frac{1}{\Omega} \frac{i}{2\pi} \int d\epsilon_{p_1} \left[-f'(\epsilon_{p_1})\right] \left(\pi^2 T^2 + \epsilon_{p_1}^2 \right) + O(1). \tag{D11}$$

Each of the ZS and ZS' contributions ends up being the opposite of the BCS contribution,

$$G'^{C,\mathrm{ZS}}_{jj'}(\Omega) = G'^{C,\mathrm{ZS'}}_{jj'}(\Omega) = -G'^{C,\mathrm{BCS}}_{jj'}(\Omega). \tag{D12}$$

therefore, using Eq. (2.10) for the $\mathbb{U}$ matrix elements, we can express the total connected contribution to the conductance to $O\left(1/T_K^2\right)$ as

$$G^C_{jj'} = -\frac{e^2}{h} \lim_{\Omega \to 0} (2\pi i \Omega) G'^{C,\mathrm{BCS}}_{jj'}(\Omega) = \frac{2e^2}{h} \int d\omega \left[-f'(\omega)\right] \mathcal{T}^C_{jj'}(\omega), \tag{D13}$$

where

$$\mathcal{T}^C_{jj'}(\omega) = -\frac{2}{V_{k_F}^4} \left[S(k_F) \Gamma^\dagger(k_F) \lambda \Gamma(k_F) S^\dagger(k_F) \right]_{jj} \left[\Gamma^\dagger(k_F) \lambda \Gamma(k_F) \right]_{j'j'} \frac{\pi^2 T^2 + \omega^2}{T_K^2}. \tag{D14}$$

We have reintroduced the coupling matrix Eq. (2.8). The ω integral can be done explicitly:

$$G^C_{jj'} = -\frac{2e^2}{h} \frac{8}{3V_{k_F}^4} \left| \left[S(k_F) \Gamma^\dagger(k_F) \lambda \Gamma(k_F) \right]_{jj'} \right|^2 \left(\frac{\pi T}{T_K} \right)^2, \tag{D15}$$

i.e. the lowest order connected contribution to the conductance is $O\left(T^2/T_K^2\right)$, characteristic of a Fermi liquid.

Eq. (D14) is in explicit agreement with Eq. (3.33). We can also check its consistency with the Eq. (3.19) and single-particle T-matrix inelasticity. Recall that, by virtue of Eq. (3.36), we should have the following approximate identity for $\omega \approx 0$ in the Fermi liquid regime:

$$\mathcal{T}^C_{jj'}(\omega) = -\frac{1}{V_{k_F}^2} \left[S(k_F) \Gamma^\dagger(k_F) \lambda \Gamma(k_F) S^\dagger(k_F) \right]_{jj} \sum_{j''} \mathcal{T}^D_{j''j'}(\omega). \tag{D16}$$

On the other hand, Eqs. (4.19) and (4.21) yield

$$\mathrm{Im}\left[-\pi\nu \mathrm{T}(\omega)\right] - \left|-\pi\nu \mathrm{T}(\omega)\right|^2 = \frac{\pi^2 T^2 + \omega^2}{2T_K^2}; \tag{D17}$$

therefore, plugging Eq. (D17) into Eq. (3.19), we find for $\omega \approx 0$

$$\sum_{j''} \mathcal{T}^{D}_{j''j'}(\omega) = \frac{\pi^2 T^2 + \omega^2}{2T_K^2} \frac{4}{V^2_{k_F}} \left[\Gamma^{\dagger}(k_F)\, \lambda \Gamma(k_F)\right]_{j'j'} . \tag{D18}$$

Eqs. (D16) and (D18) are fully consistent with Eq. (D14).

[1] J. Kondo, Prog. Theor. Phys. **32**, 37 (1964).
[2] A. Hewson, *The Kondo Problem to Heavy Fermions*, Cambridge Studies in Magnetism (Cambridge University Press, 1997).
[3] P. W. Anderson, J. Phys. C **3**, 2436 (1970).
[4] K. G. Wilson, Rev. Mod. Phys. **47**, 773 (1975).
[5] P. Nozières, J. Low Temp. Phys. **17**, 31 (1974).
[6] G. Zaránd, L. Borda, J. von Delft, and N. Andrei, Phys. Rev. Lett. **93**, 107204 (2004); L. Borda, L. Fritz, N. Andrei, and G. Zaránd, Phys. Rev. B **75**, 235112 (2007).
[7] T. Micklitz, A. Altland, T. A. Costi, and A. Rosch, Phys. Rev. Lett. **96**, 226601 (2006).
[8] F. Pierre and N. O. Birge, Phys. Rev. Lett. **89**, 206804 (2002).
[9] D. Goldhaber-Gordon, H. Shtrikman, D. Mahalu, D. Abusch-Magder, U. Meirav, and M. A. Kastner, Nature **391**, 156 (1998).
[10] S. M. Cronenwett, T. H. Oosterkamp, and L. P. Kouwenhoven, Science **281**, 540 (1998).
[11] F. Simmel, R. H. Blick, J. P. Kotthaus, W. Wegscheider, and M. Bichler, Phys. Rev. Lett. **83**, 804 (1999).
[12] W. G. van der Wiel, S. D. Franceschi, T. Fujisawa, J. M. Elzerman, S. Tarucha, and L. P. Kouwenhoven, Science **289**, 2105 (2000).
[13] M. Pustilnik and L. Glazman, J. Phys. Condens. Matter **16**, R513 (2004); L. I. Glazman and M. Pustilnik, "Nanophysics: Coherence and transport," (Elsevier, 2005) pp. 427–478.
[14] R. G. Pereira, N. Laflorencie, I. Affleck, and B. I. Halperin, Phys. Rev. B **77**, 125327 (2008).
[15] P. Simon and I. Affleck, Phys. Rev. Lett. **89**, 206602 (2002); Phys. Rev. B **68**, 115304 (2003).
[16] P. S. Cornaglia and C. A. Balseiro, Phys. Rev. Lett. **90**, 216801 (2003).
[17] J. Park, S.-S. B. Lee, Y. Oreg, and H.-S. Sim, Phys. Rev. Lett. **110**, 246603 (2013).
[18] W. B. Thimm, J. Kroha, and J. von Delft, Phys. Rev. Lett. **82**, 2143 (1999).
[19] P. S. Cornaglia and C. A. Balseiro, Phys. Rev. B **66**, 115303 (2002).
[20] R. K. Kaul, D. Ullmo, S. Chandrasekharan, and H. U. Baranger, Europhys. Lett. **71**, 973 (2005).
[21] P. Simon, J. Salomez, and D. Feinberg, Phys. Rev. B **73**, 205325 (2006).
[22] R. K. Kaul, G. Zaránd, S. Chandrasekharan, D. Ullmo, and H. U. Baranger, Phys. Rev. Lett. **96**, 176802 (2006); D. E. Liu, S. Burdin, H. U. Baranger, and D. Ullmo, Europhys. Lett. **97**, 17006 (2012); Phys. Rev. B **85**, 155455 (2012).
[23] P. Simon, O. Entin-Wohlman, and A. Aharony, Phys. Rev. B **72**, 245313 (2005).
[24] R. Yoshii and M. Eto, Phys. Rev. B **83**, 165310 (2011).
[25] I. Affleck and P. Simon, Phys. Rev. Lett. **86**, 2854 (2001); P. Simon and I. Affleck, Phys. Rev. B **64**, 085308 (2001).
[26] Y. Komijani, R. Yoshii, and I. Affleck, Phys. Rev. B **88**, 245104 (2013).
[27] L. Glazman and M. Raikh, JETP Lett. **47**, 452 (1988).
[28] C. Bruder, R. Fazio, and H. Schoeller, Phys. Rev. Lett. **76**, 114 (1996).
[29] M. Pustilnik and L. I. Glazman, Phys. Rev. B **64**, 045328 (2001).
[30] J. Malecki and I. Affleck, Phys. Rev. B **82**, 165426 (2010).
[31] Y. Meir and N. S. Wingreen, Phys. Rev. Lett. **68**, 2512 (1992); A.-P. Jauho, N. S. Wingreen, and Y. Meir, Phys. Rev. B **50**, 5528 (1994).
[32] I. V. Dinu, M. Ţolea, and A. Aldea, Phys. Rev. B **76**, 113302 (2007).
[33] M. Zaffalon, A. Bid, M. Heiblum, D. Mahalu, and V. Umansky, Phys. Rev. Lett. **100**, 226601 (2008).
[34] R. Schuster, E. Buks, M. Heiblum, D. Mahalu, V. Umansky, and H. Shtrikman, Nature **385**, 417 (1997).
[35] Y. Ji, M. Heiblum, D. Sprinzak, D. Mahalu, and H. Shtrikman, Science **290**, 779 (2000).
[36] Y. Ji, M. Heiblum, and H. Shtrikman, Phys. Rev. Lett. **88**, 076601 (2002).
[37] M. Avinun-Kalish, M. Heiblum, O. Zarchin, D. Mahalu, and V. Umansky, Nature **436**, 529 (2005).
[38] S. Takada, C. Bäuerle, M. Yamamoto, K. Watanabe, S. Hermelin, T. Meunier, A. Alex, A. Weichselbaum, J. von Delft, A. Ludwig, A. D. Wieck, and S. Tarucha, Phys. Rev. Lett. **113**, 126601 (2014).
[39] A. Carmi, Y. Oreg, M. Berkooz, and D. Goldhaber-Gordon, Phys. Rev. B **86**, 115129 (2012).
[40] A. Aharony, O. Entin-Wohlman, B. I. Halperin, and Y. Imry, Phys. Rev. B **66**, 115311 (2002).
[41] A. Aharony and O. Entin-Wohlman, Phys. Rev. B **72**, 073311 (2005).
[42] O. Entin-Wohlman, A. Aharony, and Y. Meir, Phys. Rev. B **71**, 035333 (2005); V. Kashcheyevs, A. Aharony, and O. Entin-Wohlman, Phys. Rev. B **73**, 125338 (2006).
[43] J. R. Schrieffer and P. A. Wolff, Phys. Rev. **149**, 491 (1966).
[44] I. Affleck and A. W. W. Ludwig, Phys. Rev. B **48**, 7297 (1993).
[45] T. K. Ng and P. A. Lee, Phys. Rev. Lett. **61**, 1768 (1988).

[46] G. Mahan, *Many-Particle Physics*, Physics of Solids and Liquids (Springer, 2000).
[47] I. Affleck, L. Borda, and H. Saleur, Phys. Rev. B **77**, 180404 (2008).
[48] A. E. Miroshnichenko, S. Flach, and Y. S. Kivshar, Rev. Mod. Phys. **82**, 2257 (2010).
[49] M. Vojta and L. Fritz, Phys. Rev. B **70**, 094502 (2004); L. Fritz and M. Vojta, Phys. Rev. B **70**, 214427 (2004).
[50] U. Gerland, J. von Delft, T. A. Costi, and Y. Oreg, Phys. Rev. Lett. **84**, 3710 (2000).
[51] W. Hofstetter, J. König, and H. Schoeller, Phys. Rev. Lett. **87**, 156803 (2001).
[52] P. G. Silvestrov and Y. Imry, Phys. Rev. Lett. **90**, 106602 (2003).
[53] Y. Oreg and D. Goldhaber-Gordon, Phys. Rev. Lett. **90**, 136602 (2003).
[54] R. M. Potok, I. G. Rau, H. Shtrikman, Y. Oreg, and D. Goldhaber-Gordon, Nature **446**, 167 (2007).
[55] B. Bellazzini, M. Mintchev, and P. Sorba, J. Phys. A **40**, 2485 (2007).
[56] A. Perelomov, Â. Zel'dovič, and I. Zeldovich, *Quantum Mechanics: Selected Topics*, Selected Topics Series (World Scientific, 1998).
[57] R. Shankar, Rev. Mod. Phys. **66**, 129 (1994).